KINETIC STUDY OF DIFFERENT CORROSION INHIBITORS FOR 1018 CARBON STEEL IN SEAWATER

BY

Nawaf Ibrahim Al-Bakr

A Thesis Presented to the

DEANSHIP OF GRADUATE STUDIES

KING FAHD UNIVERSITY OF PETROLEUM & MINERALS

DHAHRAN, SAUDI ARABIA

In Partial Fulfillment of the
Requirements for the Degree of

MASTER OF SCIENCE

In

Chemical Engineering

January 2010

KING FAHD UNIVERSITY OF PETROLEUM & MINERALS
DHAHRAN31261, SAUDI ARABIA

DEANSHIP OF GRADUATE STUDIES

This thesis, written by **NAWAF IBRAHIM AL-BAKR** under the direction of his thesis advisor and approved by his thesis committee, has been presented to and accepted by the Dean of Graduate Studies, in partial fulfillment of the requirements for the degree of **MASTER OF SCIENCE IN CHEMICAL ENGINEERING.**

Thesis Committee

Dr. R. A. Shawabkeh
Advisor

Dr. R. O. Rihan
Co-Advisor

Dr. Adnan M. Al-Amer
Department Chairman

Dr. S. M. Javaid Zaidi
Member

Dr. Salam A. Zummo
Dean of Graduate Studies

Dr. N. M. Faqir
Member

15/5/10
Date

DR. L. M. Al-Hadhrami
Member

DEDICATION

This thesis is dedicated to my parents who have supported me all the way since the beginning of my studies. Also, this thesis is dedicated to my wife who has been a great source of motivation and inspiration.

ACKNOWLEDGEMENTS

All praises and thanks are due to Almighty Allah for His guidance and continuous support for me to complete the present thesis. I bow my head with all submission and humility by way of gratitude due to Almighty Allah.

Acknowledgment is due to the King Fahd University of Petroleum & Minerals for supporting this research.

I wish to express my deep appreciation to my thesis committee chairman Dr. R. A. Shawabkeh for his support, friendliness, valuable advice, constant encouragement, and unlimited accessibility. Also, I want to thank him for his assisting me with recommendation in order to face all difficulties to complete this research. Thanks are also extended to my thesis committee co-chairman Dr. R. O. Rihan for assisting me during the experimental work and for teaching me the proper way to use the laboratory appliances.

In addition, I wish to express my appreciation to my committee members; DR. L. M. Al-Hadhrami for allowing me to use the Center of Research Excellence in Corrosion laboratory to conduct this research, Dr. S. M. Javaid Zaidi, and Dr. N. M. Faqir for their helpful observations to improve work and for invaluable support and advice.

Thanks are also extended to Dr. Mamdouh Al-Harthi who comes after the god to facilitate the conducting of my thesis defense. Also, I want to thank him for assisting me in the part of this work.

I would like to thank all workshop and chemical Engineering department staff for their support. Also, I would like to thank graduate students for useful suggestion and comments.

Finally, I would like to express my sincere thanks to all my family, relatives, and friends for their inspiration, encouragement, and support.

TABLE OF CONTENTS

LIST OF TABLES

LIST OF FIGURES

THESIS ABSTRACT

FULL NAME OF STUDENT	**Nawaf Ibrahim Al-Bakr**
TILTED OF STUDY	**Kinetics Study of Different Corrosion Inhibitors for 1018 Carbon Steel in Seawater**
MAJOR FIELD	**Chemical Engineering**
DATE OF DEGREE	**January 2010**

In oil and gas production industry, internal corrosion is a well-known phenomenon and has a serious problem. The major cost of maintenance for these industries is related to the severe damage by corrosion while part of operating cost in these industries is related to inhibition of this phenomenon. In Saudi oil company (Aramco), the largest oil producing and manufacturing company, for example, there was 36% of total maintenance budget in its refineries due to corrosion while production operations onshore and offshore corrosion was responsible for 28% and 60% of total maintenance costs, respectively. Carbon steel (CS) is the most widely used engineering material in petroleum production, refining, pipelines, and chemical processing industries. However, it has relatively limited corrosion resistance against corrosives such as sulfur-containing compound, salts and acidic gases. Amines are one of the groups of compounds that have improved inhibition efficiency against corrosion in carbon steel. These compounds inhibit corrosion by adsorption of the amine group to the metal surface, retarding the anodic dissolution of iron by the protective aggregate layer bonding on this surface. AR-505 AND N-211, commercial names of amine-based inhibitors, are widely used by Saudi Aramco at different environments, however, optimizing the concentration of those inhibitors according to these condition are required to minimize its operating cost.

The corrosion inhibitors in seawater are desirable to prevent or inhibit corrosion of the metal surfaces. This search has involved the study of combinations of two amine based corrosion inhibitors from Saudi Aramco (AR505 and N-211) which act together in order to reduce the sea water corrosion problems on 1018 Carbon Steel under different kinetic conditions. This study includes the measuring of the weight loss, adsorption isotherm analysis, and polarization resistance rate and potentiodynamic polarization techniques. Different operating conditions such as inhibitor concentration, fluid temperature, mixing speed and salt concentration were taken into consideration during the study.

ملخص الرسالة

الاســــــــــم: نواف إبراهيم البكر

عنوان الرسالة: دراسة حركة مختلف مثبطات التآكل ل 1018 للكربون الصلب في مياه البحر

التخصـــــص: الهندسة الكيمائية

تاريخ التخـرج: يناير 2010

التآكل الداخلي ظاهرة معروفة في إنتاج النفط والغاز , والتي تسبب مشكلة خطيرة. جزء من تكاليف التشغيل في هذه الصناعات هو متعلق بتثبيط لهذه الظاهرة. في شركة النفط السعودية (أرامكو) ، أكبر دولة منتجة للنفط ، على سبيل المثال ، 36 ٪ من مجموع ميزانية الصيانة في مصافي التكرير كانت بسبب التآكل في حين أن عمليات الانتاج في المناطق البرية والبحرية للتآكل كانت مسؤولة عن 28 ٪ و 60 ٪ من إجمالي تكاليف الصيانة ، على التوالي.
الكربون الصلب هو الأكثر استعمالا في إنتاج النفط ,التكرير ,خطوط الأنابيب ، والصناعات الكيميائية. من ناحية أخرى, لدى الكربون الصلب مقاومة محدودة ضد المواد المسببة للتأكل مثل الكبريت والأملاح والغازات الحمضية. الأمينات هي واحدة من مجموعة من المركبات التي أدت إلى تحسين كفاءة التثبيط ضد تآكل الكربون الصلب. هذه المركبات تمنع الصدأ عن طريق امتصاص المجموعة الأمينات إلى السطح المعدني. (أ.ر-505) و (ن- 211) ، تعتبر أسماء تجارية للأمين القائم على المثبطات ،و التي تستخدم على نطاق واسع من قبل شركة أرامكو السعودية في بيئات مختلفة ، ولكن ، والاستفادة المثلى من تركيز تلك المثبطات وفقا لهذه الحالة مطلوبة لتقليل تكلفة التشغيل.

إنّ مانعي التآكلَ في ماءِ البحر مرغوب لمَنْع تآكلِ السطوحِ المعدنيةِ. تَضمّنَ هذا البحثِ دراسة تأثير خليط كل من مثبط (أ.ر-505) و (ن- 211) ، والذي يستعمل في أرامكو السعوديِ لكي يُخفّضَ مشاكلَ تآكلِ ماءَ البحر في 1018 فولاذِ كاربونِ تحت الشروطِ الحركيّةِ المختلفةِ. والهدف من هذه الدراسة هو دراسة تأثير مثبط ل (أ.ر-505) و (ن- 211) ، وخليط من كل مثبط على 1018 الكربون الصلب في مياه البحر. هذه الدراسة تشمل عدة تقنيات كهروكيمائية مثل تقنية روسومات التوفل وتقنية الاستقطاب الخطي و التي تقوم بدراسة تأثير كل من تركيز المثبطات, درجة الحرارة, وتغير السرعات, و المعدل الحمضي على مقاومة و سلوك التآكل من خلال كل تجربة.

.

CHAPTER 1

1. INTRODUCTION

Oil and gas industries experience corrosion problems in their production and transportation pipelines carrying petroleum fluids from remote locations. The flow pattern in the petroleum pipelines is a multiphase complex mixture (gas, liquids and solids). The simultaneous flow of crude oil, water (usually sea water), sand particles, and some corrosive gases sulfur-containing compound, salts and acidic gases and are commonly present in petroleum pipeline systems. The presence of sea water as a corrosive solution in petroleum pipelines causes severe corrosion attack [1- 3].

The major cost of maintenance for these industries is related to the severe damage by corrosion while part of operating cost in these industries is related to inhibition of this phenomenon. In Saudi oil company (Aramco), the largest oil producing and manufacturing company, for example, there was 36% of total maintenance budget in its refineries due to corrosion while production operations onshore and offshore corrosion was responsible for 28% and 60% of total maintenance costs, respectively [4].

Carbon steels have been extensively utilized as construction materials for transmission pipelines in the oil and gas production sector [1]. Corrosion can weaken the structural integrity of pipelines and make them an unsafe vehicle for transporting potentially hazardous materials [3]. The failure of in-service components as a result of corrosion has long been responsible for major safety concerns, waste in production time, and cost in the maintenance of the materials in petroleum industries [5,6].

Four common methods were used to reduce the corrosion in pipelines, they are protective coatings and linings, cathodic protection, materials selection, and corrosion inhibitors. *Coatings and linings* normally are intended to isolate the metal from direct contact with the surrounding electrolytes. *Cathodic protection* is a technology, which uses direct electrical current to counteract the normal external corrosion of a metal pipeline. *Materials selection* refers to the selection and use of corrosion-resistant materials to enhance the lifespan of the pipeline.

Corrosion inhibitors are widely used to reduce the internal corrosion in transmission pipelines and the key solution to extend the lifetime of those pipelines and applicable to be implemented or changed without disrupting a process. However, it is not easy to select the proper corrosion inhibitor due to the variable corrosive environments in the system. The inhibitor efficiency depends on its ability to occupy the respective vacant sites forming a chemisorbed inhibitor film. Furthermore, it depends on the composition of the metal and corrodent, inhibitor structure and concentration as well as temperature. The mechanism of the corrosion inhibition can be elucidated by the adsorption of the corrosion inhibitor to the metal surface [6-12].

Several studies are reported on corrosion inhibitors in seawater such as amines, carboxylic acids or heterocyclic compounds that are in contact with the carbon steel [12-14]. Amines are one of the groups

of compounds that have improved inhibition efficiency against corrosion in carbon steel. These compounds inhibit corrosion by adsorption of the amine group to the metal surface, retarding the anodic dissolution of iron by the protective aggregate layer bonding on this surface [15, 16]. It was reported that bis-[trimethoxysilylpropyl]amine (BTSPA) filled with silica nanoparticles inhibits 1018 carbon steel corrosion in NaCl solution when added up to a certain amount, i.e. 300 ppm [12].

AR-505 and N-211 are commercial names of amine-based inhibitors, which are widely used by Saudi Aramco facilities for reducing the sea water corrosion problems in their transmission pipelines. Saudi Aramco is one of the largest producers worldwide. No study has been done to evaluate the effect of these inhibitors in reducing the corrosion rate of 1018 carbon steel in sea water solution. There are no available data in the literature about the effect of these inhibitors in reducing the corrosion rate of 1018 carbon steel in sea water solution.

There are certain conditions which must be met before a corrosion cell can function. There must be including the anode, the cathode and the electrical conductive electrolyte. Electrochemical techniques are used to detect and monitor the performance of the corrosion inhibitors in the laboratory. These techniques are selected based on the objectives of the study. Many researchers have used some electrochemical techniques such as electrochemical impedance spectroscopy, linear polarization resistance, potentiodynamic polarization, and weight loss techniques [17].

1.1 Objectives

The aim of this research was to investigate the inhibiting effect of AR-505, N-211 and mixture of each inhibitor on 1018 CS in seawater solution. The apparatus which was used in this work is an autoclave with a flow circulation system. This study includes the measuring of the weight loss method, linear polarization resistance method, potentiodynamic polarization method, Fourier Transform Infrared Spectroscopy (FTIR) and Scanning Electron Microscope (SEM). Different operating conditions such as inhibitor concentration, fluid temperature, mixing speed and the acidity were taken into consideration during the study. The results show that the corrosion rate increases with increasing solution temperature and salt concentration while decreased with increasing the concentration of the inhibitor and the mixing speed. The investigation will consider the following:

a) Effect of inhibitor concentrations (0, 5, 10, and 15 ppm) at 1000 rpm, 55^{o}C, & 8.2 pH.

b) Effect of fluid temperatures at (25 ^{o}C, 40^{o}C, 55^{o}C) at 1000 rpm, 10 ppm of inhibitor concentration, and 8.2 pH.

c) Effect of mixed speed at (0, 500, 1000 rpm) at 10 ppm of inhibitor concentration, 55^{o}C and 8.2 pH.

d) Effect of the value of pH at (4, 7, 8.2 pH) at 1000 rpm, 10 ppm of inhibitor concentration, and 55^{o}C.

CHAPTER 2

2. LITERATURE REVIEW

Several studies were conducted to evaluate the efficiency of the corrosion inhibitors in neutral and acid solution such as amines, carboxylic acids or heterocyclic compounds that are in contact with the carbon steel [12-14, 18, 19]. Some inhibitors have the ability to block the anodic reaction and called anodic inhibitor. *Ai et al.* found that the dodecanoic acid and its sodium salt (DDAS) inhibited the anodic process on coupling of N80 carbon steel (CS) and S31803 stainless steel (SS) in 1% NaCl solution with pH 4 [13]. Others inhibitor suppress the cathodic reaction or both. *Abbouda et al.* found that 2,3-Quinoxalinedione QD was mixed type inhibitor for mild carbon steel in 1.0 M HCl solution [20].

2.1 Previous Study in Evaluating of Corrosion Inhibitors in Acid Solution

Abdallah et al. investigated the effect of the aminopyrimidine derivatives *(2-aminopyrimidine (I), 2,4-diamino pyrimidine(II), 2,4-diamino-6-hydroxy-pyrimidine (III)* and *2,4,6-triaminopyrimidine (IV))* as

corrosion inhibitor on the carbon steel 1018 in 0.05M nitric acid. Inhibition appeared to result from the adsorption of molecules and ions on the metal surface according to Temkin isotherm through the protonated N-atom or via the lone pair of electrons of nitrogen atoms. The inhibition efficiency was enhanced due to the addition of the iodide ions to aminopyrimidine derivatives. Moreover, it was found that the compound 2,4,6 triaminopyrimidine was potent to protect the metal due to the presence of three active adsorption centers of amino group. In addition, this corrosion inhibitor acted as mixed corrosion inhibitor [18].

El-Etre studied the effect of the corrosion inhibitor aqueous extract of olive of 2.0M HCl solution. Inhibition appeared to result from the adsorption of molecules and ions on the metal surface according to Langmuir adsorption isotherm through the lone pairs of electrons of the oxygen atoms that surround the aromatic rings of the phenolics forming a covering film. The adsorption blocks the active on the metal surface as barrier to mass and charge transfer. Moreover, the corrosion rate was decreased when the concentration of olive leaf extract increased and, therefore, increased the degree of inhibition and the activation energy [21].

Machnikova et al. studied three types of corrosion inhibitor (*2-methylfuran, furfuryl alcohol* and *furfurylamine*) for carbon steel 1018 in 1.0M HCl. Inhibition in this study followed Langmuir isotherm through adsorption by virtue of lone pairs of electron of oxygen heteroatom. All compounds suppressed the cathodic and anodic processes and can provide the protection even at low concentrations. However, the lowest corrosion rate was found in furfuryl alcohol whereas the highest one was in furfurylamine [22].

Ying et al. studied the effect of the purines derivatives (*2,6 dithiopurine, 6- thioguanine, 2,6-diaminopurine, adenine,* and *guanine*) as corrosion inhibitors on the carbon steel in 1.0 M HCl solution. The inhibition efficiency of these derivatives enhanced with the increase concentration of the inhibitors. Both cathodic and anodic processes of corrosion were inhibited. In this study, the inhibiting efficiencies of purines derivatives increased in the order of 2,6-dithiopurine > 6- thioguanine > 2,6-diaminopurine > adenine > guanine. The adsorption of the derivatives on the carbon steel was physical adsorption [23].

Achary et al. investigated the effect of the co-polymer formed between maleic anhydride and N-vinyl-2-pyrrolidone (VPMA) as corrosion inhibitor on the mild carbon steel in 2.0 M sulphuric acid medium. It was found that the co-polymer acts as barrier by formation of adsorbed film on the metal surface and the extiance of this film was demonstared by the Scanning electron microscopy (SEM). The increase of VPMA concentration made the weight loss to be decreased. However, the increase in acid concentration will reduce the inhibition efficiency. In that paper, it was seen that for a given concentration of polymer, the corrosion rate increased with increase in temperature while the corrosion inhibition efficiency decreased. It was proved that the copolymer is effective corrosion inhibitor protected the metal from the corrosion [24].

Xometl et al. studied the effect of the new compounds alkylamides that derived from α amino acids and its derivatives as corrosion inhibitor on the carbon steel 1018 in 1.0 M HCl solution. The inhibition of those compounds obey Temkin's adsorption isotherm. The increase in inhibitor concentration leads to

increase the inhibition efficiency for all the compounds. The effect of temperature was studied from 25 to 60 Cº and found that the inhibition efficiency decreased once the temperature increased and this will increase desorption of the inhibitor. SEM illustrated that Dodecylamide of tyrosine: 2-amino-*N*-decyl-3-(4-hydroxy-phenyl)-propionamide (Tyr C-12) at 100 ppm protect the surface by the formation film. The inhibitor adsorption takes place because of the interaction of π orbital of inhibitor with d-orbital of the metal surface [25].

Priya et al. studied the effect of novel corrosion inhibitors (1- Cinnamyldine-3thiocarbohydroozide [CTCH] and 1-1'Dicinnamyldine-3thiocarbohydroozide [DCTCH]) at 500, 1000, 1500, 2000 ppm on the carbon steel in 15 % boiling hydrochloric acid solution in the temperature range from 30 ^{o}C to 110 ^{o}C. Inhibition appeared to result from the adsorption of molecules and ions on the metal surface according to Temkin adsorption Isotherm. It was found that the increase in the inhibitor concentration up to 1500 ppm, will increase the inhibition efficiency and reached 97%. Moreover, in the presence of inhibitor, the hydrogen permeation current was reduced through the metal surface [26].

Nahle´ et al. studied the effect of 4-vinylbenzyl triphenyl phosphonium chloride (VTPC) on the corrosion inhibition of carbon steel in 1.0M HCl solution in tempature range from 303 to 343 ^{o}K. It was found that the VTPC to be an efficient inhibitor to protect the metal and achieved 99% of efficiency at concentration $1*10^{-4}$ M. The adsorption of the inhibition on the metal surface occurred through the lone pair of electrons of phosphorus and p-electrons [27].

Morad et al. studied the effect of some ferrocene derivatives 1,10-diacetylferrocene (Diacetyl Fc), 1,10-diformylferrocene (Diformyl Fc) and 2 benzimidazolythioacetylferrocene (BIM Fc) on the corrosion inhibition of mild carbon steel in 0.5M H2SO4 and 1.0M HCl solution. In HCl solution, it was found that the increase in Diacetyl Fc will accelerate the corrosion of the metal and decrease the inhibition efficiency. In addition, Both Diformyl Fc and BIM Fc inhibitors were weak in HCl solution. On other hand, Both BIM Fc and Diformyl Fc were good inhibitors in H2SO4 solution but the BIM Fc was the best inhibitor in the solution through the calculation of their efficiency. In H2SO4 solution, inhibition of Diacetyl Fc and Diformyl appeared to result from the adsorption of molecules and ions on the metal surface according to Langmuir adsorption isotherm as physical adsorption while the BIM Fc is chemisorbed on the metal surface and obeyed the Frumkin's isotherm [28].

Rafiquee et al. investigated effect the influence of surfactants on the corrosion inhibition behavior of 2-aminophenyl-5-mercapto-1-oxa-3,4-diazole (AMOD) on mild carbon steel in HCl solution. Inhibition occurred due to the interaction between the compound and the metal surface and obeyed Langmuir adsorption isotherm. The inhibition efficiency of AMOD was increased obviously in presence of surfactants anionic sodium dodecylsulfate (SDS), cationic cetyltrimethylammonium bromide (CTAB),and non-ionic Triton-X-100 (TX-100) and it acted as mixed corrosion inhibitor in hydrochloric acid media. The adsorption of the compounds on the steel was spontaneous due to the low and negative value of the free energy (G_{ads}) which is less than -40.0 KJ/mol. The inhibition efficiency decreased with the increase in acid concentration from 1.0 to 5.0 mol/L HCl at all the three surfactants (SDS, CTAB, TX-100) in presence of AMOD [29].

Morad investigated the effect of some formulations composed of Sn^{2+} (as $SnSO_4$), Zn^{2+} (as $ZnSO_4$), N-acetyl- cysteine (ACC) and S-benzylcysteine (BzC) , as inhibitors for the corrosion of mild steel in 1.0 M H_2SO_4 solution. At 35 ^oC, Zn^{2+} ions acted as accelerator for mild steel corrosion in the solution since it acts as depolarizer with the higher negative potential of the interface while Sn^{2+}, ACC, and BzC provide good corrosion inhibition performance. From the result it was clear that the most effective additive inhibitor was Sn^{2+}. The Adsorption of Sn2+, ACC and BzC followed the Temkin adsorption isotherm [30].

Merah et al. studied the synergistic effect of methyl red MR and potassium iodide on inhibition of corrosion of carbon steel in 0.5M H2SO4 solution. Inhibition found to obey Langmuir adsorption isotherm. MR was found to protect the metal from the corrosion in solution and it affects on both anodic and cathodic current, therefore, it was considered as mixed type inhibitor. Furthermore, it was observed that the inhibition efficiency of MR was enhanced when the Potassium iodide (KI) added in H_2SO_4 solution [31].

Abbouda et al. Studied effect of 2,3-Quinoxalinedione (QD) as a novel corrosion inhibitor for mild carbon steel in 1.0 M HCl solution. From the result, it was clear that the inhibition efficiency increased with increasing concentration. QD was found to be as mixed type inhibitor. The adsorption of 2,3-quinoxalinedione at steel surface was a spontaneous process due to the negative value of free energy. It was found that 2,3-Quinoxalinedione acted as an effective corrosion inhibitor for mild steel in acidic bath and the highest inhibition efficiency reached 88% at concentration of10-3 [20].

Cheng et al. investigated the corrosion inhibitor effect of Carboxymenthylchitosan (CM-chitosan) on the corrosion of mild carbon steel in 1.0 M HCl. It was found that the (CM-chitsan) is a good ecofriendly inhibitor and the inhibition efficiency increased with increasing the concentration of the inhibitor but reduced with the rise of temperature. It was found that the maximum inhibition efficiency reached 93% at 200 mg/L. From the results it was showed that CM-chitosan acted as a mixed-type inhibitor by blocking the active site of anodic and cathodic processes [32].

Fouda et al. studied the effect of Pyrazolone derivatives as corrosion inhibitors for carbon steel in 2.0M hydrochloric acid solution. The results showed that all compounds were sufficient for carbon steel dissolution in the solution. It was found that the adsorption of the pryazolone derivatives to follow Frumkin's adsorption isotherm. The addition of iodide, bromide and thiocyanate ions enhances the inhibition efficiency due to synergistic effect. The compounds inhibit both the cathodic and anodic reactions based on the galvanostatic polarization data but if the external current was applied, it was found that the cathode was more polarized. The efficiency of the inhibitors decreased with a rise in temperature while it was increased with the increase in the inhibitor concentration. It was found from the slopes of anodic and cathodic Tafel lines (βa and βc) that in the presence and absence of inhibitors, the mechanism of inhibition does not change even the concentration of the compounds increased [33].

Chauhan et al. studied the inhibition effect of Zenthoxylum alatum plant extract on the corrosion of mild steel in 5% and 15% HCl solutions by using the weight loss measurement and EIS. The inhibition efficiency of mild steel in all solutions increased with increase in the concentration of plant extract till 2400 ppm. This extract showed a good performance in inhibition by compared with plant extracts of

tobacco, black pepper, etc. Surface analysis (XPS and FT-IR) showed that the compounds in plant extract formed the protective layer on the metal surface. The inhibition adsorption of the plant extract followed the Langmuir adsorption isotherm. The activation energy increased with the addition of extract but it was decreased when exceed 2400 ppm [34].

Awad studied the effect of a natural product "Quinine" (R)-(6-methoxyquinolin-4-yl)((2S,4S,8R)- 8-vinylquinuclidin-2-yl)methanol (C20H24N2O2) as corrosion inhibitor for low carbon steel in 1.0 M HCl solution. In this study the temperature range was 20 to 50 °C. From the results, it was found that Quinine performed as sufficient inhibitor and achieved the efficiency up to 96% at 20 °C. Under the conditions in that study, it was found that the corrosion irons was controlled by the charge transfer process [35].

Oguzie et al. studied the effect of 2-amino-3-mercaptopropanoic acid [cysteine (cys)] at (0.1, 0.5, 1.0, and 5.0 mmol/L) on the corrosion behavior of low carbon steel in 0.5 M H2SO4 solution. It was found that the effect of the inhibiting was manifested at (1.0 and 5.0 mmol/L of concentration). The inhibiting effect of cys suppressed the cathodic reaction at all concentration and at the same time catalyzed the anodic metal dissolution reaction. However, It was found from the results that cys accelerated the corrosion rate of the low carbon steel at low concentrations (0.1 and 0.5 mmol/L) due to stimulating effect of the Fe–cys complex on anodic reaction that greater than the cathodic inhibiting effect [36].

Ouchrif et al. studied the effect of addition of some newly synthesized diamine derivatives (1,3 diaminopropane, ({3-[(cyanomethyl)amino]propyl}amino)acetonrile, and ({3-[(bis-cyanomethyl)amino]propyl}amino) acetonrile as corrosion inhibitor on carbon steel in 0.5M H2SO4 solution using weight loss measurements, electrochemical polarization and impedance spectroscopy (EIS) methods. The results showed that diamines were considered as mixed type inhibitors. It was clear that the presence of the cyanomethyl group that facilitated the adsorption of the inhibitor leading to increase the inhibition efficiency without change the adsorption mechanism. The adsorption of the diamine on the carbon steel followed the Frumkin adsorption isotherm. It was found that there were a good agreement between the weight loss, electrochemical polarization and EIS measurement [37].

Gao et al. studied the corrosion inhibition of Quaternized polyethyleneimine (QPEI) for low carbon steel in 0.5 M H_2SO_4 solution by using weight loss method, electrochemical technique and scanning electron microscopy (SEM). It was found that QPEI was considered as polymeric quatemary ammonium salt and had excellent corrosion inhibition behavior for low carbon steel because it had double filming functions, adsorption filming and polymer filming. In addition, it achieved 92% of inhibition efficiency at 5mg/L concentration of QPEI for 72 hours of immersion time in the sulfuric acid solution. It was clear from the result that the QPEI prevented both anodic and cathodic reactions, yet, the corrosion potential shifted to the positive side and behaved as mixed type inhibitor with anodic predominance [38].

Galicia et al. studied the research corrison mechanism modification of 1018 carbon steel in alkaline sour medium (0.1M(NH4)2S and 10 ppm CN−) as a result of using an inhibitor formulation (IHF) at

concentration similar to those used in the field and it composed of hydroxyoleic imidazoline ($C_{12}H_{42}ON_2$), HI, and aminoether ($C_{20}H_{28}O_3N_2$), AE. It was found that the inhibitor modified chemical and physical properties of films of corrosion product such as thickness, porosity and (electronic and ionic) conductivity leading to increase the protective properties of iron oxi-sulfides. In the presence of HI, the topography of the film was homogenous and nonporous, also, the electronic conductivity of the HI film was lower than that observed in the film formed with AE which showed its topography was heterogeneous. It was found that the presence of both HI and AE improved the film passivity due to the synergetic effect of both species [39].

Amin et al. studied the inhibition behavior of succinic acid (SA) as a corrosion inhibitor for the low carbon steel in aerated non-stirred 1.0 M HCl solutions (pH 4) within the temperature range (15-65 ^{o}C) by using weight loss, potentiodynamic polarization and EIS (electrochemical impedance spectroscopy) techniques. The results showed that the increase in temperature leading to decrease the inhibition efficiency. Moreover, the inhibition of the corrosion by SA was due to the formation of physisorbed film on the electrode surface. The adsorption of the inhibitor on low carbon steel obeyed the Temkin adsorption isotherm. The addition of SA concentration to the solution led to increase in the activation corrosion energy. It was found that the results obtained from those techniques are in a good agreement [40].

Babu et al. studied the effect N-cetyl-N,N,N-trimethylammonium bromide (CTAB) and orthophenylenediamine (OPD) as corrosion inhibitor on carbon steel in 1 mol/L HCl by electrochemical techniques. It was found that CTAB has high inhibition efficiency in the system when

it was used above a concentration of 100 mmol/L. Moreover, CTAB was combined with 20 mmol/L of OPD and found that the inhibition efficiency was slightly enhanced and acted better than CTAB alone, as well as, the hydrogen permeation reduced. The inhibitor performed as mixed inhibitor type and followed the Langmuir adsorption isotherm in 1 mol/L HCl solution. SEM showed that these inhibitors had the control on the corrosion of the metal [41].

Rahman et al. studied the aptitude of new cyclic nitrones containing hydrophobic substituent with concentration varied between 50 to 400 ppm as corrosion inhibitors on carbon steel in 1 M HCl solution at 60 ^{o}C by using electrochemical techniques. The evaluations of those compounds were conducted for first time. It was found that the performance of those compounds had an excellent inhibition behavior and achieved 90% to 98.3% of the inhibition efficiency in the solution [42].

2.2 Previous Study in Evaluating of Corrosion Inhibitors in Neutral Solution

Amar et al. studied the effect of the corrosion inhibitor on the carbon steel by phosphonic acids (thiomorpholin-4-ylmethyl-phosphonic acid (TMPA) and morpholin-4-methyl-phosphonic acid (MPA)) in natural seawater. It was found that the corrosion potential was shifted towards the positive direction and this proved that these compounds have protective action on the carbon steel in this

solution. It was clear that the current density decreased with the presence of phosphonic acids and this indicated that their compounds were adsorbed on the metal surface and hence the metal was protected from the corrosion. The presences of phosphonic acids were effective on carbon steel even with small concentration in natural seawater [8].

Tosun et al. studied the inhibitor effect of single, binary and ternary mixture of chromate, molybdate, nitrite, tetraborate, ortophosphate, benzoate, acetate, ascorbic acid on the corrosion of carbon steel in neutral aqueous solution containing 100ppm Cl^- at room temperature. The best inhibitor effect was a mixture of 1 ppm chromate, 6 ppm nitrite and 3ppm molybdate, and it was found to be more economic than the single and binary component systems. The inhibitor effect decreased with increasing temperature and decreased in acidic medium. The use of sodium chromate or sodium nitrite increased the efficiency of individual components [43].

Chirkunov et al. conducted a study on the effect of Lignosulfonate Inhibitors (zinc hydroxyethylidenediphosphonate ZnHEDP, lignosulfonates LS1 and LS2, and their mixtures) on low carbon steel in neutral solution. The Addition of lignosulfonates was enhanced the protection of low-carbon steel by ZnHEDP in corrosive soft water at 20 and 80°C. In the presence of ZnHEDP, LS1 the cathodic reaction on steel was inhibited by ZnHEDP, while LS2 favors the inhibition of both electrode reactions [44].

Amadeh et al. studied the use of rare earth (RE) cations as corrosion inhibitors for carbon steel in aerated NaCl solution. It was showed that increasing in the temperature and increase in Cl_2 ion concentration from room temperature to 50 and 70°C lead to the increase in the corrosion rate of the steel. The optimum inhibitor concentration was 500 ppm with inhibition efficiency reached to 76%. The inhibitors were considered as cathodic inhibitors at low concentrations, however, the (RE) acted as mixed inhibitor at higher concentration [45].

Srisuwan et al. studied the evaluation of the corrosion rate in the presence of the mixture fatty amines (FA) and phosphonocarboxylic acid salts (PCAS) and the determination of the influence of the presence of two layers covering the electrode surface. It was clear that the cathodic current densities increased with the increase of electrode rotation rate while the anodic current densities decreased. The results showed that the increase of the electrode rotation rate lead to the corrosion current density to be non monotonic which was explained by the presence of the two layers on the electrode surface, moreover, the corrosion potential was shifted in the anodic direction [46].

Ai et al. investigated the effect of dodecanoic acid and its sodium salt (DDAS) as corrosion inhibitor on coupling of N80 carbon steel (CS) and S31803 stainless steel (SS) in 1% NaCl solution with pH 4 in the presence and absence of DDAS. It was found that the anodic process of galvanic corrosion was inhibited by DDAS and it was considered as anodic inhibitor. From the result, it was clear that the protective layer that formed on the coupled CS is more compact than which on the single CS electrode in the same solution. The experiments showed that the adsorption behavior of DDAS on metal surface was highly influenced by positive and negative excess charges in 1% NaCl solution [13].

Alsabagh et al. studied the effect of polyester aliphatic amine surfactants at 40-200 ppm as corrosion inhibitors on the carbon steel in the formation water (deep well water). This solution considers the most corrosive environments in oil field operations containing huge quantities of carbon dioxide and hydrogen sulfide as well as the presence of aggressive salts such as chloride and sulfate causes severe corrosion attack. From the results, the corrosion rate was reduced in all the surfactants especially at a high concentration (200 ppm). The inhibition efficiency of the surfactants increased up to 96% of efficiency with the total number of carbon atoms in the aliphatic hydrocarbon chain. The results show carbon steel was protected by the surfactants as anodic inhibitor. The adsorption of the surfactant molecules block the reactive site on the surface and transport away from the surface. It was deduced that the inhibition process by surfactants was affected by the length of the hydrocarbon chain which controlled the process. Scanning electron microscopy (SEM) was utilized to recognize the surface morphology of carbon steel alloy in the absence and presence of the surfactants [47].

Rajendran et al. studied the effect of polyvinyl alcohol (PVA) as corrosion inhibitor on the carbon steel in natural aqueous solution contiaing 60 ppm of Cl^- in the absence and the presence of Zn^{2+}. Moreover, the effects of sodium sulfate Na2SO4, sodium dodecyl sulphate (SDS), pH and the duration of the immersion of PVA-Zn^{2+} were investigated. It was found that the highest inhibition efficiency to the carbon steel in the solution was 81% at100 ppm of PVA and 75 ppm of Zn^{2+}. In the study, it was observed that the combination of PVA and Zn^{2+} had a synergetic effect on the inhibition efficiency. The maximum inhibition efficiency was found at the critical micelle concentration (200ppm) of SDS as anodic surfactant. The inhibition efficiency of PVA-Zn^{2+} system decreased when the value of pH

was increased. Moreover, when the immersion period of the system was increased, the protective film was ruptured by constant attack of the Cl^-, therefore, the inhibition efficiency was decreased [48].

Gao et al. studied the effect of some tertiary amines in the series of 1,3-di-amino-propan-2-ol, referred as 1,3-di-morpholin-4-ylpropan- 2-ol (DMP) and 1,3-bis-diethylamino-propan-2-ol (DEAP) on carbon steel under electrolyte solution that simulated atmospheric corrosion water (0.1 g/L NaCl, 0.1 g/L NaHCO3, 0.1 g/L Na2SO4). The results proved that the DMP and DEAP acted as anodic inhibitor for carbon steel. Moreover, the performance of the DMP was enhanced with the increasing of the concentration and the maximum inhibition efficiency was found at 2.5x10-2M. It was found that the performance of the DEAP is better than that of DMP and the highest value of inhibition efficiency of DEAP was 95% at 2.5x10-2M [15].

Suegama et al. studied the corrosion behavior of bis-[trimethoxysilylpropyl] amine (BTSPA) films filled with silica nanoparticles at (100, 200, 300, 400 and 500 ppm) for carbon steel in 0.1 mol/ L NaCl solution. The results showed that the barrier properties of the silane layer with silica addition improved the anticorrosion performance in the system. It was found that the addition of 300 ppm of silica nanoparticles achieved the best electrochemical response. However, when the amount of silica nanoparticles was added highly, then, the corrosion protection decreased because of the agglomeration was obtained leading to cracked films and permeable structure [12].

Naderi et al. studied the performance of inhibitive properties of zinc aluminum polyphosphate (ZAPP) pigment extract compared to those involving conventional zinc phosphate (ZP) pigment extract and also no pigment (blank) on low carbon steel in 3.5% NaCl aqueous solution by using as

electrochemical impedance spectroscopy (EIS), linear polarization (LP) and SEM. From the results it was found that ZAPP pigment showed superior performance as a modified phosphate based anti-corrosion pigment in comparison with ZP pigment. SEM results and energy dispersive X-ray analysis (EDX), were demonstrated that a layer precipitated on the surface exposed to solution containing ZAPP extract. . However, there was no film in ZP and it was just scattered corrosion products around the surface [49].

Deyab et al. studied the behavior of the pitting corrosion on carbon steel in carbonate-formation water solution in the presence of adding chloride ions as well as the effect of addition of Na_2WO_4, Na_2MoO_4 and $NaNO_2$ salts by using potentiostatic current–time measurements and complemented by scan electron microscope (SEM). The pitting potential was shifted to more negative potential due to the increase in the anodic peak current and the addition of the concentrations of Cl- ions. The addition of the inorganic anions directed the pitting potential to shift to more positive direction and the rate of pit initiation reduced. It was found from SEM that the inhibiting effect of these anions on carbon steel increased in the following order: $(WO_4)_2^- > (MoO_4)_2^- > (NO_2)^-$ [5].

Sahin et al. conducted experimental and theoretical study of some heterocyclic compounds, 3-amino-1,2,4-triazole (3-ATA), 4-hydroxy-2H-1-benzopyran-2-one (4-HQ) and 4-hydroxy-3-(1H-1,2,4-triazole-3-ylazo)-2H-1-benzopyran- 2-one (3-ATA-Q) as corrosion inhibitors on the low carbon steel in 3.5% NaCl medium by Tafel extrapolation and linear polarization methods. It was found that the increase in the concentration of 3-ATA and 3-ATA-Q led to increase in the surface coverage and obeyed the Langmuir adsorption isotherm. On the other hand, the corrosion rate was accelerated once

4-HQ was used in this study. This study showed an excellent agreement between the theoretical and the experimental results [14].

Yao et al. studied the behavior of aggregated polyaniline (PANI) and polyaniline (PANI) nanofibers on Carbon Steel (0.25-0.45% of carbon content) in 5% NaCl solution. It was indicated that the surface of carbon steel coated with PANI nanofibers formed better passive layer. However, the presence of hydrophilic groups impaired PANI anticorrosion ability. Furthermore, the dispersion stability of the PANI nanofibers in ethanol was better than the aggregated polyaniline. Moreover, it provided the protection to carbon steel by formation of passive layer [50].

Salasi et al. studied the effect sodium silicate and 1-hydroxyethylidene-1,1-diphosphonic acid (HEDP) on the carbon steel in aerated soft water solution. From the results, it was found that the optimum enhanced inhibition, at 15 ppm silicate and 10 ppm HEDP, therefore, the synergistic effects of the inhibitors mixtures were shown at lower value of HEDP while the antagonistic behavior is observed at 15 ppm silicate and 15 ppm HEDP. The study revealed that the inhibitor acted as mixed type inhibitor. Scanning electron microscopy (SEM) images, showed that in the presence of inhibitor molecule, the surface layer increases and this illustrated the corrosion ability to protect the metal [1]. Salasi et al. also studied the inhibition effect of the sodium silicate and HEDP as eco-friendly inhibitors to protect the carbon steel pipelines from red water in aerated soft water by utilizing electrochemical impedance and Tafel polarization measurements. It was demonstrated that the sodium silicate and HEDP have a synergistic effect at low concentration under static conditions. It was found that the inhibition efficiency and synergistic effect was increased with the increase of the electrolyte turbulence. The synergistic effect of the inhibitors increased the inhibition efficiency due to incorporation of organic phosphorous bonds of HEDP through sodium silicate gel-like network [1, 51].

In a previous work, it was shown that the electrode rotation rate depend on the properties of the protective layers formed on the metal surface. *Srisuwan* et al. studied the mechanism of inhibition of a carbon steel by a non-toxic multicomponent inhibitor (fatty amines associated with phosphonocarboxylic acid salts) in the treatment of water in cooling circuits. The corrosion rate was measured from impedance diagrams obtained at the corrosion potential for different electrode rotation rates. The cathodic current densities increased with the increase of electrode rotation rate and shifted to infinity when infinite rotation rate was carried out. It was demonstrated that the low rotation speed rate lead to increase the inhibition efficiency because it will distribute the inhibitor and cover the layer on the surface while at high rotation rate the efficiency will reduced and the surface becomes bright [52].

CHAPTER 3

3. EXPERIMENTAL SET-UP AND PROCENDURE

The apparatus which was used in this project is an autoclave with a flow circulation system. The experimental apparatus was manufactured by Cortest as shown in Figure 3-1. The main components of the corrosion testing apparatus are the following:

3.1 Autoclave

The autoclave acts as a reservoir for the solution. It is a 5.6 liter pressure vessel. It is surrounded by an electric heater to heat the solution. The autoclave is made from 316 stainless steel internally clad with Hastelloy C276. It is equipped with a variable speed motor to rotate the impeller, a pocket to house a thermocouple for measuring the temperature of the solution inside the autoclave, and a gas connection. The design pressure is 20.7 MPa at 260^{o}C. The diagram of the autoclave is shown in Figure 3-2.

3.2 Electrodes

The autoclave is equipped with the following electrodes in order to perform electrochemical measurements:

3.2.1 Reference Electrode

There is only one external Ag/AgCl reference electrode attached to the autoclave. The reference electrode is a simple Ag rod (1.5 mm diameter and 50 mm long) coated by AgCl which was prepared by anodically polarizing the Ag rod in a saturated KCl solution at room temperature. A current density of 10 mA/cm^2 was used for three minutes in order to coat the rod with a durable AgCl layer. In the experiments the reference electrode was continuously wetted by the solution which was extracted from the autoclave and cooled to room temperature, by natural convection. The DC voltage drop ("IR"drop) resulting from varying distance between the reference electrode and the two working electrodes was measured to be very small due to the high conductivity of the solution.

3.2.2 Counter Electrode

The counter electrode is a circular ring placed around the working electrodes in order to ensure a symmetrical current distribution during electrochemical polarization measurements as illustrated in Figure 3-2. The counter electrode is made from Hastelloy C276.

Figure 3-1: The experimental apparatus was an autoclave with a flow circulation system.

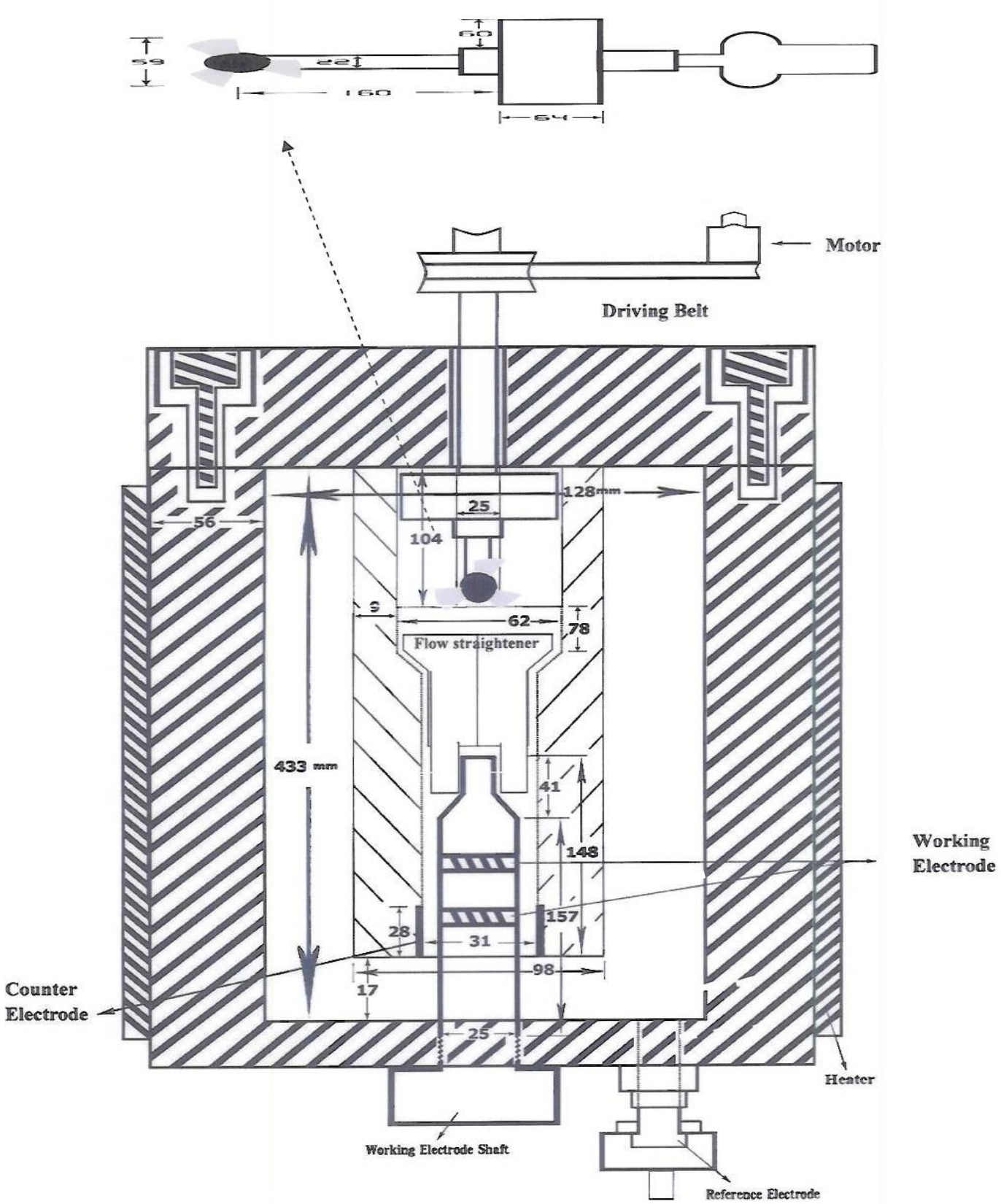

Figure 3-2: Schematic diagram of the experimental apparatus.

3.2.3 Working Electrode (WE)

There are two working electrodes inserted on the working electrode shaft as illustrated in Figures 3-2 and 3-3. One electrode was used for electrochemical measurements, while the other electrode was used for weight loss measurements. The working electrode is a circular ring inserted on the working electrodes shaft. The dimensions of the working electrode are illustrated in Figure 3-4. The working electrodes are made from the material to be tested, which is 1018 carbon steel in this study.

3.3 Flow Straightener

The flow straightener is placed just before the working electrodes shaft as shown in Figure 3-2 in order to stabilize the flow. The flow straightener allows the flow to pass through four separate paths and recombine again before passing over the working electrodes shaft.

3.4 Test Solution

In this investigation, the test solutions for all experiments was prepared from substitute ocean water ASTM 1141D that produced by Lake Products Company, Inc. The chemical, substitute ocean water, is analytical reagent (AR) grade. The chemical compositions of the sea salt mixture are illustrated in Table 3-1.

The procedures to prepare the test solution were carried out as follows:

1) 41.9534 grams sea-salt was dissolved in distilled water.

2) Enough distilled water was added to make one liter total solution.

After mixing, the pH was adjusted to 8.2 using 0.1 N solution of sodium hydroxide or hydrochloric acid.

The solution was placed in the autoclave and the solution was heated to 55^{o}C while running the motor at a speed of 1000 rpm, then the electrochemical measurements started.

Table 3-1: Chemical composition of Sea Salt

Constituent	wt %
NaCl	58.49
MgCl2.6 H2O	26.46
Na2SO4	9.75
CaCl2	2.765
KCl	1.645
NaHCO3	0.477
KBr	0.238
H3BO3	0.071
SrCl2.6H2O	0.095
NaF	0.007

Density of seawater equal 1.025 @ 15 °C

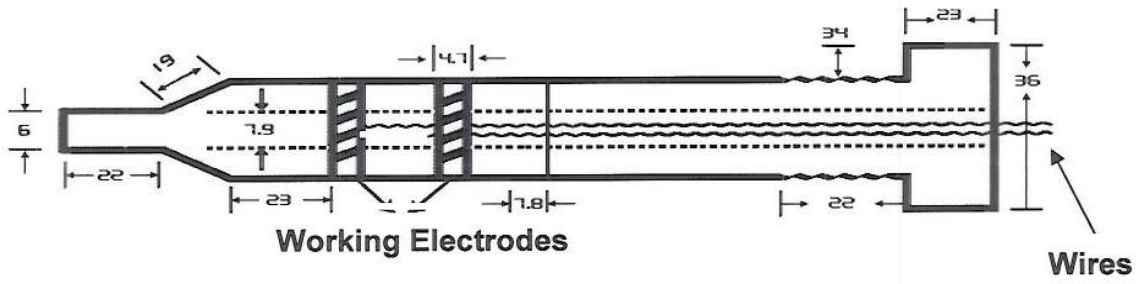

Figure 3-3: Working electrode shaft (Measurements in mm)

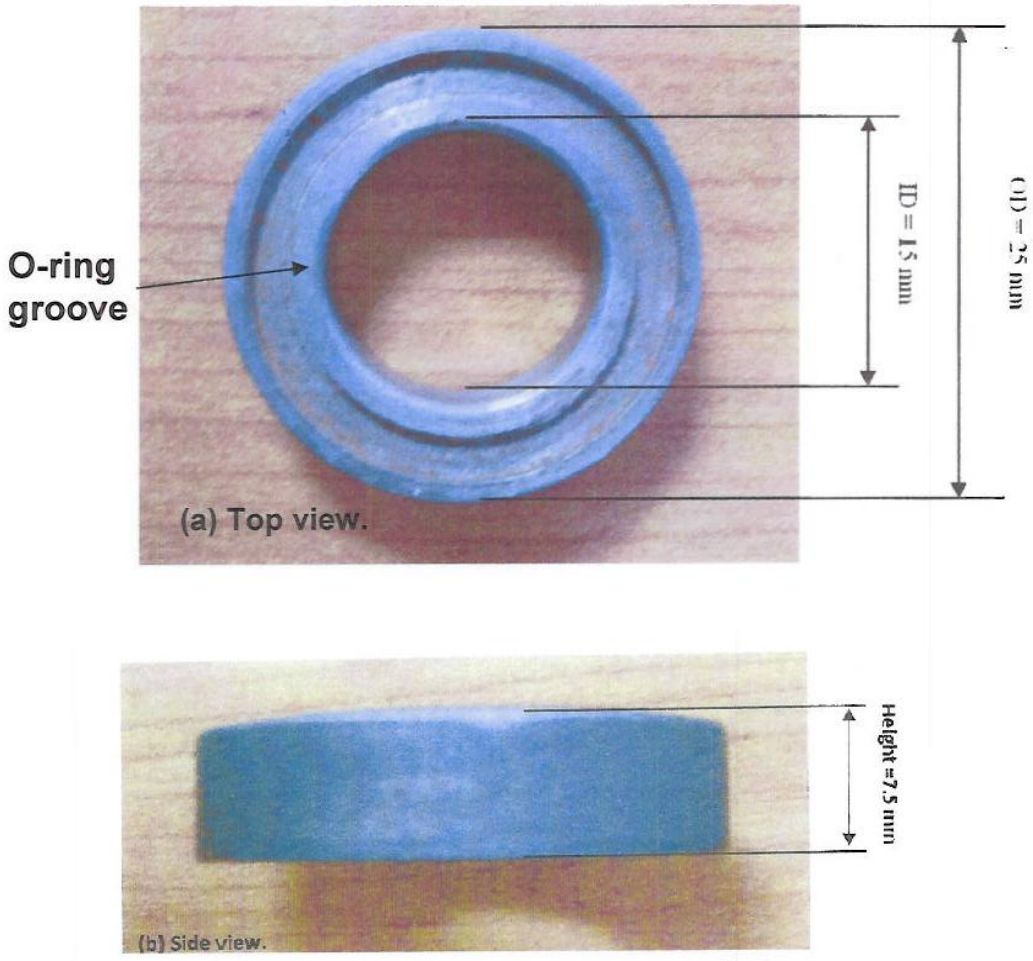

Figure 3-4: The dimensions of the working electrode: (a) Top view; (b) side view.

3.5 Kinetic Experiments of Corrosion Inhibitors

The inhibiting effects of AR-505 and N-211 on 1018 CS in seawater solution were studied and the kinetic experiments were conducted to study the followings:

- Effect of inhibitor concentration (0, 5, 10, and 15 ppm) on the rate of corrosion of the 1018 CS specimens by adding the inhibitor to the test solution. Each experiment was conducted at 1000 rpm, 55°C, and 8.2 pH.

- Effect of fluid temperatures at (25, 40, 55°C) on the rate of corrosion of 1018 CS specimens. Each experiment was conducted at 1000 rpm, 10 ppm of inhibitor concentration, and 8.2 pH.

- Effect of mixed speed at (0, 500, 1000 rpm) on the rate of corrosion of 1018 CS specimens. Each experiment was conducted at 10 ppm of inhibitor concentration, 55°C and 8.2 pH.

- Effect of the value of pH at (4, 7, 8.2 pH) on the rate of corrosion of 1018 CS specimens. Each experiment was conducted at 1000 rpm, 10 ppm of inhibitor concentration, and 55°C.

3.6 Corrosion Testing Methods

Potentiodynamic polarization method was used to investigate the corrosion mechanism of 1018 carbon steel in substitute ocean water. This technique considers generating the Tafel plots for each sample by polarizing the test electrode about ±300 mV anodically and cathodically at scan rate of 2 mV/s. The potential current data is recorded for each sample step, then, the data will be plotted as applied potential against log current density as shown in Figure 3-5. As a result, the corrosion current, i_{corr} is obtained from a Tafel plot by extrapolation of region of Tafel behavior or the intersection of the two lines. An EG&G Princeton/Applied Research (Potentiostat/Galvanostat Model 263A) was used to perform the electrochemical measurements as shown in figure 3-6.

Linear polarization resistance method was used to obtain the polarization resistance (R_p) from the slope of the potential versus current curve as shown in Figure 3-7. The R_p was determined at different time intervals during the experiment. The measurements were performed by polarizing the working electrode 6 mV above and below the open circuit potential at a scan rate of 0.1 mV/s.

The corrosion current (i_{corr}) was calculated using Equation1:

$$i_{corr} = \frac{B}{R_p} \qquad (1)$$

Where: i_{corr} is the corrosion current density in A/m^2, R_p is the polarization resistance in $\Omega.m^2$, and B is the proportionality constant in V/decade (Equation 2) which depends on the anodic (β_a) and cathodic (β_c) Tafel constants.

$$B = \frac{\beta_a * \beta_c}{2.3 * (\beta_a + \beta_c)} \quad (2)$$

The corrosion rate (CR) measured by the electrochemical method was calculated by using Equation 3.

$$CR = \frac{i_{corr} * w}{\rho * F} \quad (3)$$

Where w is the equivalent weight of steel, F is Faraday constant, and ρ is the density of the steel.

Also, the weight loss method was used to determine the corrosion rate for each completed experiment by weighing the specimen before and after the experiment. The corrosion rate measured by weight loss was calculated by using Equation 4:

$$CR = \frac{K * W}{A * t * \rho} \quad (4)$$

Where $K = 8.76 \times 10^6$ (mm/m)(h/y), t is the time of exposure in hour, A is the exposed area of the electrode in m^2, W is the mass loss in kg, and ρ is the specimen density in kg/m^3.

The inhibition efficiency, IE , was calculated as a ratio of the difference between corrosion rate in the presence of the inhibitor to that in the absence of inhibitor as

$$IE(\%) = \frac{CR_{blank} - CR_{inh}}{CR_{blank}} * 100 \qquad (5)$$

Where (CR_{blank}), (CR_{inh}) are the corrosion rate in the absence and presence of the inhibitor.

Fourier Transform Infrared Spectroscopy (FTIR) which is a powerful technique for characterization of organic materials and provides the identification of unknown materials as well as the identification of functional groups.

Scanning Electron Microscope (SEM) is employed to investigate the morphology of microstructures.

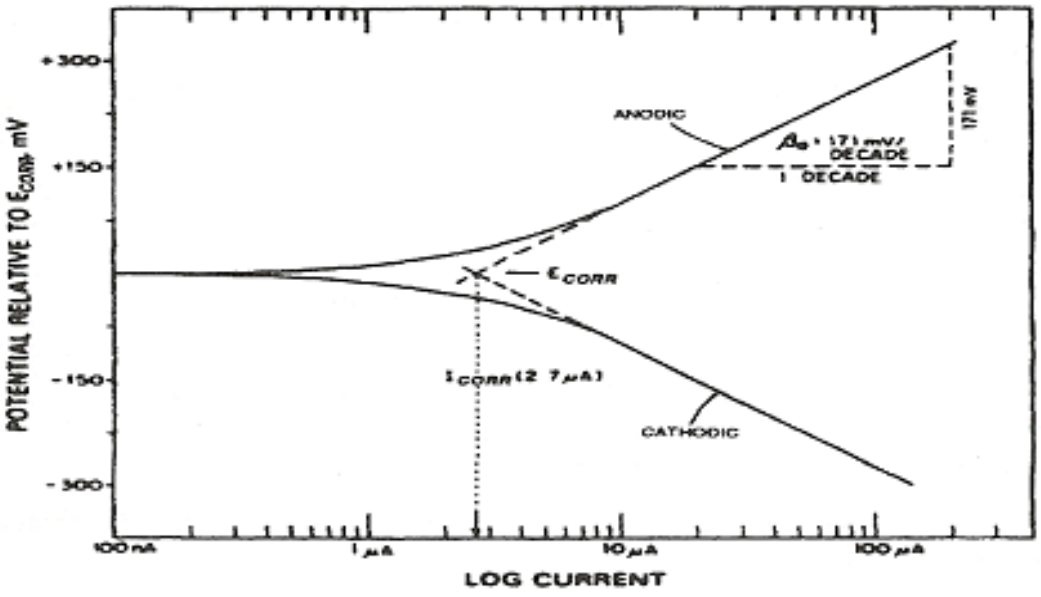

Figure 3-5: Experimentally measured Tafel plot.

Figure 3-6: (Potentiostat/Galvanostat Model 263A) used for electrochemical experiment

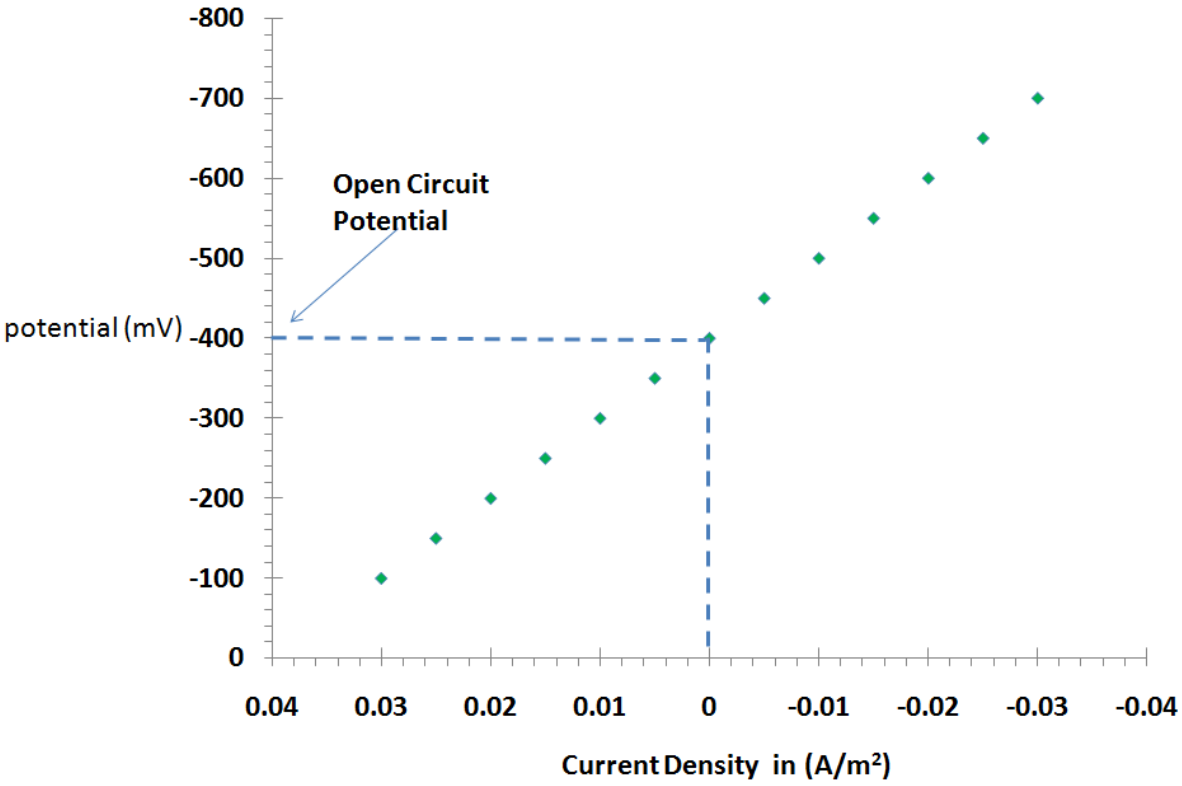

Figure 3-7: Experimentally measured Linear Polarization

CHAPTER 4

4. EXPERIMENTAL RESULTS AND DISCUSSIONS

4.1 AR-505 Amine based Inhibitor

An amine-based corrosion inhibitor (CORTRON AR-505) was used in this work. It is manufactured by Champion Technologies-USA and was provided by Saudi Aramco. It belongs to Alkyl pyridine benzyl chloride quaternary family. It is a dark brown liquid with specific gravity of 1.05 at 15.5^{o}C.

Kinetic experiments were conducted to study the effect of inhibitor concentration (5, 10, and 15 ppm), solution temperature (25, 40, and 55^{o}C), agitation speed (0, 500, and 1000 rpm), and solution pH (4, 7, and 8.2) on the rate of corrosion of the 1018 CS specimens and compare results with results in the absence of inhibitor. This has been investigated by different electrochemical techniques using weight loss, polarization resistance and potentiodynamic polarization methods.

4.1.1 Fourier Transform Infrared Spectroscopy (FTIR)

(FTIR) of AR-505 is represented in Figure 4-1 in order to identify the amine functional groups. It has five major peaks at 1248, 1456, 1636, 2068, and 3446 cm^{-1} all of which are mainly related to $N-NO_2$, $N-N=O$, $C=N-$, $-N=C=S$,and, $-NH_2$ functional groups respectively. Other peaks for alkenes, and hydroxyl groups appeared at 937, 1346 and 2949 cm^{-1}. These amines are generally chemisorbed at the metal surface and displace the adsorbed water and electrolytes from the surface. It is assumed these N-containing functional groups act as electron pair donors to electron-depleted dehydrated metal surface.

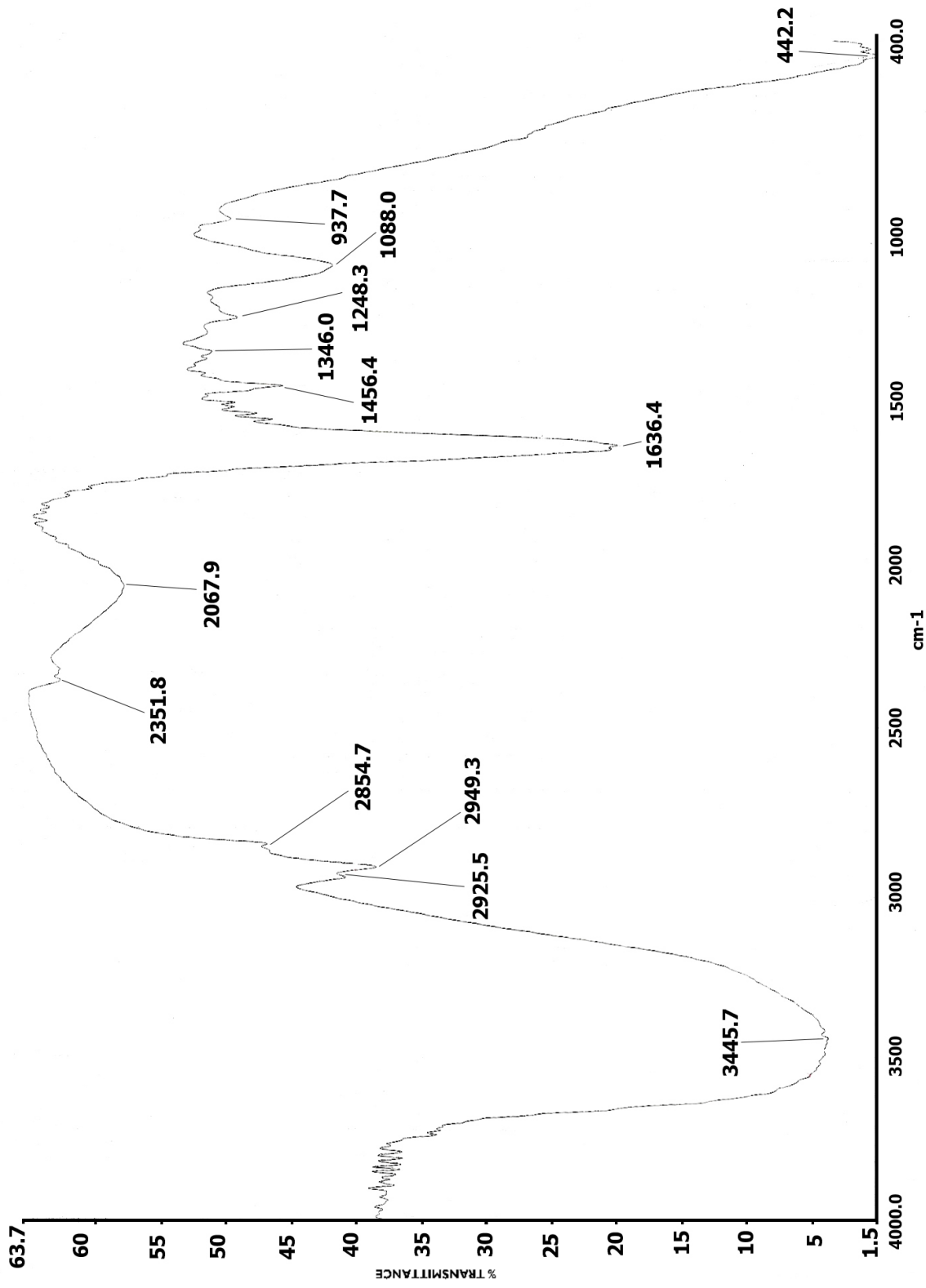

Figure 4-1. FTIR spectrum for AR505 Corrosion inhibitor

4.1.2 Surface analysis

The SEM of the corroded Carbon steel 1018 surfaces after exposure to salt solution for 48 hours in the presence and absence of AR505 are shown in Figure 4-2. Figure 4-2a shows the corrosion layer on the specimen in the presence of AR505 where part of the surface was polished by sand paper. It is clear that the corroded surface is very porous which could be attributed to the corrosion product of γ-FeOOH [55, 56]. Moreover, the corrosion of specimens is distributed over the whole surface area with uniform appearance. Figure 5b shows presence of intense white spots as compared to that in Figure 4-2c. This is probably due to the presence of calcium on the inhibited surface as illustrated by Energy Dispersive Spectroscopy (EDS) analysis in Figure 4-3 and Table 4-1. The surface was mostly of composed oxides of iron, calcium, and magnesium with trace amounts of S, Cr and Si. The specimen that was exposed to the solution containing AR505 inhibitor shows a distinctive peak of calcium with a percentage of 5.57. On the other hand, the percentage of iron on this surface is low compared to that not treated with Corrosion Inhibitor (CI). This presumably is due to the enhancing of the adsorption of calcium ions by the surface in the presence of CI, which blocks part of the surface from being exposed to solution. The percentage of oxygen to iron on the surface of the specimen in the presence and absence of corrosion inhibitor are 32.3% and 24.4%, respectively. The higher oxygen content at the surface that was exposed to the CI is attributed to the formation of the oxides of Mg, Ca and Si which prevent part of the surface from corroding.

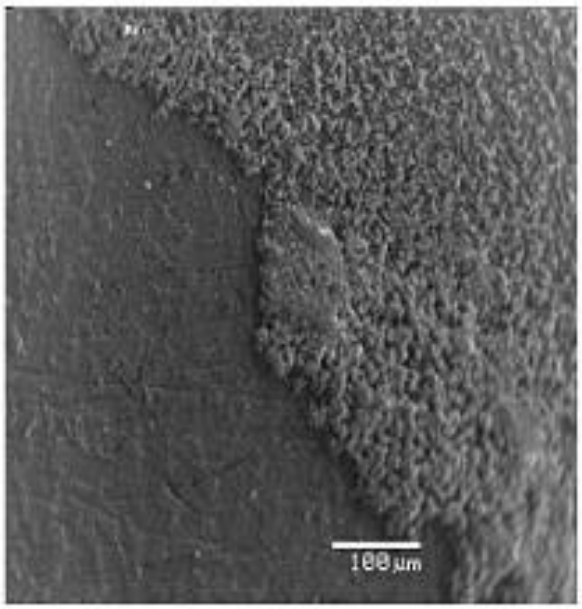

(a)

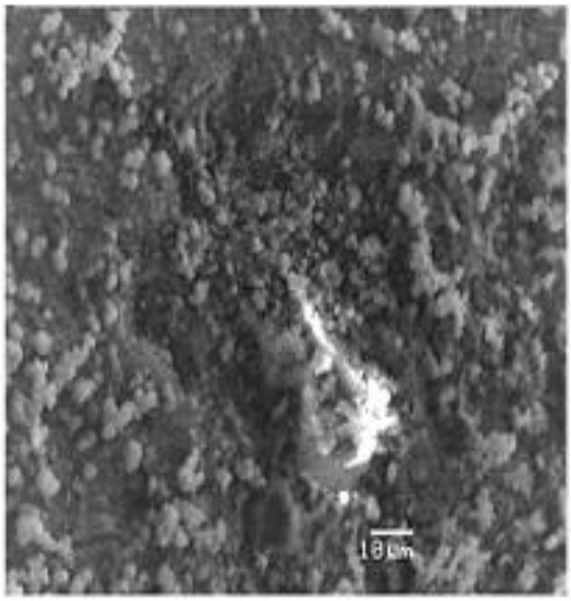

(b)

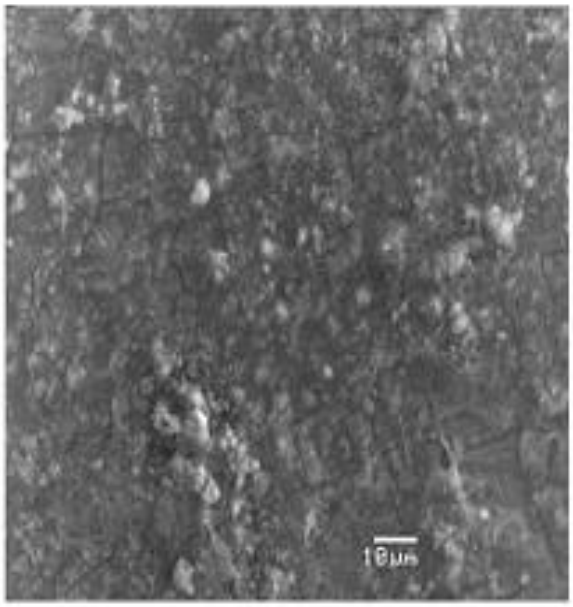

(c)

Figure 4-2: SEM micrograph taken on the surface of a specimen exposed to sea salt; (a,b) mixed with 10 ppm AR505, and (c) without corrosion inhibitor

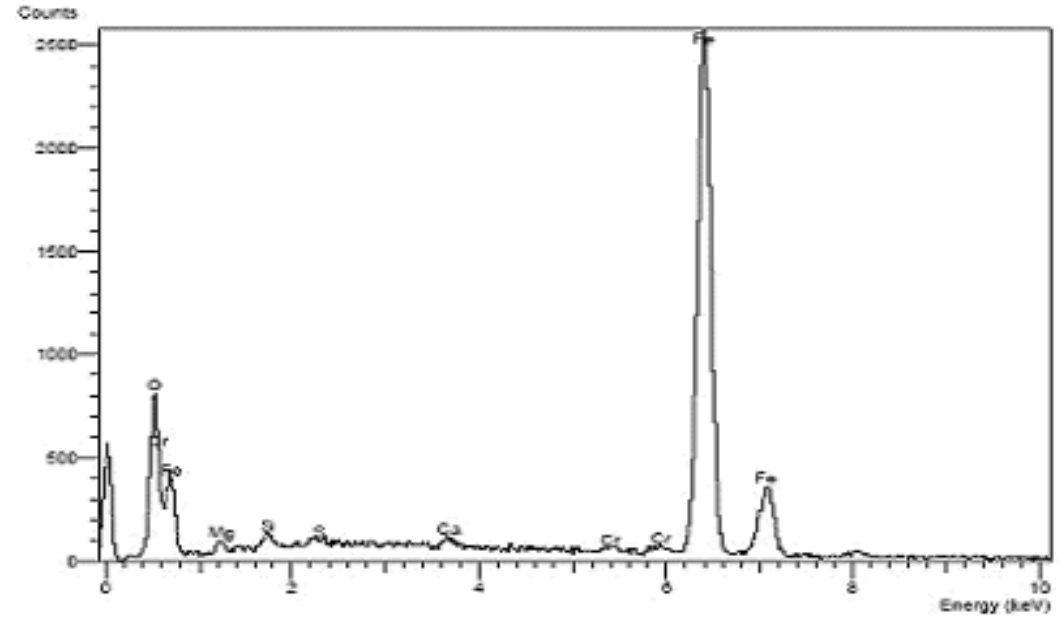

(a)

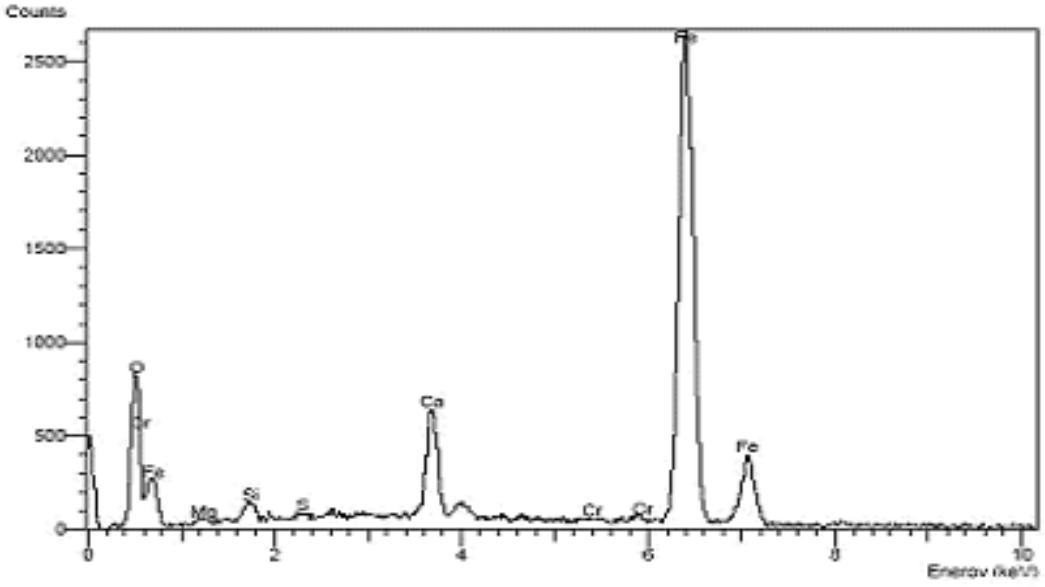

(b)

Figure 4-3: Energy dispersive X-ray analysis of corroded CS1018 specimen; (a) in the absence, and (b) presence of corrosion inhibitor.

TABLE 4-1. EDS ELEMENTAL ANALYSIS OF CORRODED CS1018 SPECIMEN; (A) IN THE ABSENCE, AND (B) PRESENCE OF CORROSION INHIBITOR.

Element	**Elemental Percentage in the Absence of AR 505 CI (%)**	**Elemental Percentage in the presence of AR505 (%)**
O	17.31	21.79
Mg	9.48	4.44
Si	0.77	0.93
S	0.20	-
Ca	0.50	5.57
Cr	0.42	-
Fe	71.30	67.26
Total	100.00	100.00

4.1.3 Weight loss studies

The measured corrosion rate (CR) by weight loss method of 1018 carbon steel specimen in salt water solution as a function of corrosion inhibitor concentration is shown in Figure 4-4 and Table 4-2 and was determined after removing the corrosion products from the surface as blocked the reaction sites [45, 47]. For the sample that was immersed in inhibitor-free solution the CR was 2.47 mm/y while this value was decreased to 1.52 mm/y when 5 ppm of inhibitor was added to the solution. Extra addition of the inhibitor has significant effect in reducing the CR where 0.868 mm/y was achieved when the inhibitor concentration was 15 ppm as shown in Figure 4-4a.

The corrosion rate has increased with increasing the temperature from 25 to 55 $^{\circ}$C as shown in figure Figures 4-4b. It can be seen that at 25 $^{\circ}$C, the corrosion rate was 0.93 mm/y and increased up to 1.29 at 55 $^{\circ}$C, therefore, diminish the efficiency of the inhibitor [43, 45].

Also, the corrosion rate has increased with increasing mixing speed from 0 to 1000 rpm as shown in and 4-4c. It was found that the corrosion rate reduced to 0.34 mm/y. hence, the inhibition efficiency increased with decreased the mixing speed [52]. However, the decrease in the value of pH from 4 to 8.2 pH, led to increase the corrosion rate as shown in Figure 4-4d. Consequently, the inhibition efficiency was reduced [43].

Also, the corrosion rate and inhibition efficiency at different kinetic conditions are shown in Table 4-2.

TABLE 4-2. CORROSION RATE AND INHIBITION EFFICIENCY FOR 1018 CS AT DIFFERENT KINETIC CONDITIONS.

Effect of Parameter	Inhibitor Concentration (ppm)	Speed rpm	Temperature (^{o}C)	pH	CR (mm/y)	Inhibition Efficiency (%)
Inhibitor Concentration	0	1000	55	8.2	2.47	0.0
	5	1000	55	8.2	1.52	38.5
	10	1000	55	8.2	1.29	47.8
	15	1000	55	8.2	0.868	64.9
Temperature	10	1000	25	8.2	0.93	62.4
	10	1000	40	8.2	1.01	59.1
	10	1000	55	8.2	1.29	47.8
pH	10	1000	55	4	3.67	-
	10	1000	55	7	1.98	19.8
	10	1000	55	8.2	1.29	47.8
Speed	10	0	55	8.2	0.34	86.2
	10	500	55	8.2	1.18	52.2
	10	1000	55	8.2	1.29	47.8

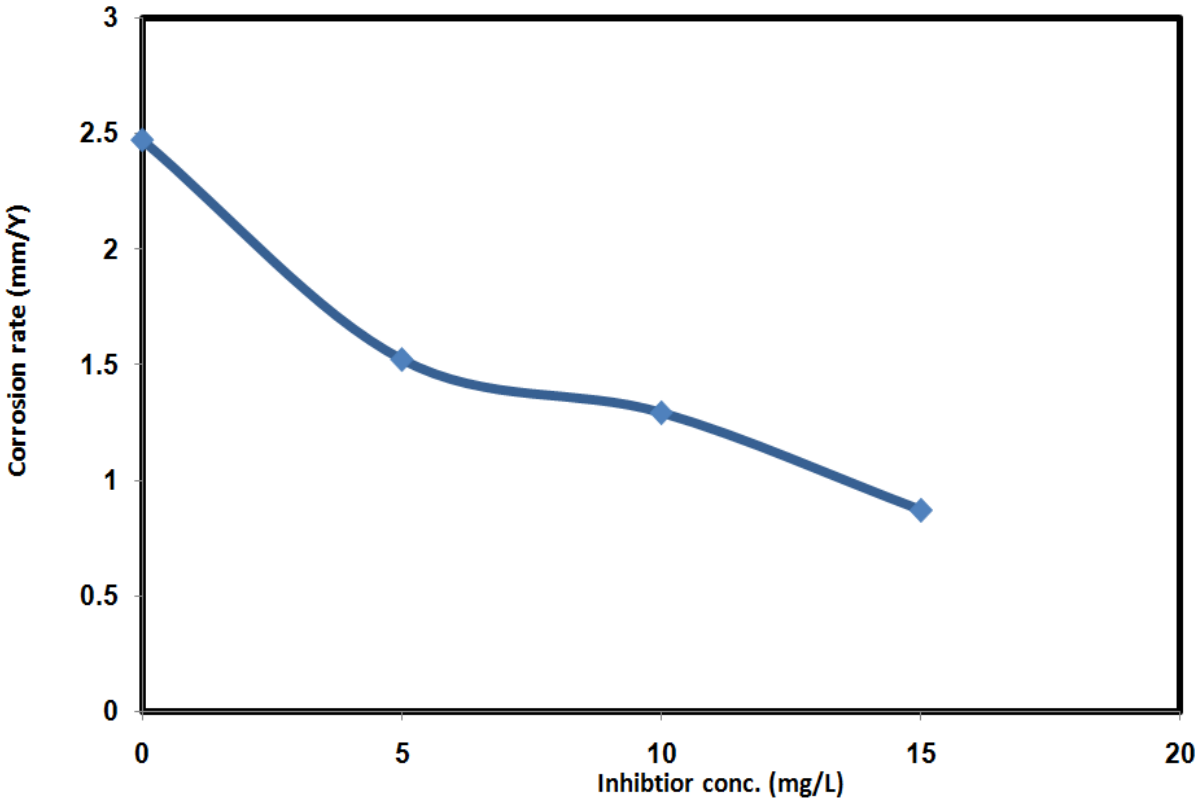

Figure 4-4 a: Effect of inhibitor concentration on the corrosion rate of 1018 CS in sea water obtained by weight loss method at 55^{o}C, 1000 rpm, and pH 8.2.

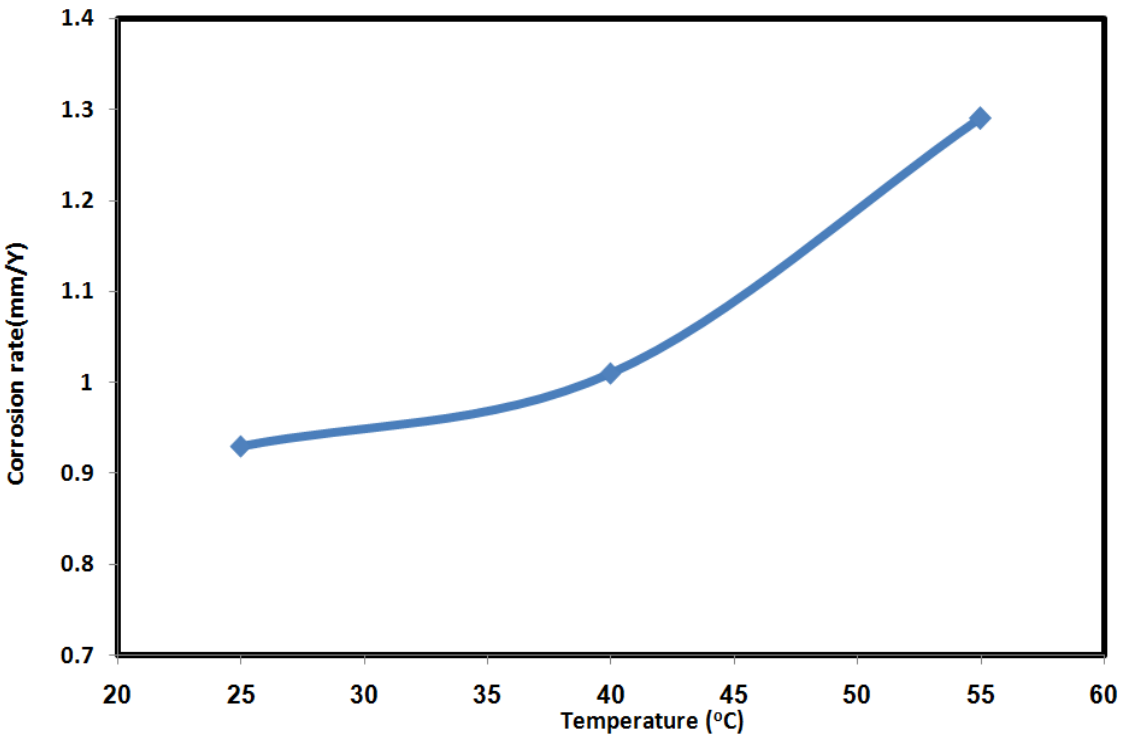

Figure 4-4 b: Effect of solution temperature on the corrosion rate of 1018 CS in sea water obtained by weight loss method at 1000 rpm, 10 ppm inhibitor concentration and pH 8.2.

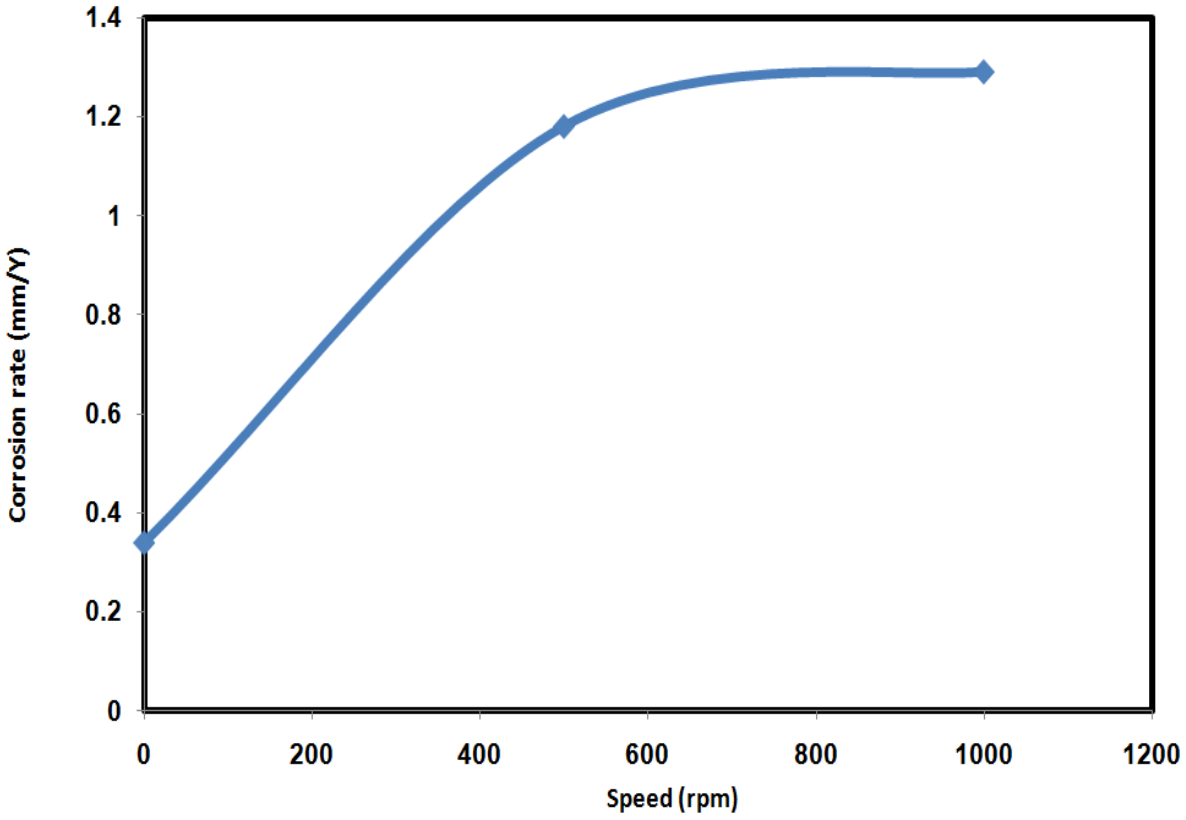

Figure 4-4 c: Effect of mixing speed on the corrosion rate of 1018 CS in sea water obtained by weight loss method at 55^{o}C, 10 ppm inhibitor concentration and pH 8.2.

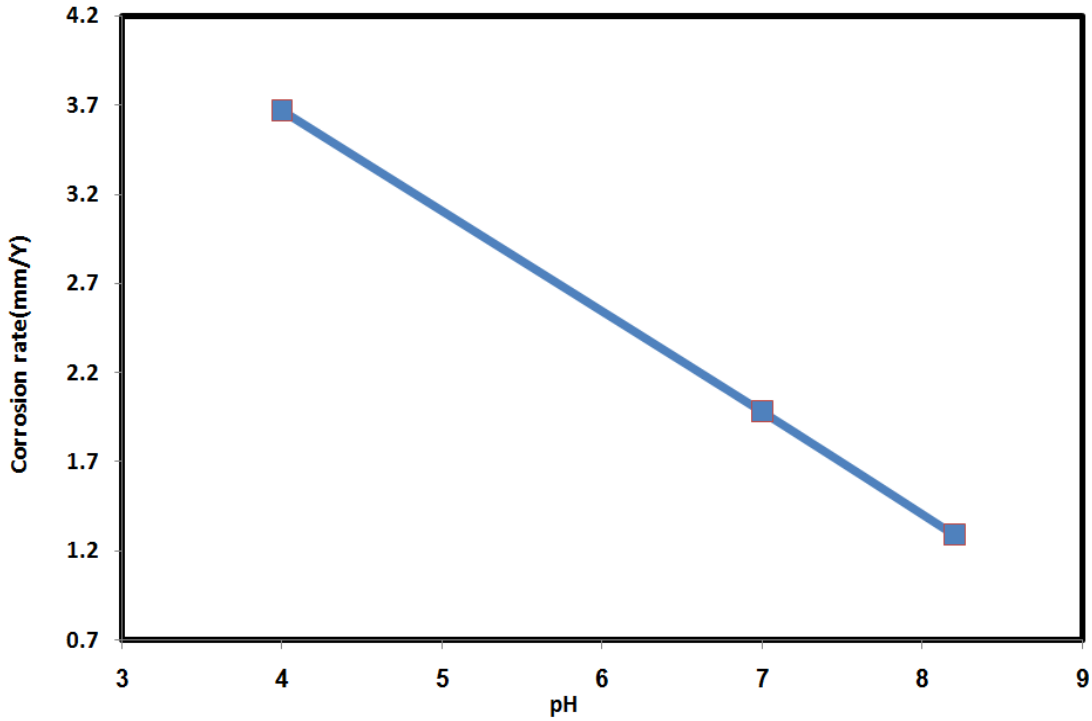

Figure 4-4 d: Effect of solution pH on the corrosion rate of 1018 CS in sea water obtained by weight loss method at 10 ppm inhibitor concentration, 55^{o}C and 1000 rpm.

4.1.4 Adsorption isotherm analysis

The mechanism of corrosion inhibition can be explained by adsorption of the corrosion inhibitor to the surface of the metal. The efficiency of this inhibitor depends on its ability to occupy the respective vacant sites forming a chemisorbed inhibitor film. This efficiency depends on the composition of the metal and corrodent, inhibitor structure and concentration as well as temperature [3, 7, 9-11]. Therefore, the adsorption equilibrium for AR505 by CS surface was investigated at 1000 rpm, 55°C, and the pH was adjusted to 8.2 pH. The degree of surface coverage by the inhibitor, θ_m can be related to the weight loss in the absence and presence of corrosion inhibitor, m_{free} and $m_{inh.}$, respectively as illustrated by Equation 6.

$$\theta_m = \frac{m_{free} - m_{inh}}{m_{free}} \qquad 0 \le \theta_m \le 1 \qquad (6)$$

The values of θ_m corresponding to the inhibitor concentration were plotted in Figure 4-5 and fitted to the isotherm models of Equations 7 and 8.

Langmuir model [53] $$\theta_m = \frac{\theta_{max} bCe}{1 + bCe} \qquad (7)$$

Shawabkeh-Tutunji relation [54] $$\theta_m = q_o(1 - \alpha Ce^{\beta}) \qquad (8)$$

Where θ_{max} is the maximum adsorption capacity could be reached by the inhibitor-surface

system, Ce is the equilibrium concentration of the inhibitor in solution, and q_0, b, α, and β are constants and presented in Table 4-3. It can be seen that Shawabkeh-Tutunji correlation best fits the experimental data with regression coefficient of 0.990 which is applied for chemisorption adsorbent-adsorbate system; however, Langmuir model predicts the physical adsorption isotherm with regression coefficient (R^2) of 0.983. The maximum adsorption capacity that covers monolayer of inhibitor by the 1018 CS surface is estimated using Langmuir model as 0.097 mg AR505.

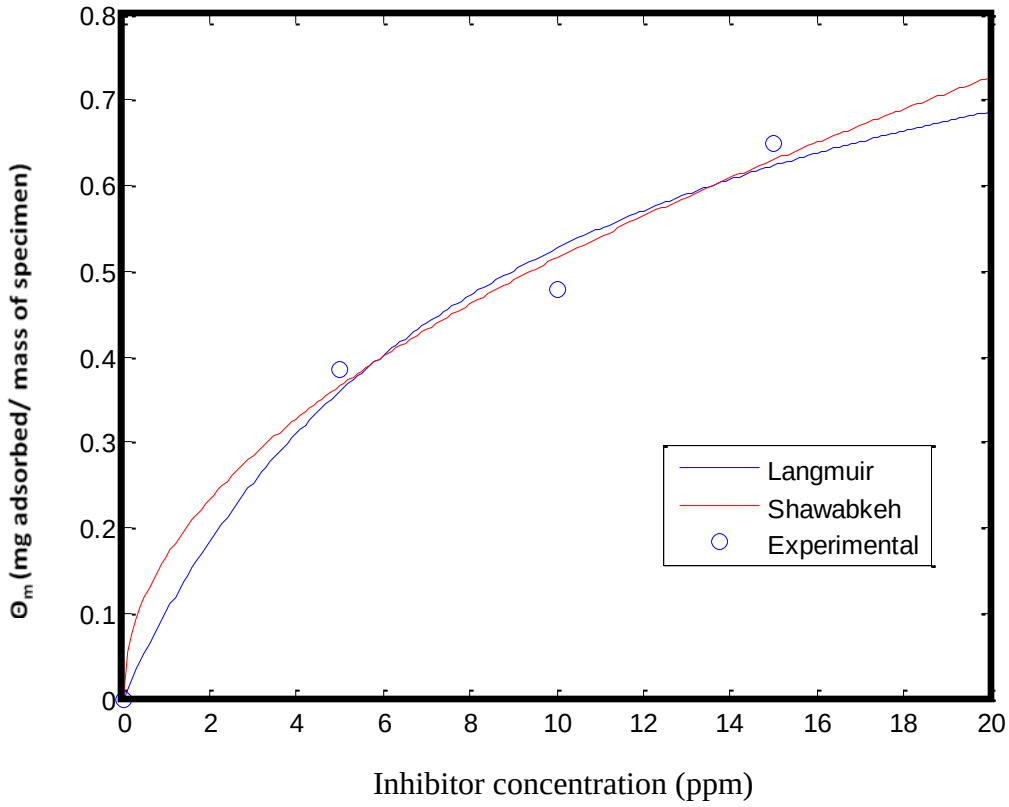

Figure 4-5. Adsorption isotherm of AR505 CI using 1018 CS at 1000 rpm, 55°C, and pH 8.2.

TABLE 4-3. ADSORPTION ISOTHERM PARAMETERS

Model	Parameter	Value	R^2
Langmuir	maxθ (mg/g)	9.685×10^{-2}	0.983
	b	1.204×10^{-2}	
Shawabkeh-Tutunji	q_0	1.333×10^{-3}	0.990
	α	-126.747	
	β	0.485	

4.1.5 Linear Polarization Resistance (LPR) Method

The corrosion rates versus time at different experimental conditions are shown in Figure 4-6. It was conducted for the first four hours, then, it continued on it continued after 15 hours till the performance became steady. Figure 4-6a shows the effect of different CI concentrations on the corrosion rate. It is apparent that the increase in CI concentration has decreased the corrosion rate. A rapid decrease in corrosion rate was achieved within the first hour of conducting the experiments which is related to the formation of a protective oxide film. However, it is shown that the increase in CI has little effect on percentage of inhibition. It is also concluded that a 10 ppm CI could be assumed as an optimum concentration to inhibit the surface where an approximate CR of 1mm/y regardless of the amount of inhibitor in solution. At 10 ppm CI, the corrosion rate was further studied by varying the solution temperature (Figure 4-6b). The solution temperature has a noticeable effect on CR where a value of 0.88 mm/y was achieved at 55^{o}C within 4h compared to 0.35 mm/y obtained at 25^{o}C within the same period of time. As expected, the higher solution temperature yields a higher corrosion rate. This is due to the increase in desorption of the inhibitor with increasing temperature and hence increase the rate of electrochemical reactions and diffusion processes which stimulates corrosive attack. The effect of mixing speed is presented in Figure 4-6c. The corrosion rate has increased within 4 h from 0.2 mm/y for stagnant solution to 0.85 mm/y at mixing speed of 500 rpm. A similar corrosion rate was obtained when the mixing speed has increased to 1000 rpm. Increasing mixing speed will reduce the thickness of the diffusion layer at the electrode surface and thus maintaining the concentration of the salt adjacent to surface is relatively equal to that in the bulk of the solution [52]. The

corrosion rate at 1000 rpm was severely affected by decreasing the solution pH (Figure 4-6d). It is expected that decreasing the solution pH will increase hydrogen ions in solution and the later becomes more aggressive to attack the surface. A value of 2.6 mm/y was reached within 4 hours at this condition.

The studies of the corrosion potential (E_{corr}) versus time noticeably show the capability to maintain the passivity of the 1018 CS at different experimental conditions as shown in Figures 4-7. Figure 4-7a shows that the E_{corr} became more positive as the inhibitor concentration increased. However, it can be seen from Figure 4-7b that the decrease in temperature assists the passivation of the steel surface and the adherence of the passive film is high. The passivity of the carbon steel was decreased as the rotating speed increased as illustrated in Figure 4-7c. It is seen that, under the static condition, the E_{corr} shift to highest positive values. Apparently, an increase of rotating speed leads to acceleration of the diffusion of oxygen, thus the oxide film will be removed. It is extrapolated from Figure 4-7d that the corrosion potential decreases with increase in acidity and this is demonstrated that oxide film have a tendency to dissolve in the solution swiftly when it reached to pH 4.

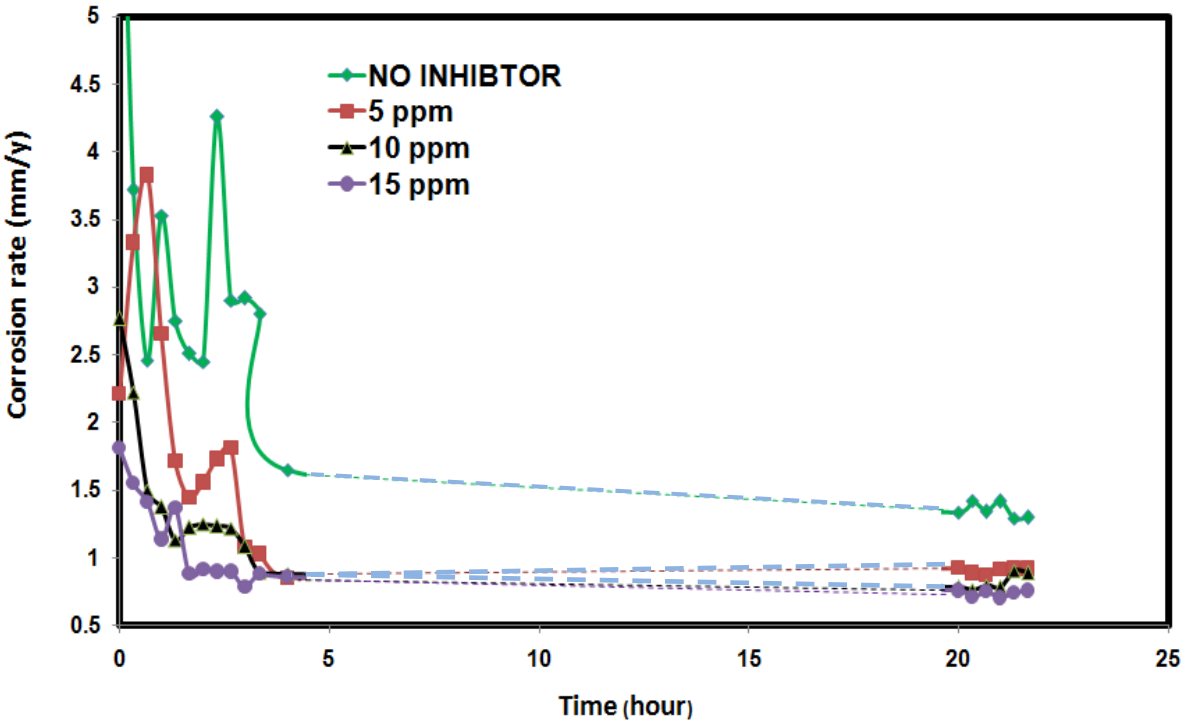

Figure 4-6 a: Effect of inhibitor concentration on the corrosion rate 1018 CS in sea water obtained by (LPR) Method at 55^{o}C, 1000 rpm, and pH 8.2.

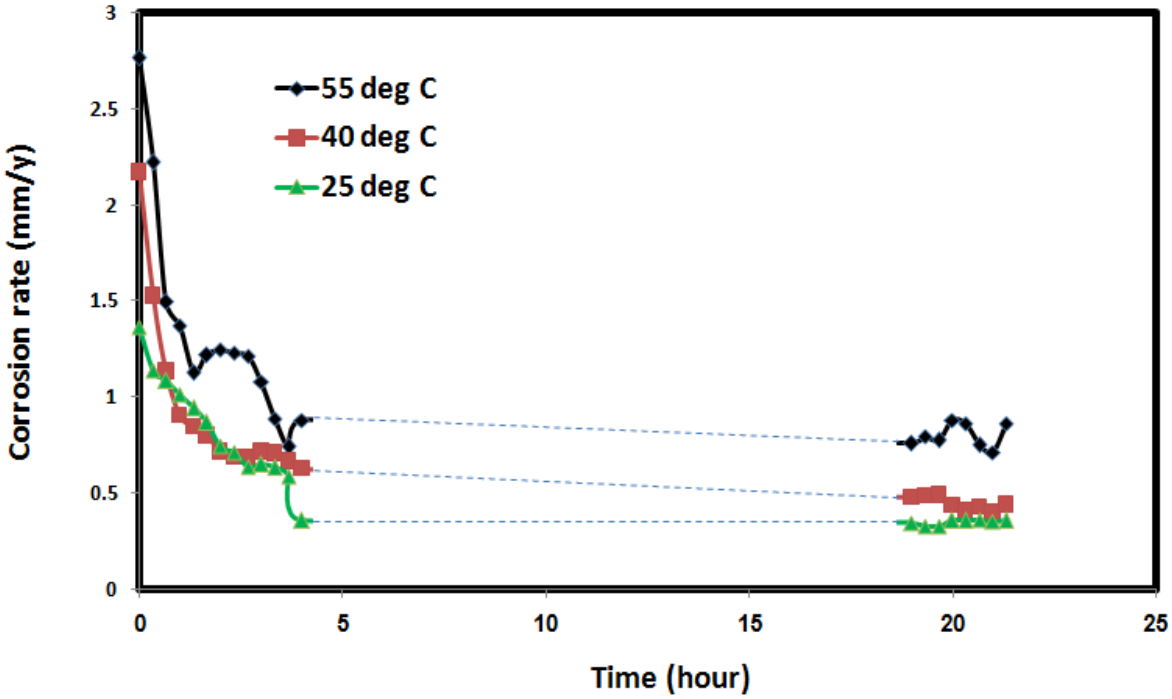

Figure 4-6 b: Effect of solution temperature on the corrosion rate of 1018 CS in sea water obtained by (LPR) Method at 1000 rpm, 10 ppm inhibitor concentration and pH 8.2.

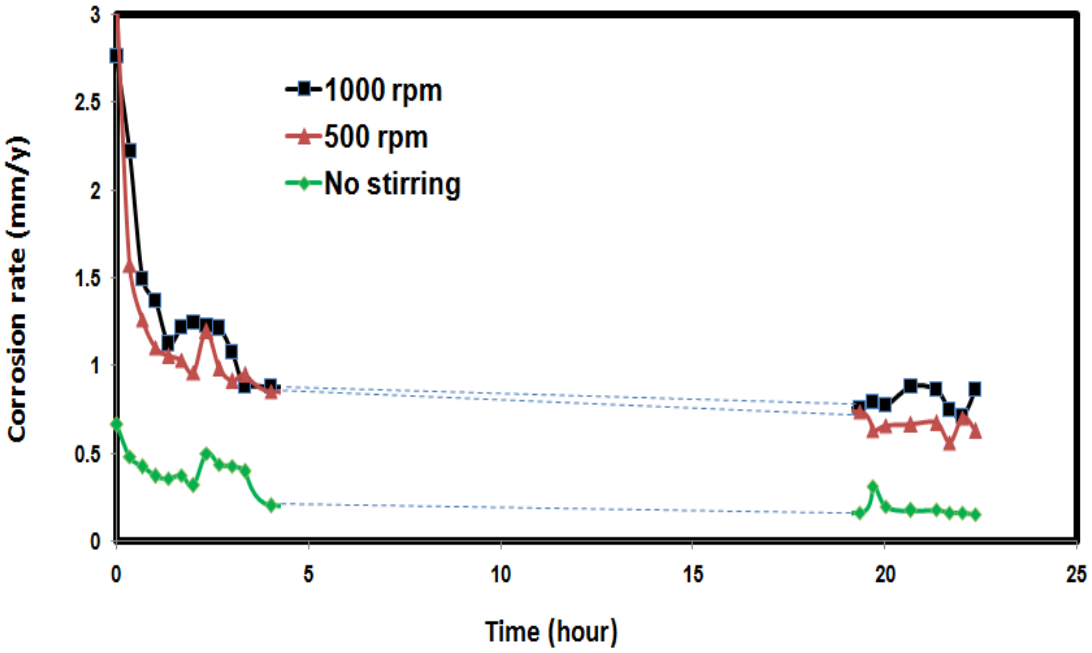

Figure 4-6 c: Effect of mixing speed on the corrosion rate 1018 CS in sea water obtained by (LPR) Method at 55^{o}C, 10 ppm inhibitor concentration and pH 8.2.

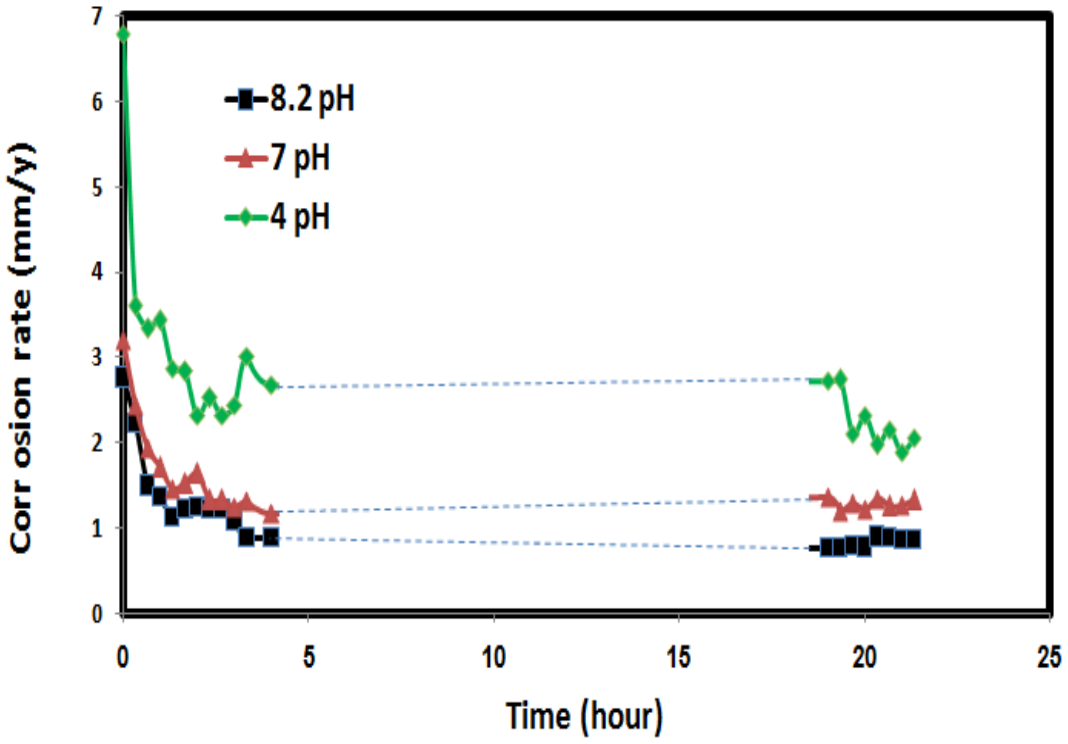

Figure 4-6 d: Effect of solution pH on the corrosion rate 1018 CS in sea water obtained by (LPR) Method at 10 ppm inhibitor concentration, 55^{o}C and 1000 rpm.

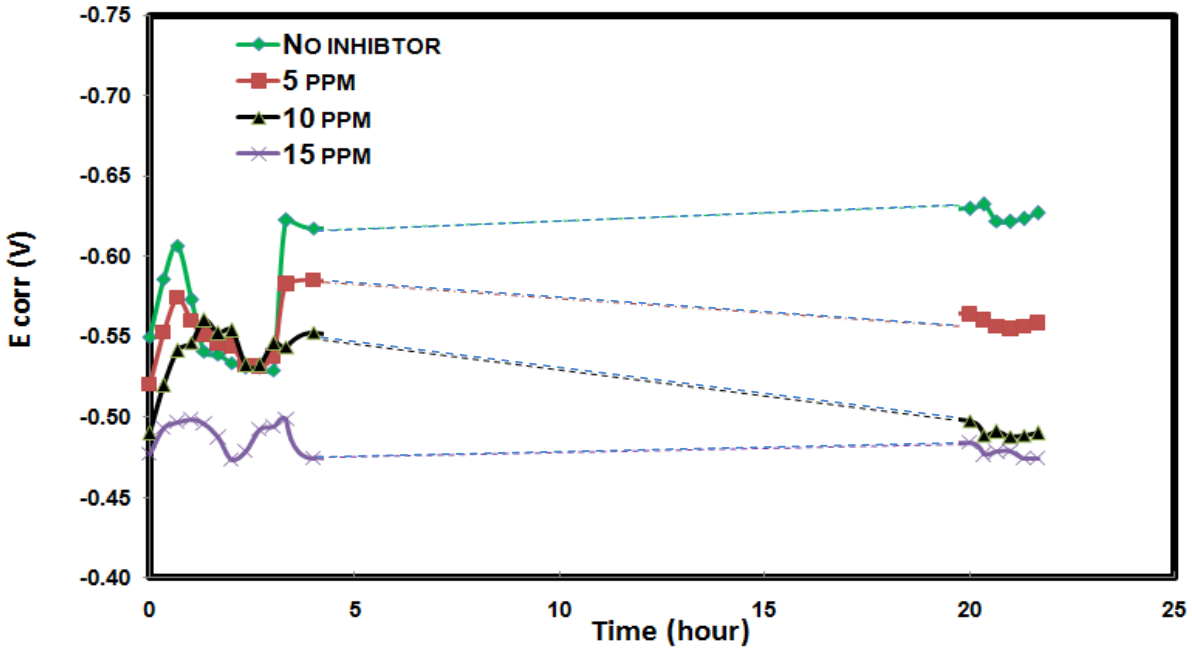

Figure 4-7 a: Effect of inhibitor concentration on the corrosion potential (E_{corr}) 1018 CS in sea water obtained by (LPR) Method at 55^{o}C, 1000 rpm, and pH 8.2.

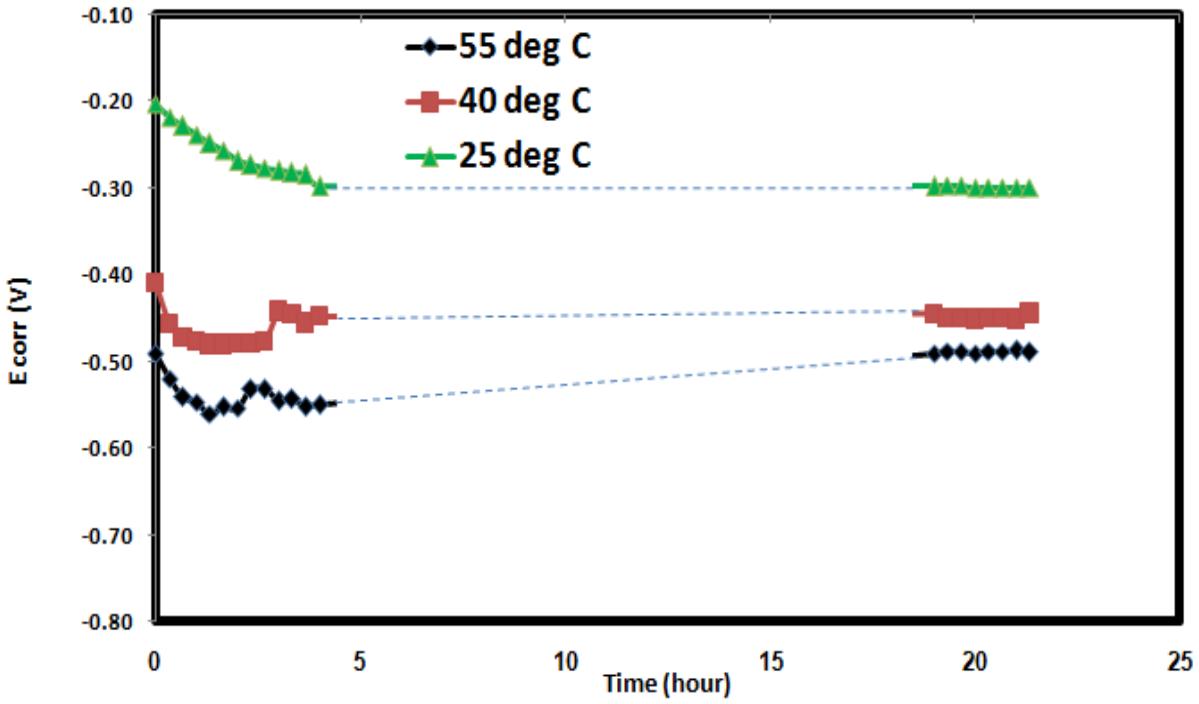

Figure 4-7 b: Effect of solution temperature on the corrosion potential (E_{corr}) of 1018 CS in sea water obtained by (LPR) Method at 1000 rpm, 10 ppm inhibitor concentration and pH 8.2.

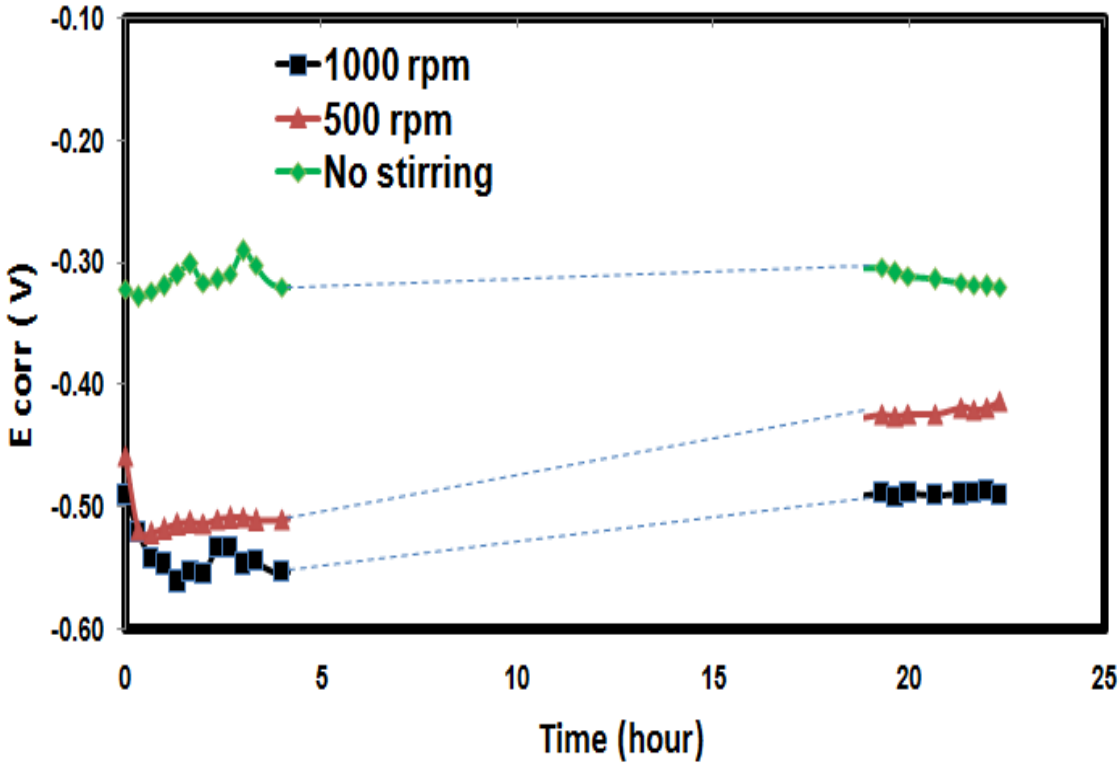

Figure 4-7 c: Effect of mixing speed on the corrosion potential (E_{corr}) 1018 CS in sea water obtained by (LPR) Method at 55^{o}C, 10 ppm inhibitor concentration and pH 8.2.

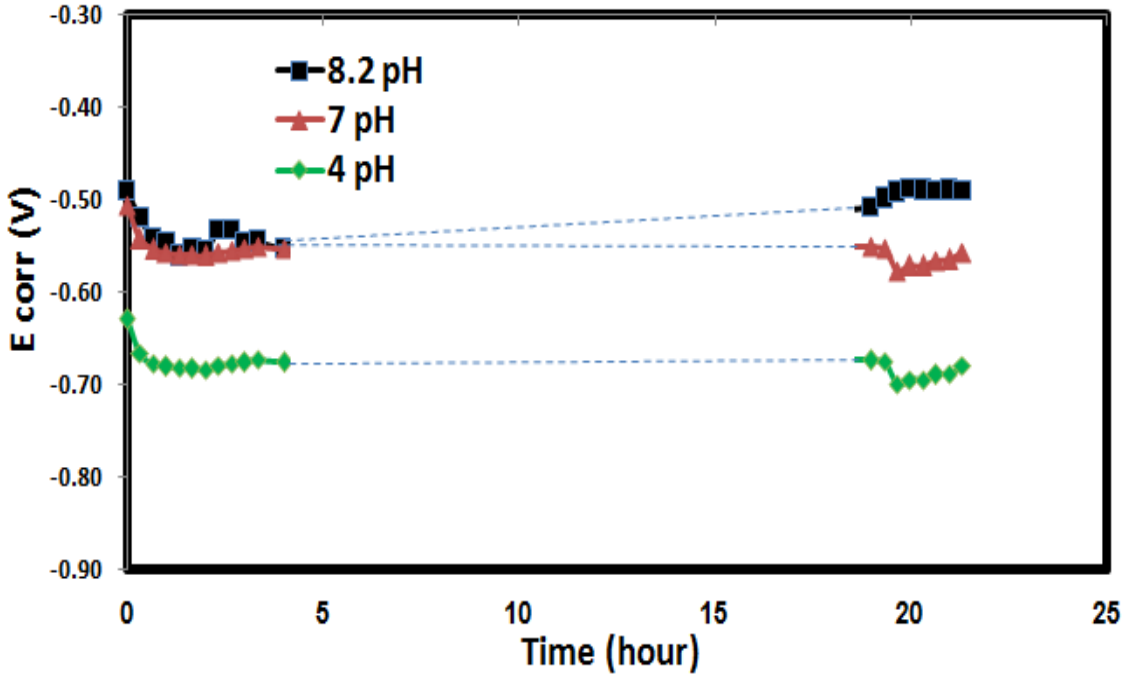

Figure 4-7 d: Effect of solution pH on the corrosion potential (E_{corr}) 1018 CS in sea water obtained by (LPR) Method at 10 ppm inhibitor concentration, 55^{o}C and 1000 rpm.

4.1.6 Potentiodynamic Polarization

The potentiodynamic polarization curves are shown in Figure 4-8 where the corrosion potential (E_{corr}) has shifted to more positive value with increasing the concentration of the inhibitor, which indicates that the anodic process of CS is inhibited by AR505 (Figure 4-8a). The relation between current density and potential in the experimental data was fitted using the Butler-Volmer Equation (BVE) to obtain the anodic (α_a) and cathodic (α_c = 1- α_a) transfer coefficients and hence to estimate the value of both anodic and cathodic current densities according to Equation 9:

$$i = i_o[e^{\alpha_a F\eta/RT} - e^{(1-\alpha_a)F\eta/RT}] \quad (9)$$

Where i is the net current density of the electrode, i_o is the exchange current which equals to the anodic current at equilibrium, and η is the over potential which equals to the difference between the equilibrium and the applied potentials. Table 4-4 shows the values of the transfer coefficients, corrosion currents and corrosion potentials for these polarization data. It is cleared that the anodic transfer coefficients are generally greater than 0.5 and hence the contribution of the anodic current is in the average of 80% of the total corrosion current. This anodic current is attributed to the dissolution of the metal surface where a charge transfer reaction at the surface of the CS take place leading to mass transport of the metal ions into bulk solution. Increasing the concentration of CI has decreased the anodic corrosion current and increased the corrosion potential which results in increase in the polarization resistance at the surface. Therefore, the

corrosion rate has decreased. On the other hand, the contribution of the cathodic current is due to the deposition of hydrated iron oxide and oxygen and hydrogen reduction at the surface especially at lower potential.

Corrosion of CS has noticeably been affected by both solution temperature and pH (Figures 4-8b and 4-8d). The current density has increased with increasing temperature which suggests a higher corrosion rate at 55°C. With increasing the temperature from 25 to 55°C the corrosion potential decreased from -286 mV to -501mV while the corrosion current is increased from 63.1 to 251 $\mu A/cm^2$. The anodic transfer coefficient has also increased from 0.68 to 0.82. Increasing the temperature will increase the rate of electrochemical reaction and thus the corrosion rate [43, 45]. Similarly, the decrease in solution pH from 8.2 to 4 resulted in a decrease of potential from -501 to -638 mV and increase in the total current and anodic transfer coefficient from 251 to 1260 $\mu A/cm^2$ and 0.82 to 0.92, respectively. This is due to the increasing of hydrogen ions in the solution which is adsorbed to the CS surface and reduced to the hydrogen gas [43]. Figure 4-8c shows the polarization curves for the effect of stirring speed on corrosion parameters. As the stirring speed increases from 0 to 500 rpm the potential decreased from -328 to -498 mV and the total current is increased from 97.7 to 280 $\mu A/cm^2$. However, further increase in mixing speed has little effect on corrosion. Increasing the mixing speed will decrease the external mass transfer resistance for the electrolytes to reach the CS surface where this resistance will become negligible at higher agitation speed of the solution [52].

TABLE 4-4. POLARIZATION KINETIC PARAMETERS FOR CORROSION OF 1018 CS IN SEA WATER SOLUTION.

Parameter	value	E_{corr} (mV)	i_{corr} (A/cm^2)	Transfer coefficients		BVE slopes		R_p
				α_a	α_c	β_a (mV/decade)	β_c (mV/decade)	
Concentration (ppm)	0	-520	4.46E-04	0.87	0.13	32.5	217.4	2.76E+04
	5	-510	3.16E-04	0.84	0.16	33.7	173	3.88E+04
	10	-501	2.51E-04	0.82	0.18	34.6	156	4.91E+04
	15	-475	2.51E-04	0.83	0.17	34.0	168	4.90E+04
Temperature (^oC)	25	-286	6.31E-05	0.68	0.32	36.4	87.4	1.77E+05
	40	-446	2.00E-04	0.79	0.21	34.1	129	5.86E+04
	55	-501	2.51E-04	0.82	0.18	34.6	156	4.91E+04
pH	4	-638	1.26E-03	0.92	0.08	30.8	341	9.75E+03
	7	-545	6.31E-04	0.91	0.09	31.1	314	1.95E+04
	8.2	-501	2.51E-04	0.82	0.18	34.6	156	4.91E+04
Speed (rpm)	0	-328	9.77E-05	0.56	0.44	50.5	64.2	1.26E+05
	500	-498	2.80E-04	0.85	0.16	33.5	182	4.39E+04
	1000	-501	2.51E-04	0.82	0.18	34.6	156	4.91E+04

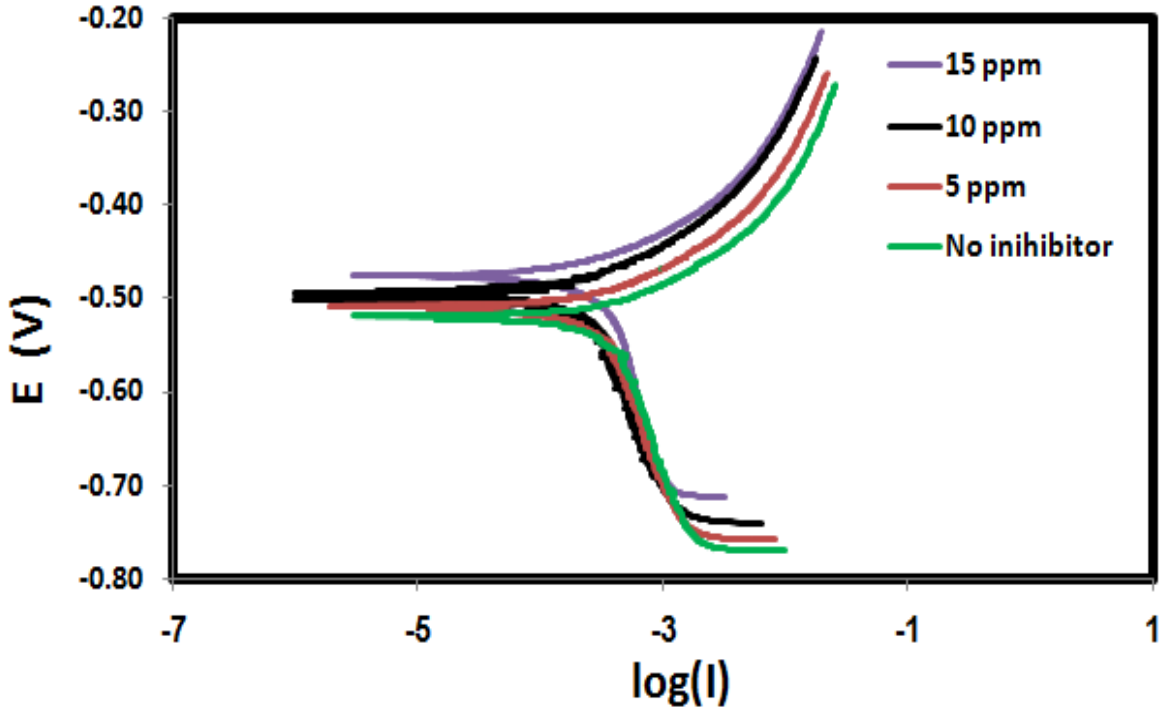

Figure 4-8 a: Effect of inhibitor concentration based on Potentiodynamic polarization curves of 1018 CS in seawater at 55^{o}C, 1000 rpm, and pH 8.2.

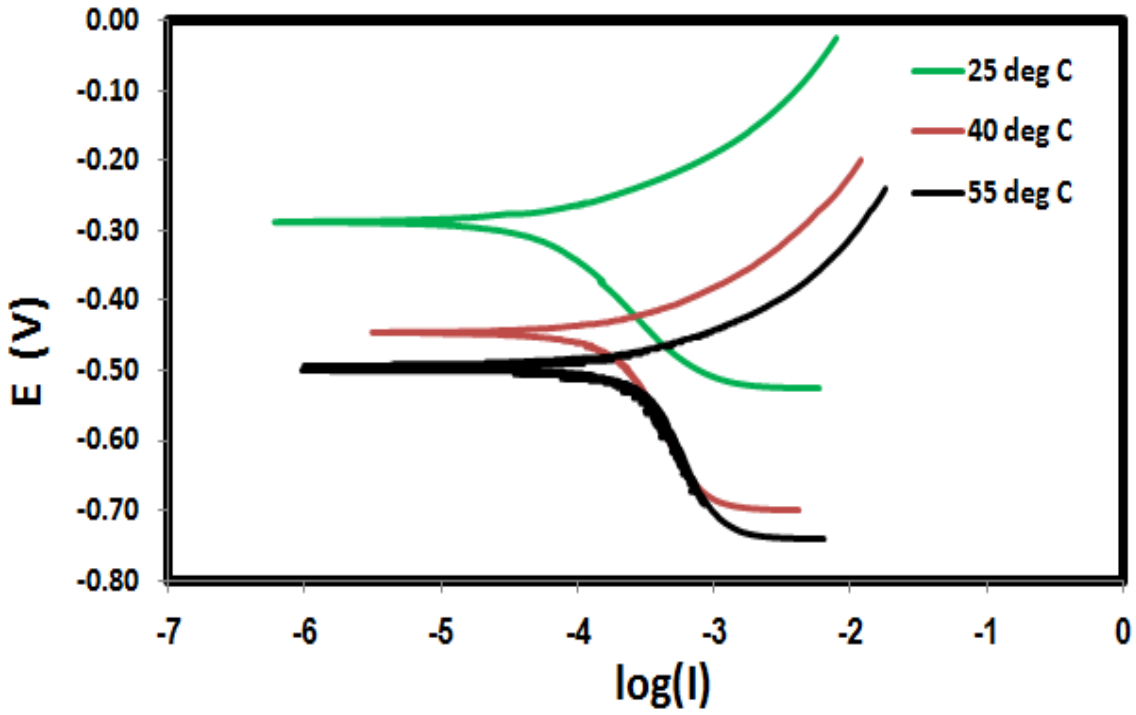

Figure 4-8 b: Effect of solution temperature based on polarization curves of 1018 CS in seawater at 1000 rpm, 10 ppm inhibitor concentration and pH 8.2.

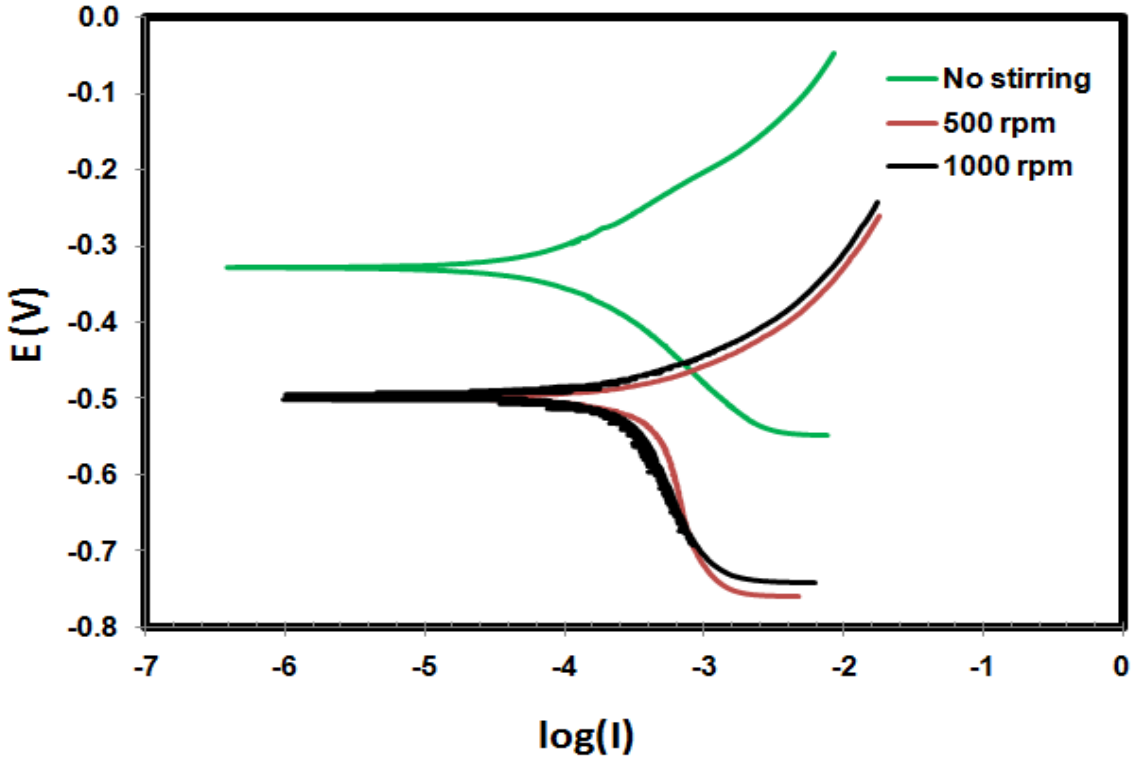

Figure 4-8 c: Effect of mixing speed based on Potentiodynamic polarization curves of 1018 CS in seawater at 55^{o}C, 10 ppm inhibitor concentration and pH 8.2.

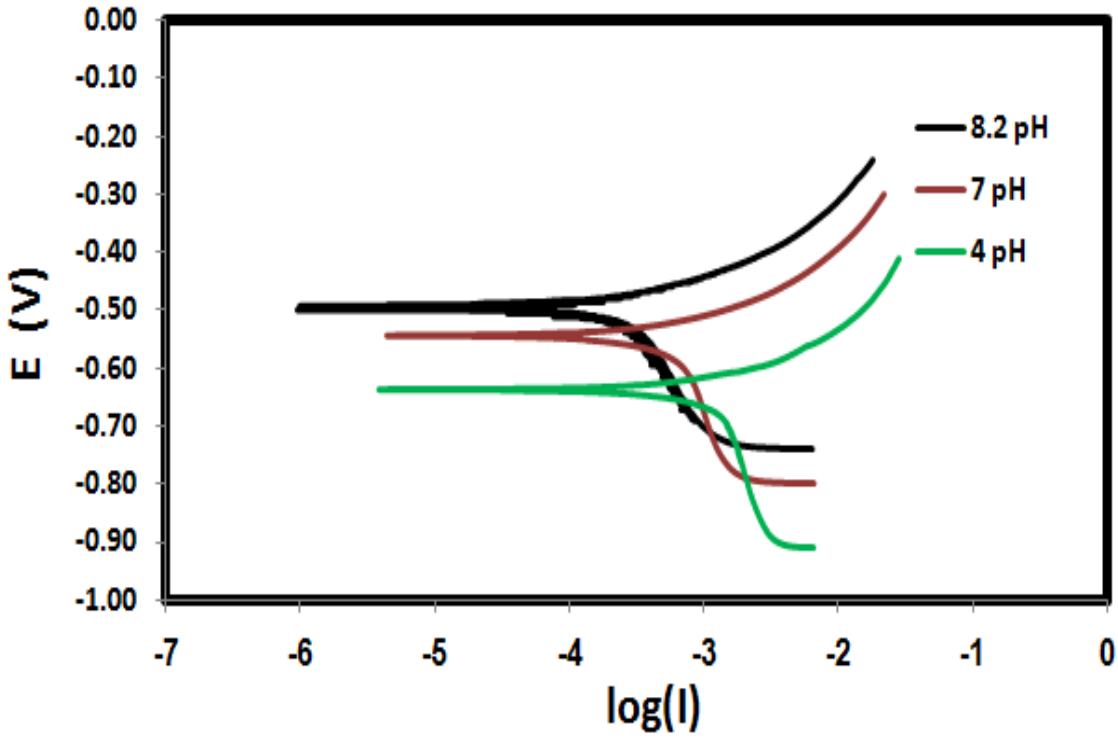

Figure 4-8 d: Effect of solution pH based on Potentiodynamic polarization curves of 1018 CS in seawater based on at 10 ppm inhibitor concentration, 55 ^{o}C and 1000 rpm.

4.1.7 Activation energy calculation

The apparent activation energy (E_a) for the corrosion of 1018 CS in the presence of corrosion inhibitor was calculated from the Arrhenius equation (Equation 10).

$$k = A_f e^{-E_a / RT} \qquad (10)$$

Where k is the rate of metal dissolution, A_f is the frequency factor, R is the ideal gas constant (J/mole.K), and T is the temperature ($^{\circ}$K). A plot of ln (k) versus 1/T yields a straight line with a slope of -1060.7 K and hence the activation energy is $8.818 \frac{KJ}{mole}$ as shown in Figure 4-9. Abdullah et al. (2006) showed similar results for C-steel in presence and absence of different concentrations of Aminopyrimidine derivatives inhibitor in 0.05M HNO_3, where the activation energy was varied from 8.63 to $12.04 \frac{KJ}{mole}$ when inhibitor concentration was varied from 0 to 15 ppm, respectively [18].

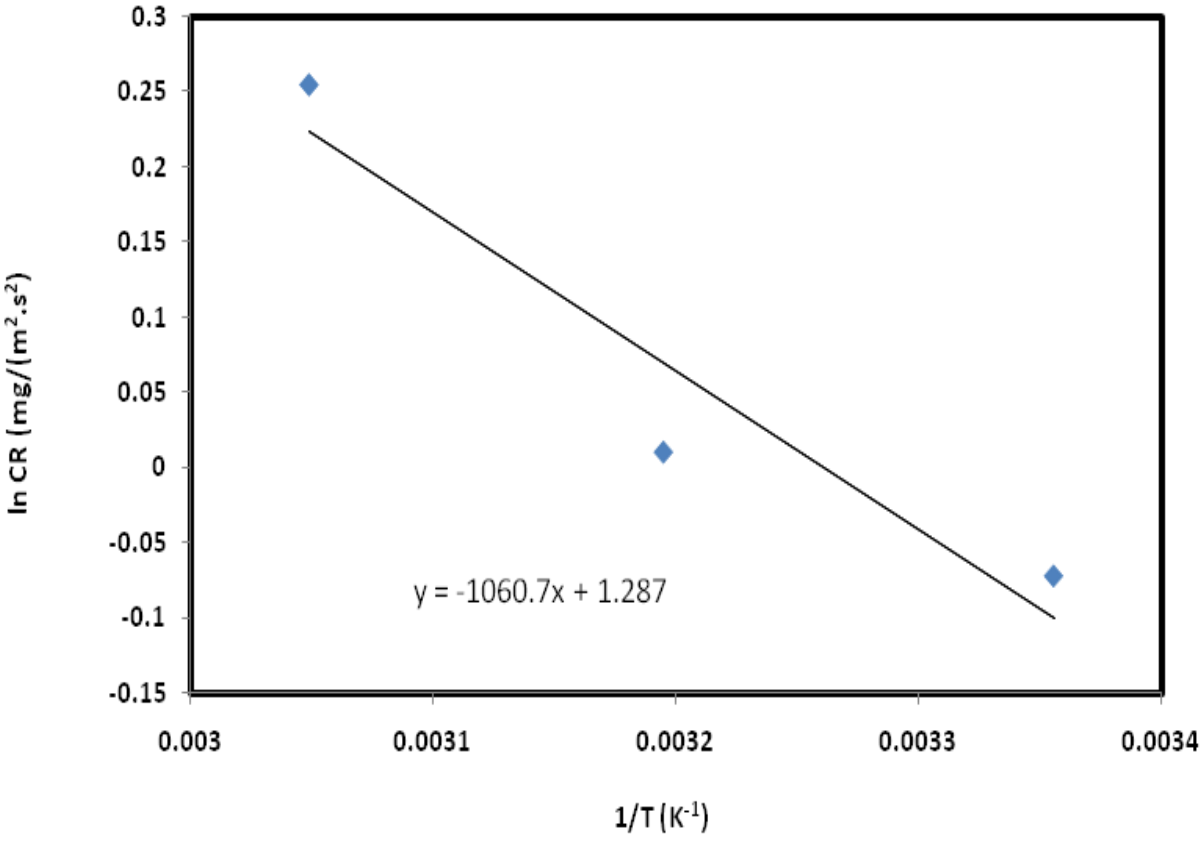

Figure 4-9: Log corrosion rate vs. 1/T for 1018 CS in the presence of AR505 CI.

4.2 N-211 Amine based Inhibitor

An amine-based corrosion inhibitor (**NORUST** N-211) was used in this work. It is manufactured by CECA ARKEMA Group in France and was one of the inhibitors that were used in Saudi Aramco. It belongs to Alkyl amines family. It is a water soluble corrosion inhibitor with specific gravity of 1.1 at 15.5^{o}C.

Kinetic experiments were conducted to study the effect of inhibitor concentration (5, 10, and 15 ppm), solution temperature (25, 40, and 55^{o}C), agitation speed (0, 500, and 1000 rpm), and solution pH (4, 7, and 8.2) on the rate of corrosion of the 1018 CS specimens and compare results with results in the absence of inhibitor. Thus the inhibition efficiency of N-211 was investigated at different electrochemical techniques using weight loss, polarization resistance and potentiodynamic polarization methods.

4.2.1 Fourier Transform Infrared Spectroscopy (FTIR)

Fourier Transform Infrared Spectroscopy (FTIR) for this compound is illustrated in Figure 4-10. It has five major peaks at 1248, 1456, 1636, 2078.7 and 3448 cm^{-1} which related to N $-NO_2$, N $-N=O$, C $=N-$, $-N=C=S$ and $-NH_2$ functional groups, respectively. Other peaks for alkenes, and hydroxyl groups appeared at 698, 1376, 2923 and 2963 cm^{-1}. These amines are generally chemisorbed at the metal surface and displace the adsorbed water and electrolytes from the surface. It is assumed these N-containing functional groups act as electron pair donors to electron-depleted dehydrated metal surface.

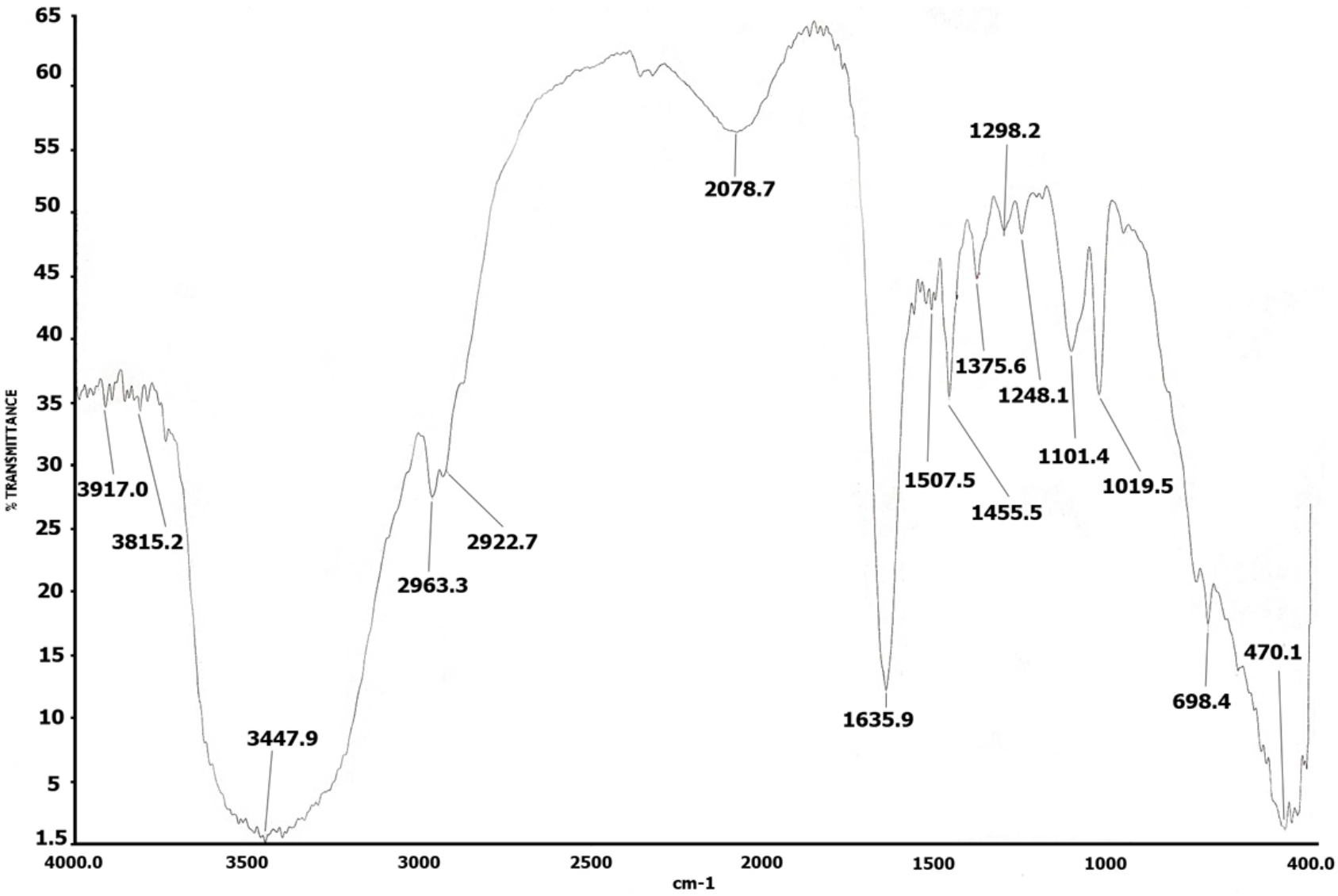

Figure 4-10. FTIR Spectrum for N-211 corrisob inhbitor

4.2.2 Surface Analysis

The SEM of the corroded CS1018 surfaces after exposure to salt solution for 48hours in the presence and absence of N-211 are shown in Figure 4-11. Image 4-11a shows the corrosion layer on the specimen in the presence of N-211 where part of the surface was polished by sand paper. It is cleared that the corroded surface is very porous which could be attributed to corrosion product of γ-FeOOH [55, 56]. Moreover, the corrosion of specimens is distributed over the whole surface area with uniform appearanc. It was illustrated by EDS analysis that the surface was mostly of composed oxides of iron and magnesium with trace amounts of S, Ca, Cr and Si as shown in Figure 4-12 and Table 4-5. The percentage of oxygen to iron on the surface of the specimen in the presence and absence of corrosion inhibitor are 38.1% and 24.3%, respectively. The higher oxygen content at the surface that was exposed to the CI is attributed to the formation of the oxides of Mg, Ca, Cr and Si which prevented part of the surface from corroding.

(a)

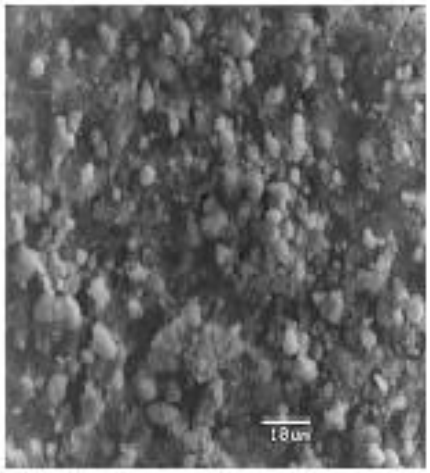

(b)

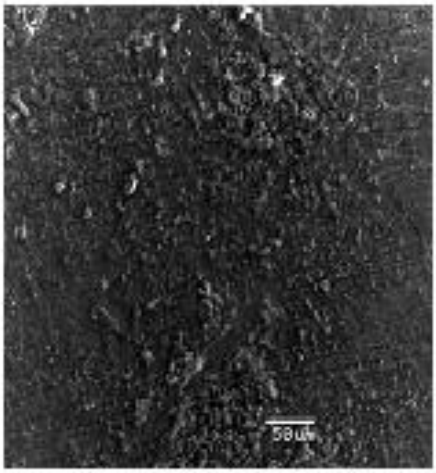

(c)

Figure 4-11. SEMmicrograph taken on the surface of a specimen exposed to Sea salt; (a,b) mixed with 10 ppm N-211 , and (c) without corrosion inhibitor

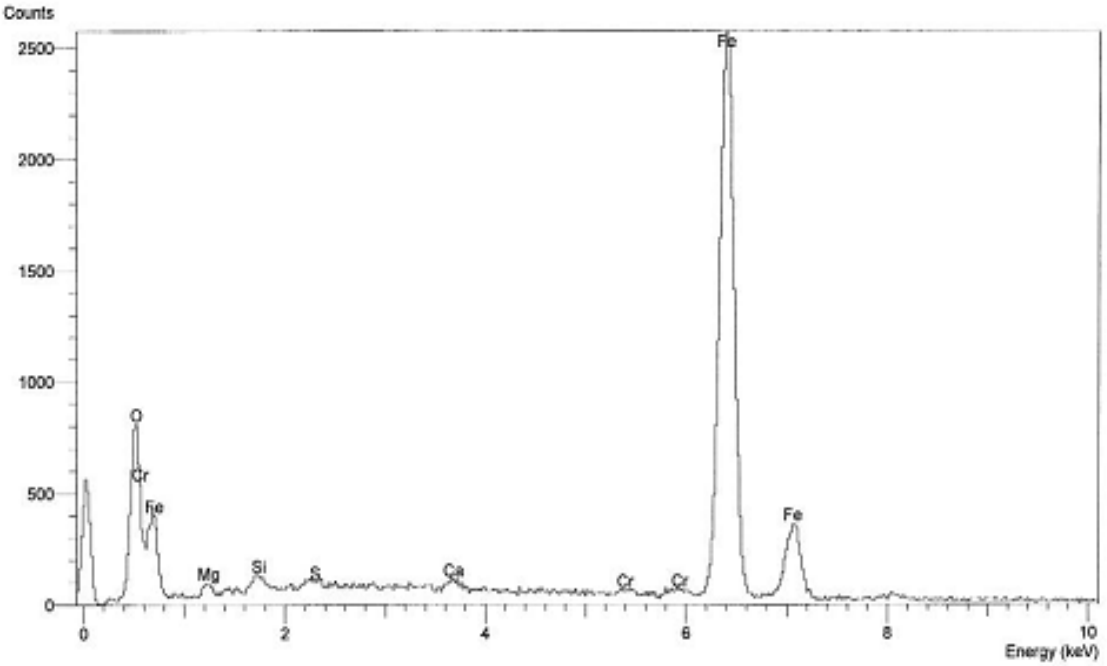

(a)

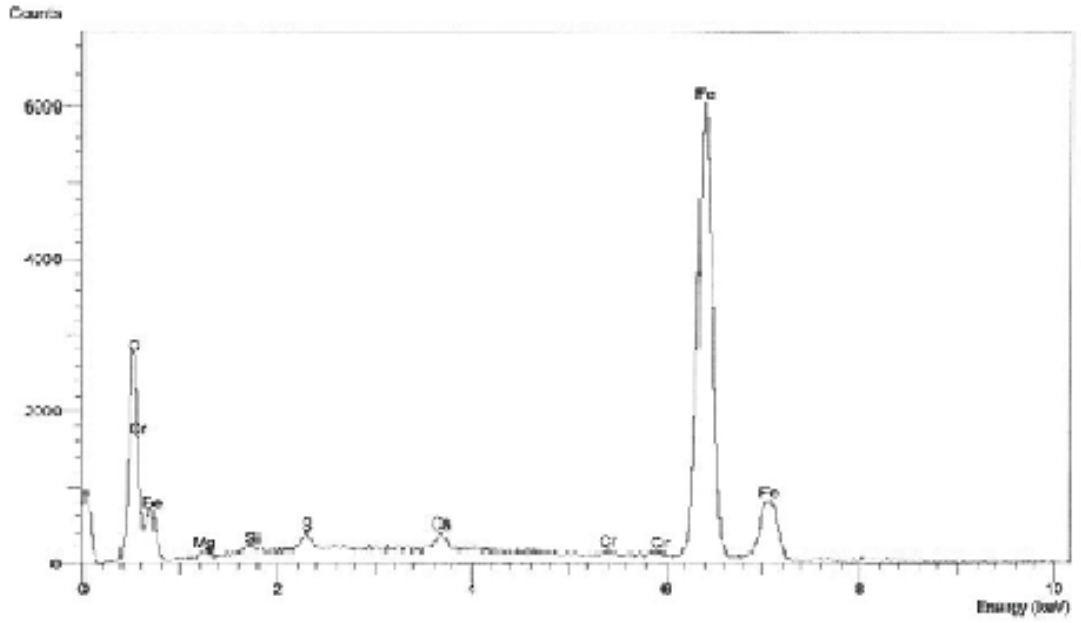

(b)

Figure 4-12: Energy dispersive X-ray analysis of corroded CS1018 specimen; (a) in the absence, and (b) presence of corrosion inhibitor

TABLE 4-5. EDS ELEMENTAL ANALYSIS OF CORRODED CS1018 SPECIMEN; (A) IN THE ABSENCE, AND (B) PRESENCE OF CORROSION INHIBITOR.

Element	**Elemental Percentage in the Absence of N-211 CI (%)**	**Elemental Percentage in the presence of N-211 (%)**
O	17.31	25.29
Mg	9.48	6.32
Si	0.77	0.29
S	0.20	0.72
Ca	0.50	0.87
Cr	0.42	0.29
Fe	71.30	66.22
Total	100.00	100.00

4.2.3 Weight Loss Studies

The weight loss, in term of corrosion rate (CR) of the carbon steel specimen in salt water solution as a function of corrosion inhibitor concentration is shown in Figure 4-13 and Table 4-6. As can be observed, the corrosion rate is decreased with increasing inhibitor concentration. For the sample that immersed in inhibitor-free solution the CR was 2.47 *mm/y* while this value decreased to 1.22 *mm/y* when 5 ppm of inhibitor was added to the solution. Extra addition of the inhibitor has significant CR where 0.52 *mm/y* was achieved when the inhibitor concentration was 15 ppm. Also it can be noticed that CR is decreased with increasing solution pH with a value from 2.88 *mm/y* at pH 4 to 1.08 *mm/y* at pH 8.2. On the other hand, increasing both solution temperature and mixing speed have increased the corrosion rate to a value of 1.08 *mm/y* at 55 ^{o}C and 1000 rpm.

It is obvious that an increase in inhibition efficiency (IE) from 50.6% to 78.9% when the inhibitor concentration was increased from 5 to 15 ppm. The highest IE was achieved when the solution was stagnant and inhibited by 10 ppm CI, while the lowest value obtained at pH 4 and mixing speed of 1000 rpm.

TABLE 4-6. CORROSION RATE AND INHIBITION EFFICIENCY FOR 1018 CS AT DIFFERENT KINETIC CONDITIONS

Effect of Parameter	Inhibitor Concentration (ppm)	Speed rpm	Temperature (^{o}C)	pH	CR (mm/y)	Inhibition Efficiency (%)
Inhibitor Concentration	0	1000	55	8.2	2.47	0.00
	5	1000	55	8.2	1.22	50.6
	10	1000	55	8.2	1.08	64.1
	15	1000	55	8.2	0.52	78.9
Temperature	10	1000	25	8.2	0.68	72.5
	10	1000	40	8.2	0.86	65.2
	10	1000	55	8.2	1.08	50.6
pH	10	1000	55	4	2.88	-
	10	1000	55	7	1.43	42.1
	10	1000	55	8.2	1.08	50.6
Speed	10	0	55	8.2	0.16	93.5
	10	500	55	8.2	0.73	70.5
	10	1000	55	8.2	1.08	50.6

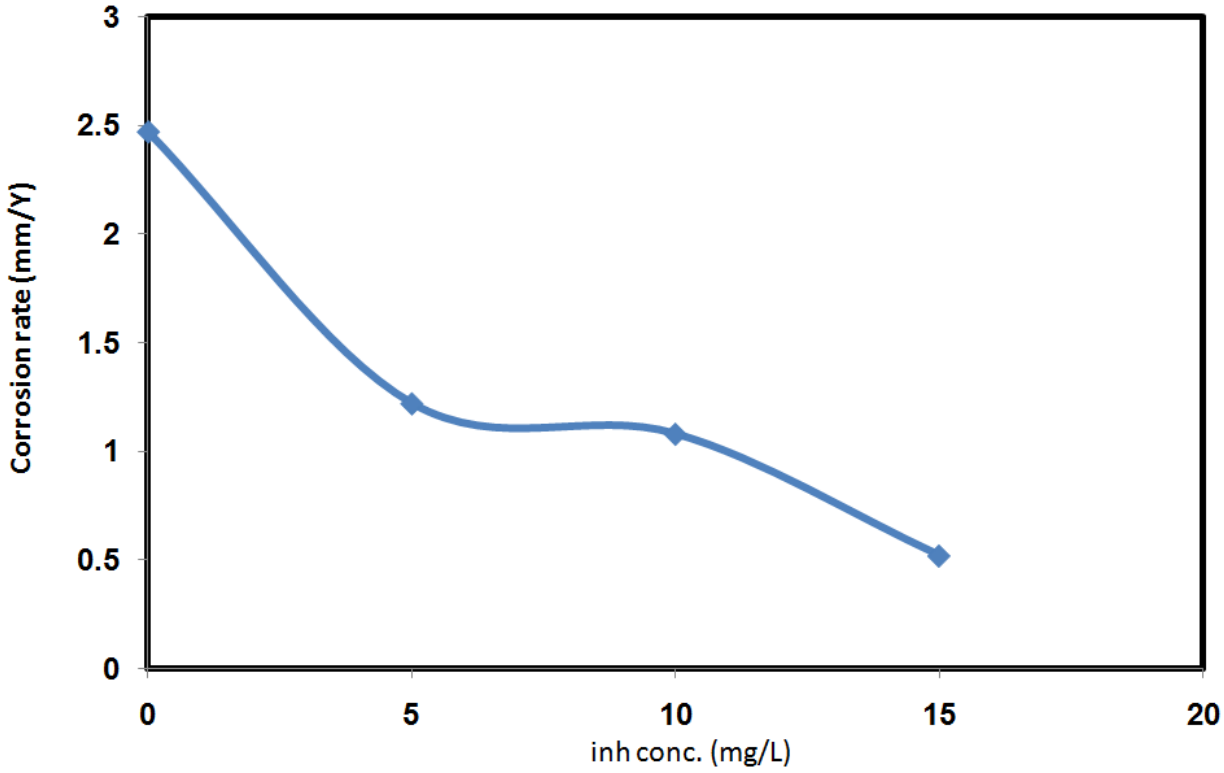

Figure 4-13 a: Effect of inhibitor concentration on the corrosion rate of 1018 CS in sea water obtained by weight loss method at 55^{o}C, 1000 rpm, and pH 8.2.

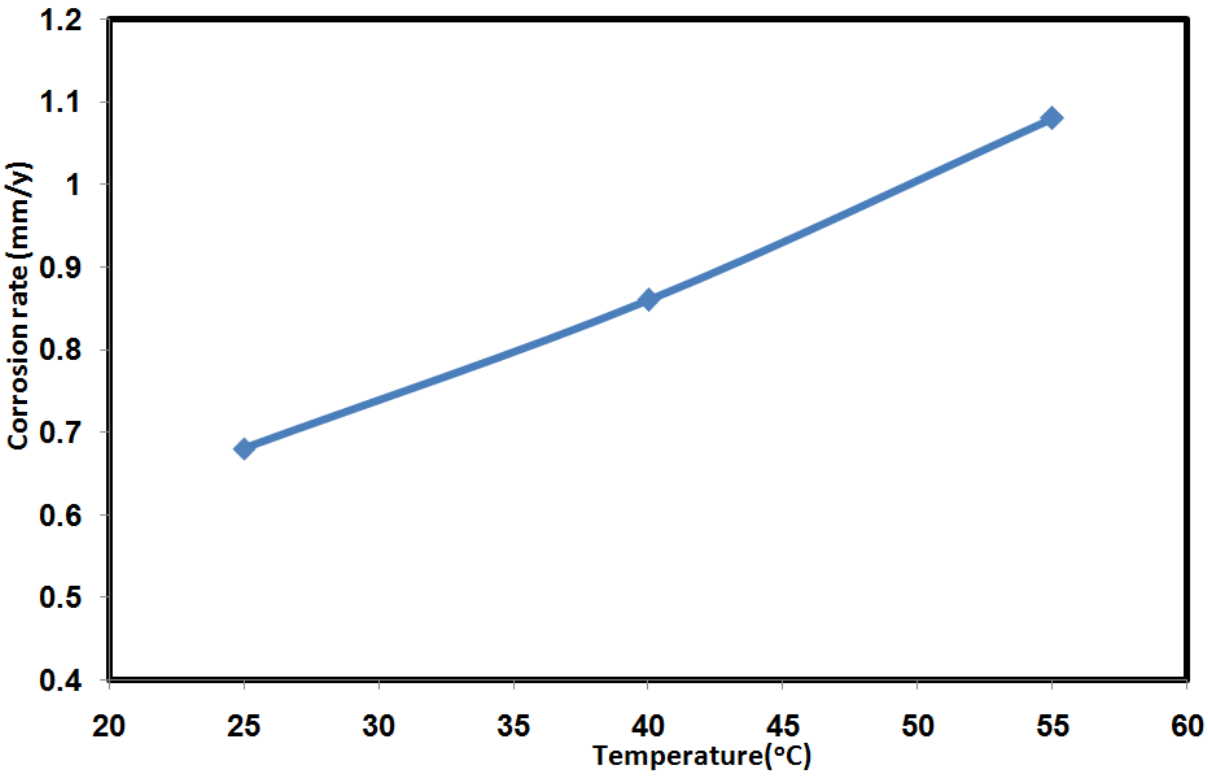

Figure 4-13 b: Effect of solution temperature on the corrosion rate of 1018 CS in sea water obtained by weight loss method at 1000 rpm, 10 ppm inhibitor concentration and pH 8.2.

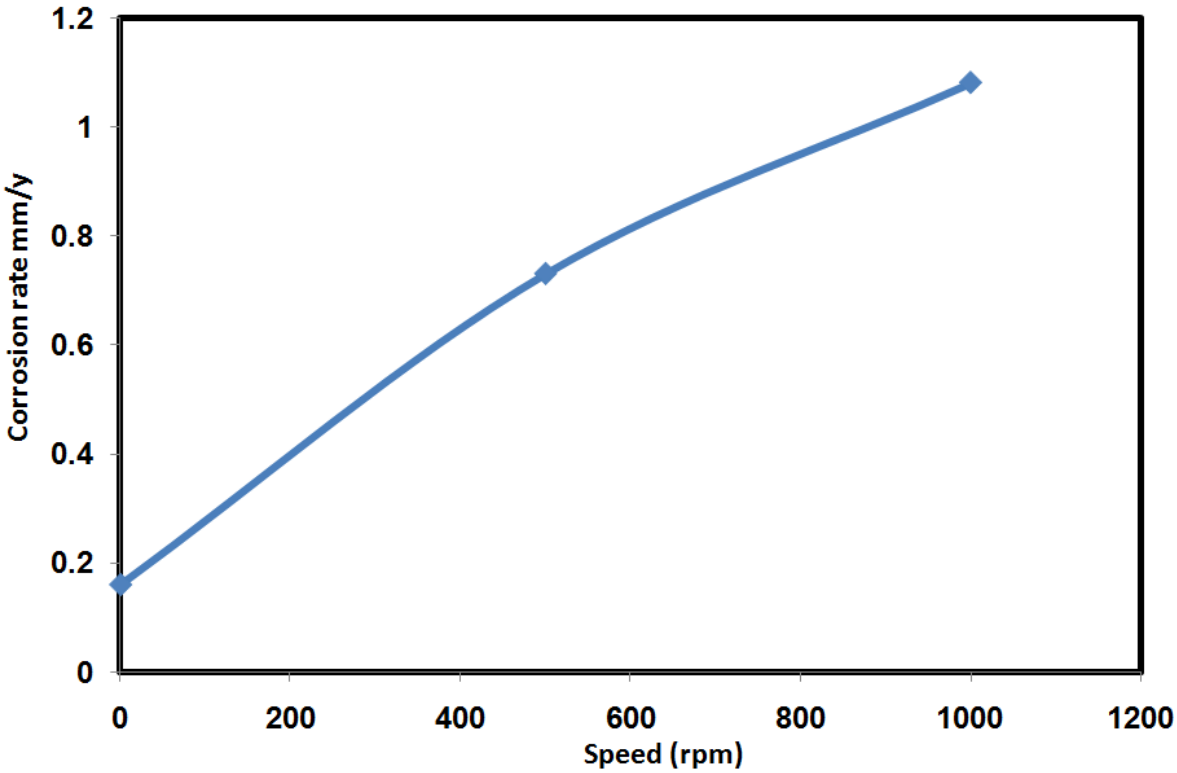

Figure 4-13 c: Effect of mixing speed on the corrosion rate of 1018 CS in sea water obtained by weight loss method at 55^{o}C, 10 ppm inhibitor concentration and pH 8.2.

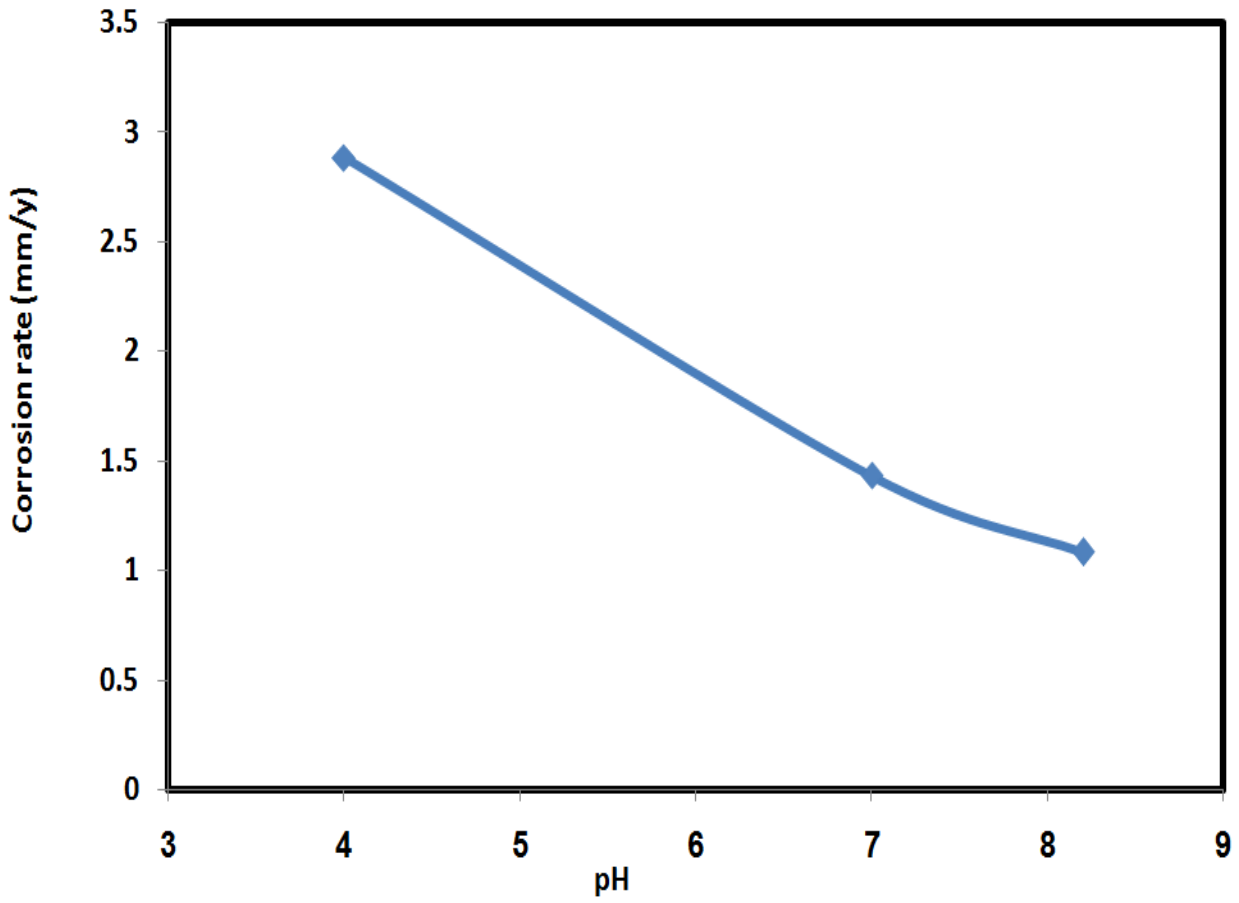

Figure 4-13 d: Effect of solution pH on the corrosion rate of 1018 CS in sea water obtained by weight loss method at 10 ppm inhibitor concentration, 55^{o}C and 1000 rpm.

4.2.4 Adsorption Isotherm Analysis

Therefore, the adsorption equilibrium for N-211 by CS surface was investigated at 55^{o}C, 1000 rpm, and the pH was adjusted to 8.2. The degree of surface coverage by the inhibitor, θ_m can be related to weight loss in the absence and presence of corrosion inhibitor, m_{free} and $m_{inh.}$, respectively as:

$$\theta_m = \frac{m_{free} - m_{inh}}{m_{free}} \tag{6}$$

The values of θ_m corresponding to the inhibitor concentration were plotted in Figure 4-14 and fitted to the isotherm models of equations 7 &8:

Langmuir model [53] $$\theta_m = \frac{\theta_{max} bCe}{1 + bCe} \tag{7}$$

Shawabkeh-Tutunji relation [54] $$\theta_m = q_o(1 - \alpha Ce^{\beta}) \tag{8}$$

Where θ_{max} is the maximum adsorption capacity could be reached by the inhibitor-surface system, Ce is the equilibrium concentration of the inhibitor in solution, and q_0, α, β and b are constants and presented in Table 4-7. It can be seen that Shawabkeh-Tutunji correlation best fits the experimental data with regression coefficient of 0.9987 which is applied for chemisorption adsorbent-adsorbate system; however, Langmuir model predicts the physical adsorption isotherm with regression coefficient of 0.9952. The maximum adsorption capacity that covers monolayer of inhibitor by the CS 1018 surface is estimated using Langmuir model as 1.0771 mg N-211.

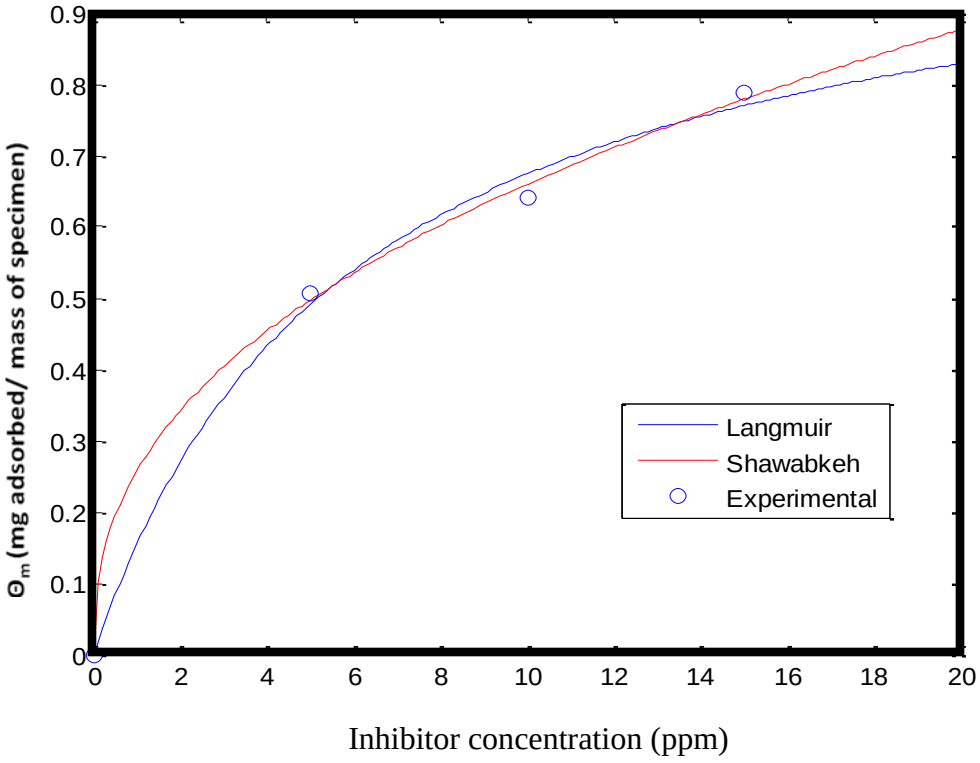

Figure 4-14. Adsorption isotherm of N-211 using 1018 CS at 55^{o}C, 1000 rpm, and pH 8.2.

TABLE 4-7. ADSORPTION ISOTHERM PARAMETERS

Model	Parameter	Value	R^2
Langmuir	maxθ (mg/g)	1.0771	0.9952
	b	0.1672	
Shawabkeh-Tutunji	q_0	0.0037	0.9987
	α	-69.6975	
	β	0.41	

4.2.5 Linear Polarization Resistance (LPR) Method

The corrosion rates versus time at different experimental conditions are shown in Figures 4-15. Figure 4-15a shows the effect of different CI concentrations on the corrosion rate. It is apparent that the increase in CI concentration has decreased the corrosion rate. A rapid decrease in corrosion rate was achieved within the first hour of conducting the experiments. However, it is shown that the increase in CI has little effect on percentage of inhibition which is related to the formation of a protective oxide film. However, it is also concluded that a 10 ppm CI could be assumed as an optimum concentration to inhibit the surface. At 10 ppm CI the corrosion rate was further studied by varying the solution temperature (Figure 4-15b). The solution temperature has a noticeable effect on the corrosion rate where a value of 0.52 mm/y was achieved at 55 ^{o}C within 4h compared to 0.32 mm/y obtained at 25 ^{o}C within the same period of time. As expected, the higher solution temperature yields a higher corrosion rate. This is due to the increase in desorption of the inhibitor with increasing temperature and hence increase the rate of electrochemical reactions and diffusion processes which stimulates corrosive attack. Effect of mixing speed is presented in Figure 4-15c. The corrosion rate has increased within 4 h from 0.14 mm/y for stagnant solution to 0.52 mm/y at mixing speed of 1000 rpm. Increasing mixing speed will reduce the thickness of the diffusion layer at the electrode surface and thus maintaining the concentration of the salt adjacent to surface is relatively equal to that in bulk of the solution [52]. The corrosion rate at 1000 rpm was severely affected by decreasing the solution pH (Figure 4-15d). It is expected that decreasing the solution pH will increase hydrogen ions in solution and the later becomes

more aggressive to attack the surface. At pH 4, a value of 2.22 mm/y was reached within 4 hours at this condition.

The studies of the corrosion potential (E_{corr}) versus time noticeably show up the capability to maintain the passivity of the 1018 CS at different experimental conditions as shown in Figures 4-16. Figure 4-16a shows that the E_{corr} became more positive as the inhibitor concentration increased. However, it can be seen from figure 4-16b that the decrease in temperatures assists the passivation the surface of iron and the adherence of the passive film is high. The passivity of the carbon steel was decreased as the rotating speed increased as illustrated in figure 4-16c. It is seen that, under the static condition, the E_{corr} shift to highest positive values. Apparently, an increase of rotating speed lead to accelerate the diffusion of oxygen, thus the oxide film will be removed. It is extrapolated from figure 4-16d that the corrosion potential decreases with increase in acidity and this is demonstrated that oxide film have a tendency to dissolve in the solution swiftly when it reached to pH4.

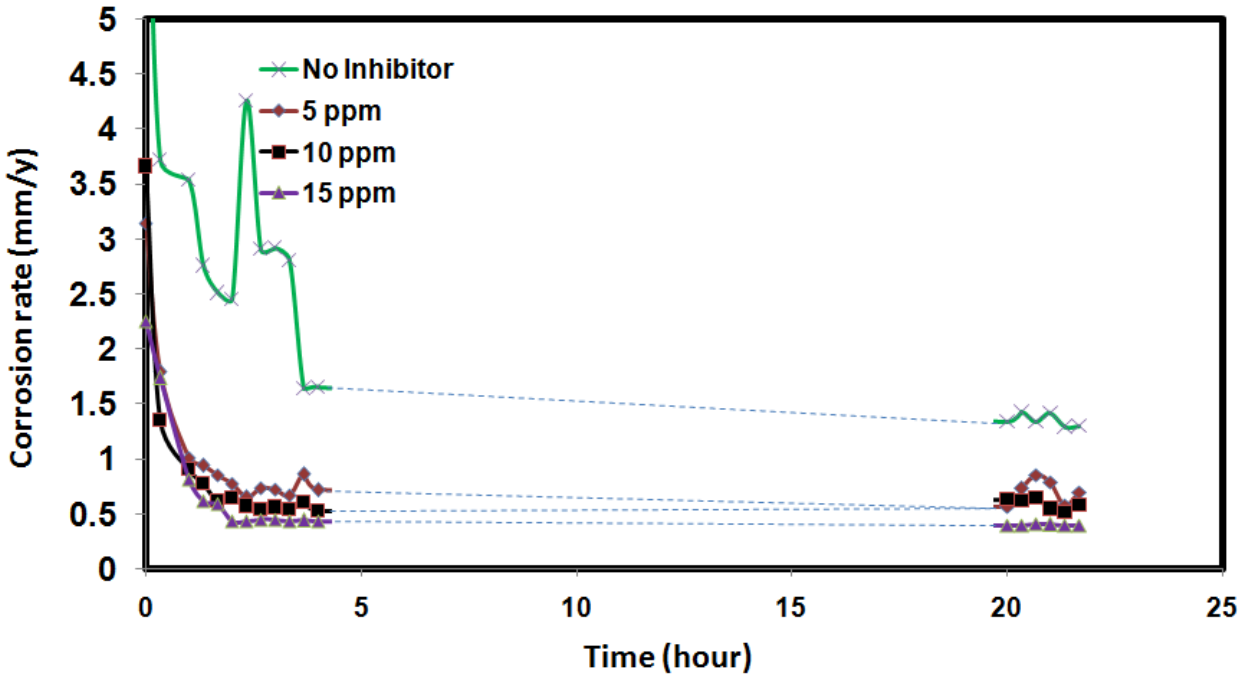

Figure 4-15 a: Effect of inhibitor concentration on the corrosion rate 1018 CS in sea water obtained by (LPR) Method at 55^{o}C, 1000 rpm, and pH 8.2.

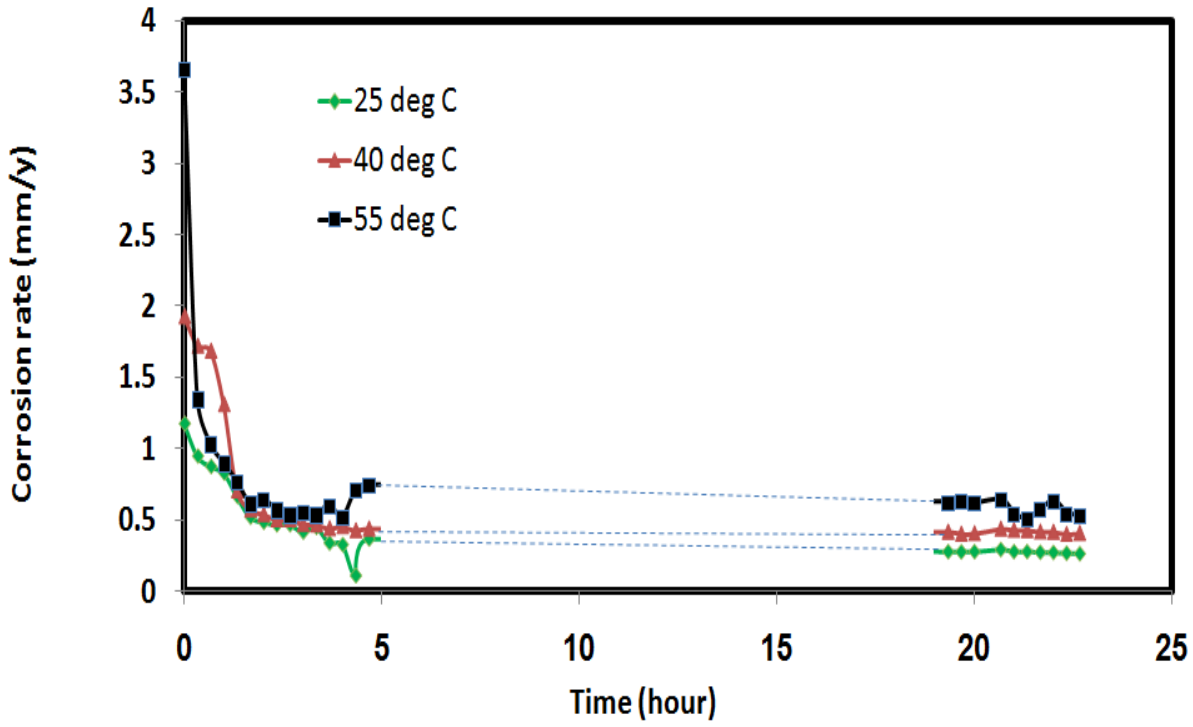

Figure 4-15 b: Effect of solution temperature on the Corrosion rate of 1018 CS in sea water obtained by (LPR) Method at 1000 rpm, 10 ppm inhibitor concentration and pH 8.2.

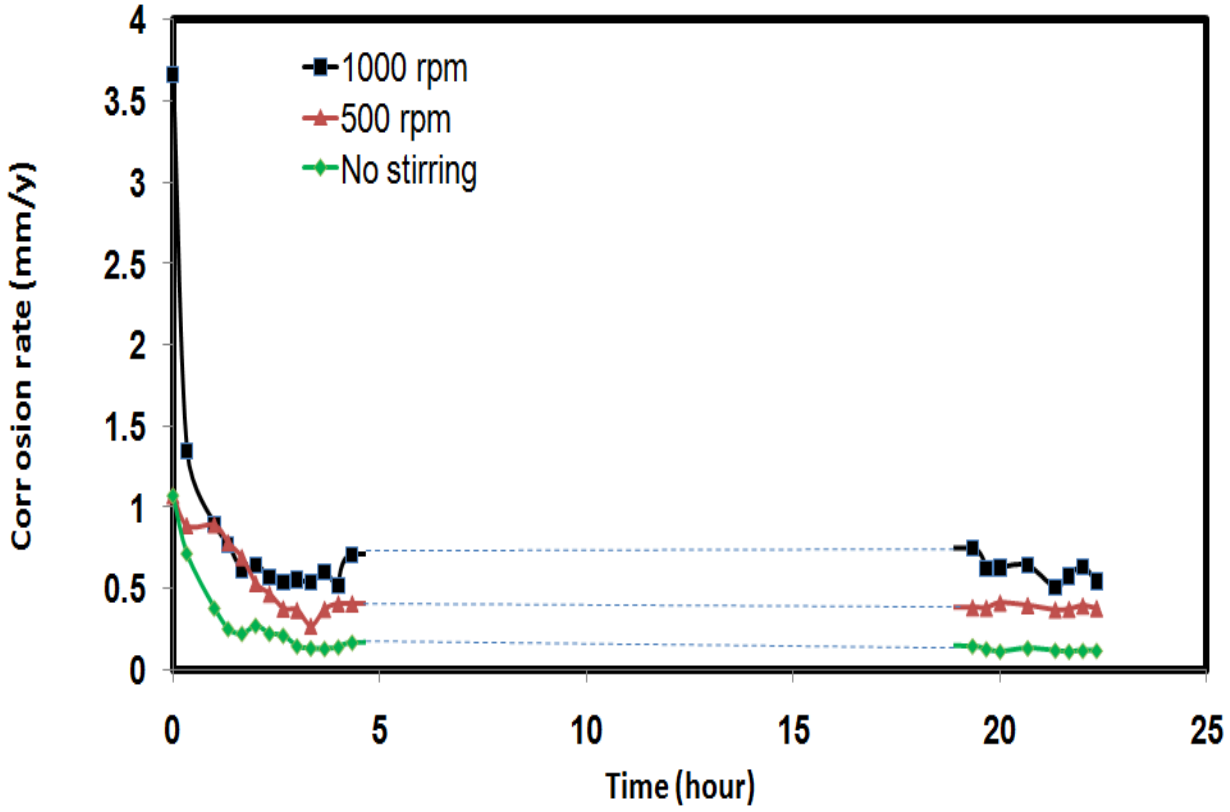

Figure 4-15 c: Effect of mixing speed on the corrosion rate 1018 CS in sea water obtained by (LPR) Method at 55^{o}C, 10 ppm inhibitor concentration and pH 8.2.

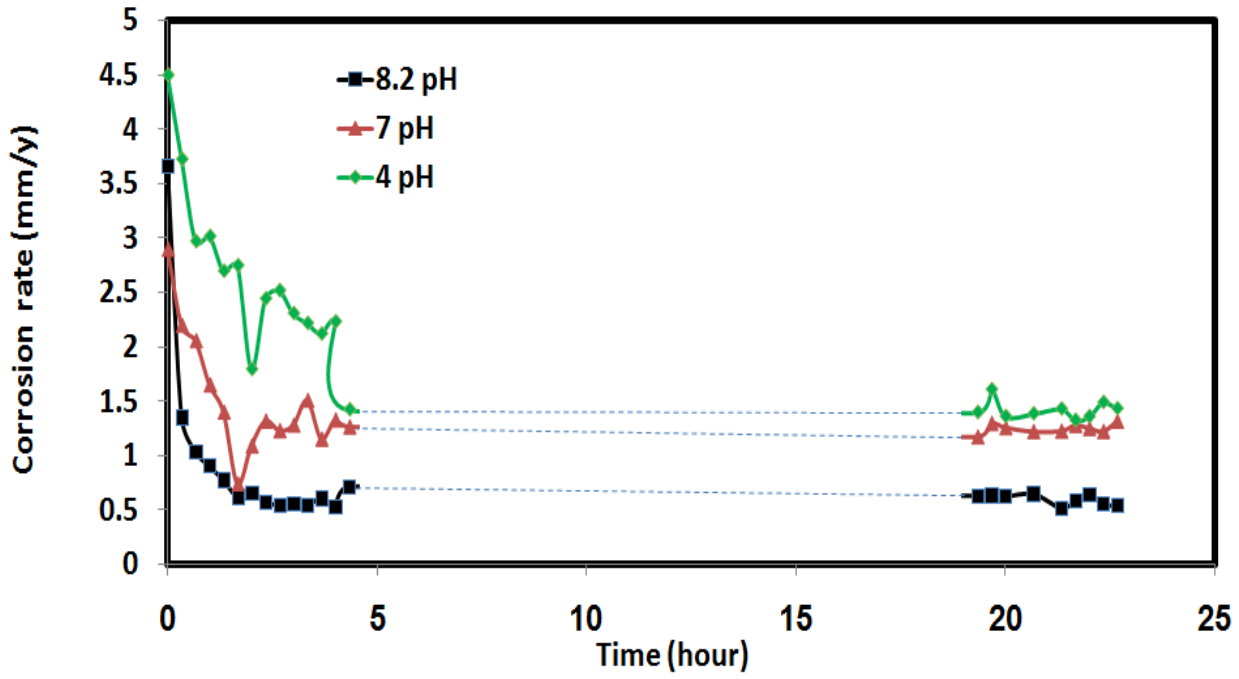

Figure 4-15 d: Effect of solution pH on the corrosion rate 1018 CS in sea water obtained by (LPR) Method at 10 ppm inhibitor concentration, 55^{o}C and 1000 rpm.

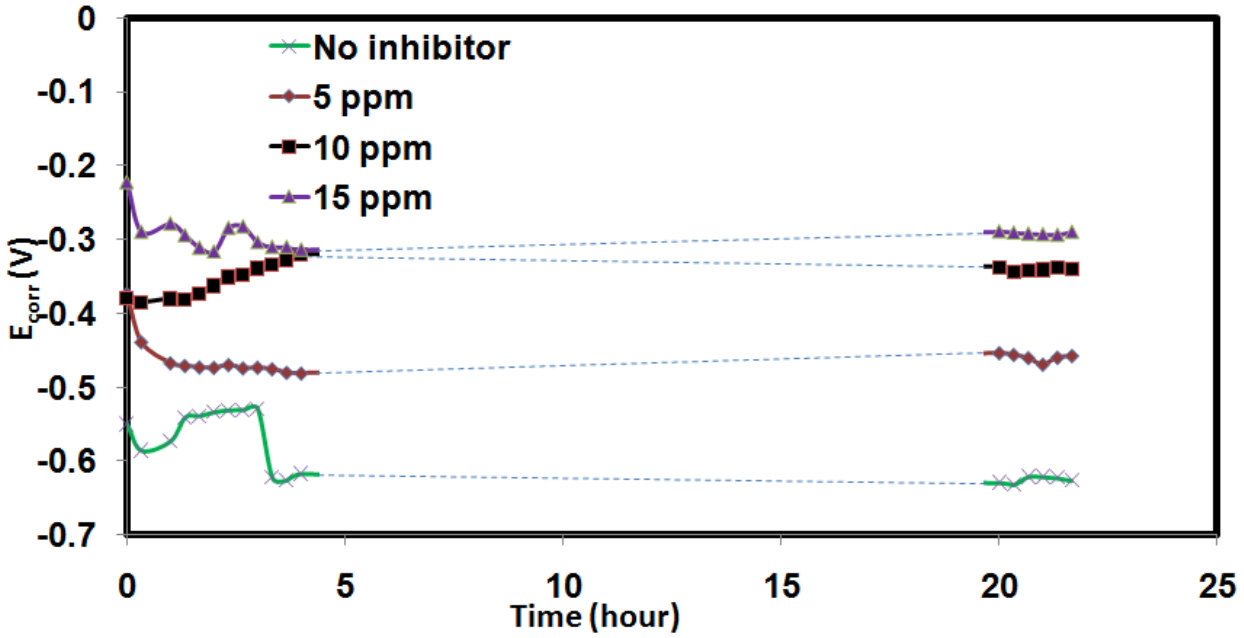

Figure 4-16 a: Effect of inhibitor concentration on the corrosion potential (E_{corr}) 1018 CS in sea water obtained by (LPR) Method at 55^{o}C, 1000 rpm, and pH 8.2.

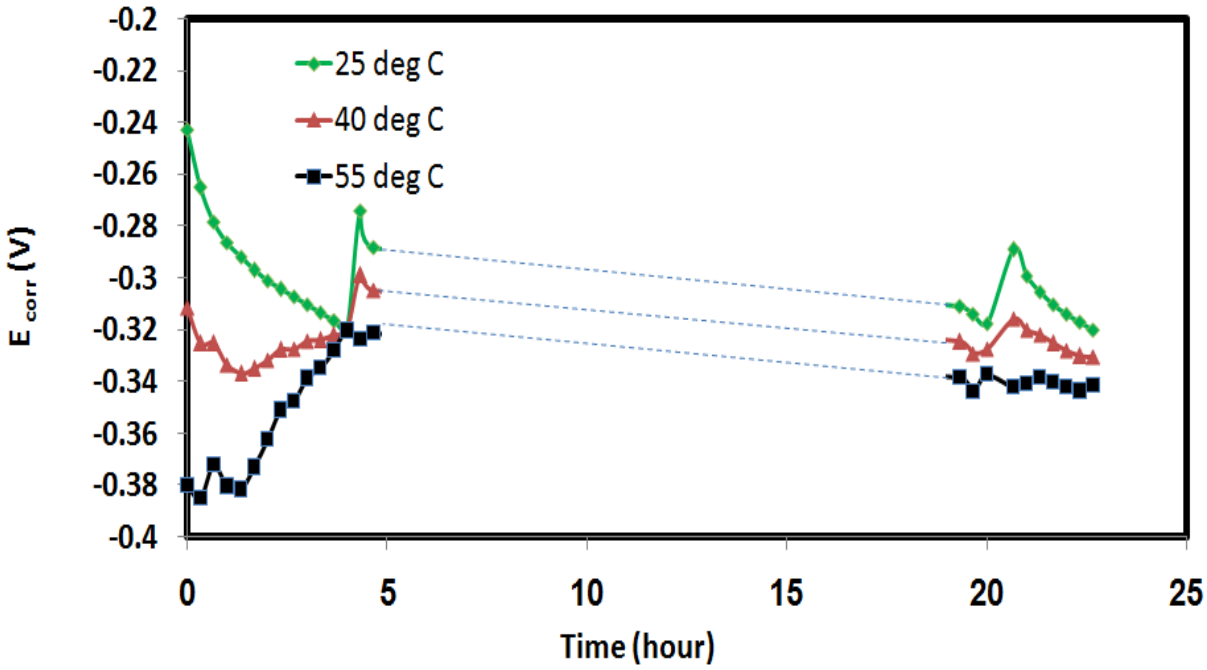

Figure 4-16 b: Effect of solution temperature on the corrosion potential (E_{corr}) of 1018 CS in sea water obtained by (LPR) Method at 1000 rpm, 10 ppm inhibitor concentration and pH 8.2.

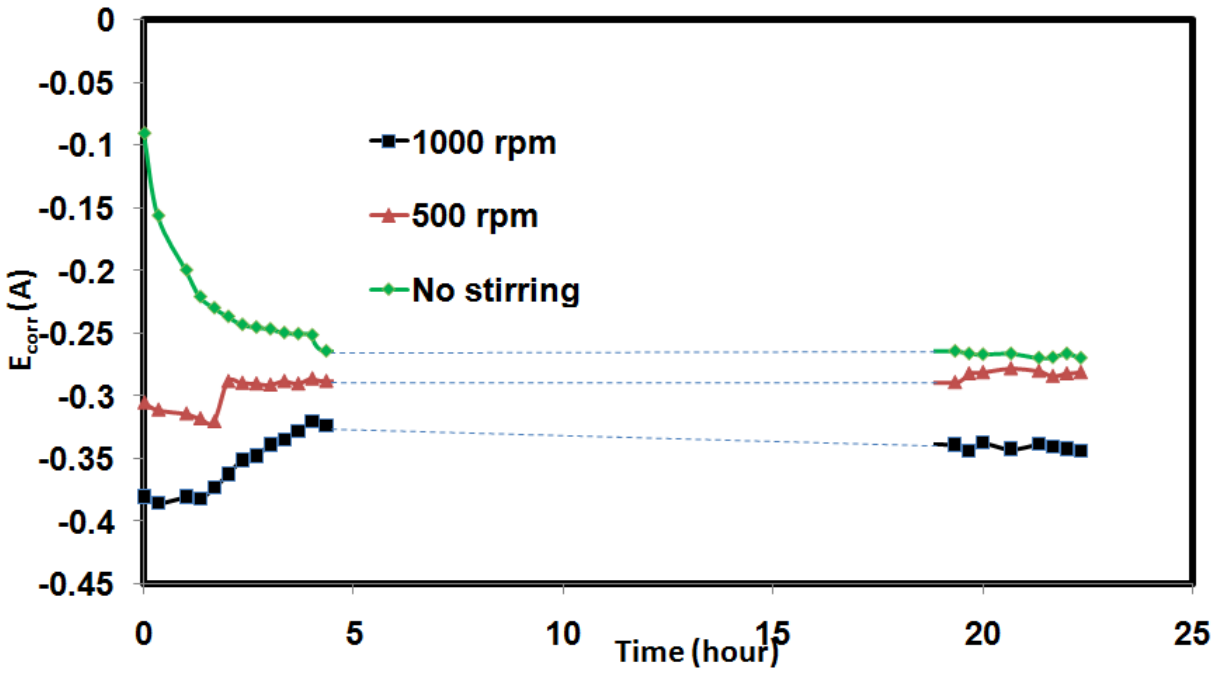

Figure 4-16 c: Effect of mixing speed on the corrosion potential (E_{corr}) 1018 CS in sea water obtained by (LPR) Method at 55^{o}C, 10 ppm inhibitor concentration and pH 8.2.

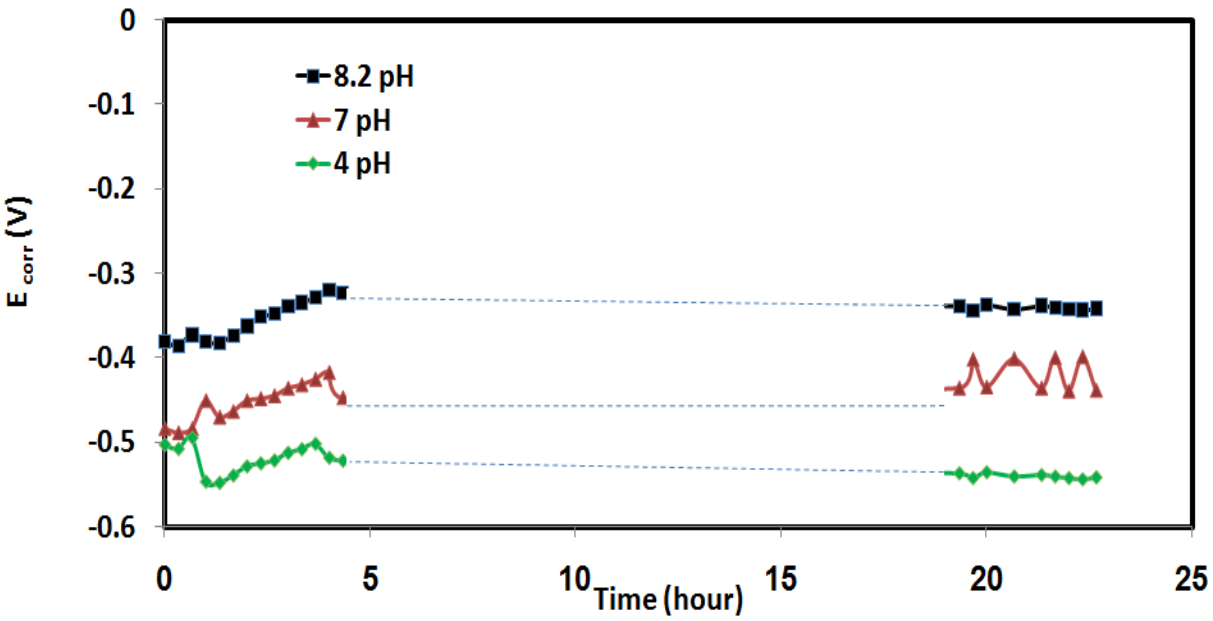

Figure 4-16 d: Effect of solution pH on the corrosion potential (E_{corr}) 1018 CS in sea water obtained by (LPR) Method at 10 ppm inhibitor concentration, 55^{o}C and 1000 rpm.

4.2.6 Potentiodynamic Polarization

The *Potentiodynamic* polarization curves are shown in Figure 4-17 where the corrosion potential, (E_{corr}), has shifted to more positive value with increasing the concentration of the inhibitor, which indicates that the anodic process of CS is inhibited by N-211 (Figure 4-17a). The relation between current density and potential in the experimental data was fitted using Butler-Volmer Equation (BVE) to obtain the anodic,(α_a) and cathodic, ($\alpha_C = 1-\alpha_a$), transfer coefficients and hence to estimate the value of both anodic and cathodic current densities according to Equation 9:

$$i = i_o[e^{\alpha_a F\eta/RT} - e^{(1-\alpha_a)F\eta/RT}] \qquad (9)$$

Where i is the net current density of the electrode, i_0 is the exchange current which equals to the anodic current at equilibrium, ηis the over potential which equals to the difference between the equilibrium and the applied potentials. Table 4-8 shows that the anodic transfer coefficients is generally greater than 0.5 and hence the contribution of the anodic current is in the average of 80% of the total corrosion current. This anodic current is attributed to the dissolution of the metal surface where a charge transfer reaction at the surface of the CS take place leading to mass transport of the metal ions into bulk solution. Increasing the concentration of CI has decreased the anodic corrosion current and increased the corrosion potential which results in increase in the linear polarization resistance at the surface. Therefore, the corrosion rate has decreased. On the other hand, the contribution of the cathodic current is due to the deposition of hydrated iron oxide and oxygen and hydrogen reduction at the surface especially at lower potential.

Corrosion of CS has noticeably affected by both solution temperature and pH (Figures 4-17b and 4-17c). The current density has increased with increasing temperature which suggests a higher corrosion rate at 55 °C. With increasing the temperature from 25 to 55 °C the corrosion potential decreased from -283 mV to -310 mV while the corrosion current is increased from 79.4 to 224 $\mu A/cm^2$. The anodic transfer coefficient has also increased from 0.73 to 0.80. Increasing the temperature will increase the rate of electrochemical reaction and thus the corrosion rate. Similarly, the decrease in solution pH from 8.2 to 4 resulted in a decrease of potential from -310 to -529 mV and increase in the total current and anodic transfer coefficient from 224 to 1260 $\mu A/cm^2$ and 0.80 to 0.90, respectively. This is due to increasing the hydrogen ions in solution which adsorb to the CS surface and reduced to hydrogen gas. Figure 4-17d shows the polarization curve for the effect of stirring speed on corrosion parameters. As the stirring speed increases from 0 to 1000 rpm the potential decreased from -285 to -310 mV and the total currant is increased from 69.3 to 224 $\mu A / cm^2$. However, further increase in mixing speed has little effect on corrosion. Increasing the mixing speed will decrease the external mass transfer resistance for the electrolytes to reach the CS surface where this resistance will become negligible at higher agitation speed of the solution.

Table 4-8. Polarization kinetic parameters for corrosion of CS in Sea water solution.

Parameter	value	E_{corr} (mV)	i_{corr} (A/cm^2)	Transfer coefficients		BVE slopes		Rp
				α_a	α_c	β_a (mV/decade)	β_c (mV/decade)	
Concentration (ppm)	0	-519	4.46E-04	0.87	0.13	32.5	217.4	2.76E+04
	5	-493	3.10E-04	0.82	0.18	34.5	160.8	3.99E+04
	10	-310	2.24E-04	0.80	0.20	35.4	138.8	5.47E+04
	15	-280	2.00E-04	0.72	0.28	39.3	101	6.15E+04
Temperature (^oC)	25	-283	7.94E-05	0.73	0.27	38.7	95.7	1.51E+05
	40	-293	1.95E-04	0.75	0.25	36.0	107.3	6.01E+04
	55	-310	2.24E-04	0.80	0.20	35.4	138.8	5.47E+04
pH	4	-529	1.26E-03	0.90	0.10	31.4	285.7	9.76E+03
	7	-380	6.21E-04	0.87	0.13	32.5	218.7	1.98E+04
	8.2	-310	2.24E-04	0.80	0.20	35.4	138.8	5.47E+04
Speed (rpm)	0	-285	6.93E-05	0.61	0.39	46.6	72.1	1.78E+05
	500	-293	2.00E-04	0.75	0.25	37.8	112.7	6.15E+04
	1000	-310	2.24E-04	0.80	0.20	35.4	138.8	5.47E+04

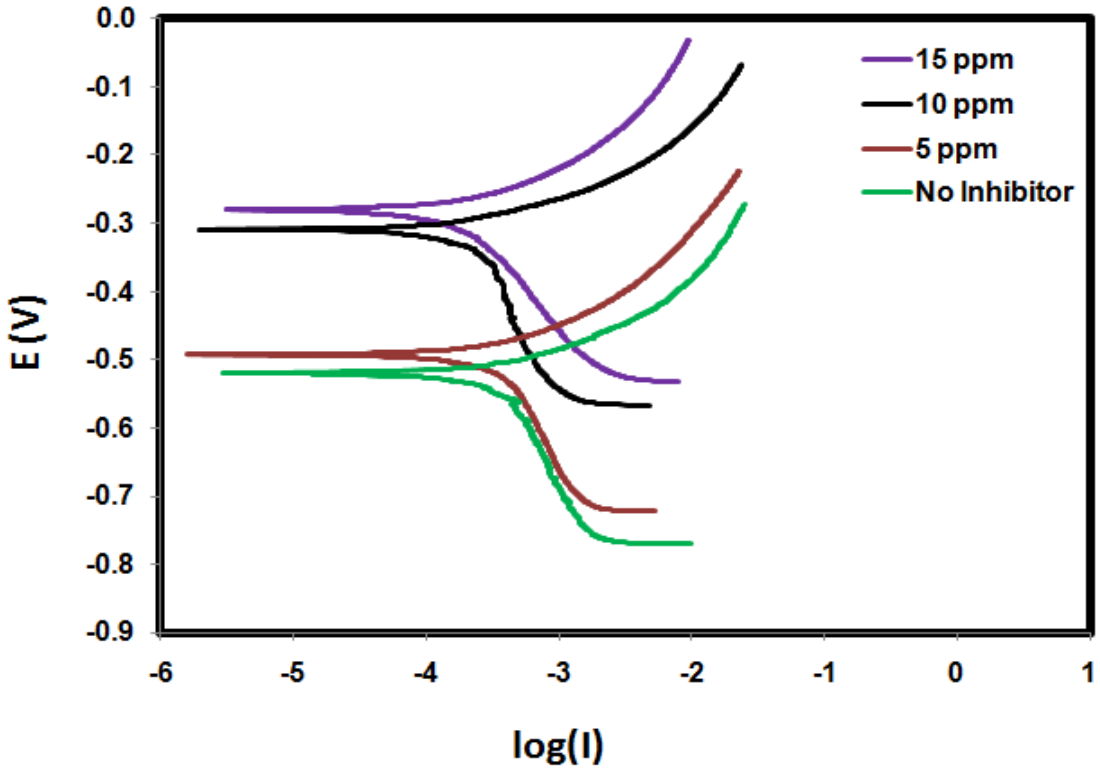

Figure 4-17 a: Effect of inhibitor concentration based on Potentiodynamic polarization curves of 1018 CS in seawater at 55^{o}C, 1000 rpm, and pH 8.2.

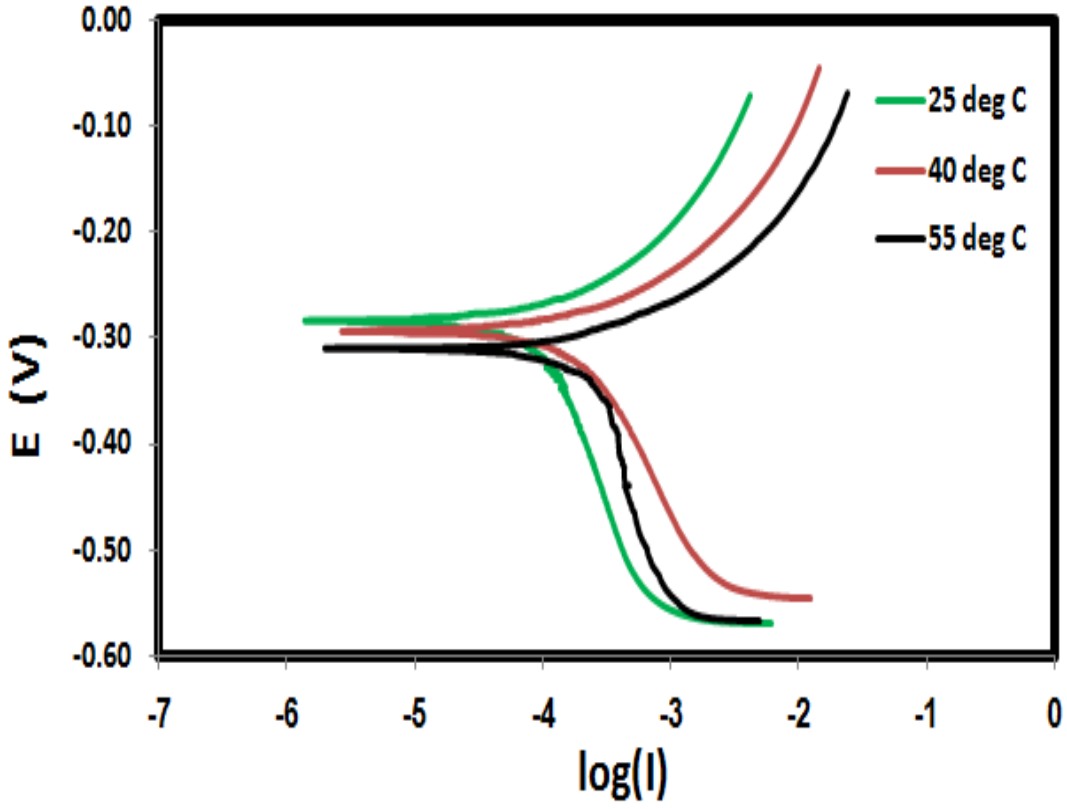

Figure 4-17 b: Effect of solution temperature based on polarization curves of 1018 CS in seawater at 1000 rpm, 10 ppm inhibitor concentration and pH 8.2.

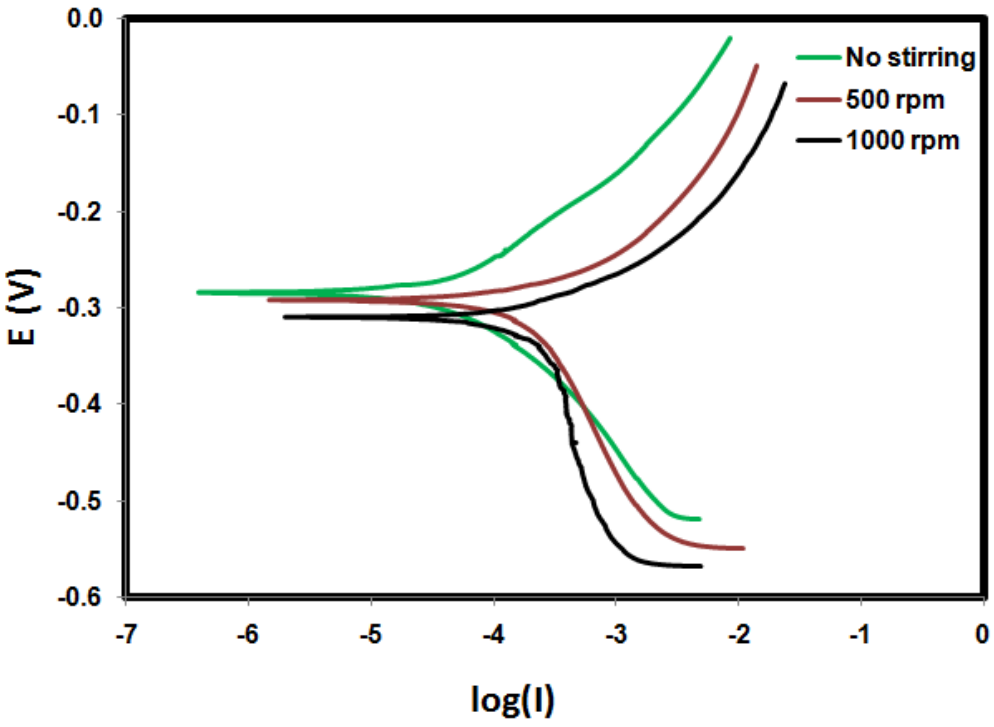

Figure 4-17 c: Effect of mixing speed based on Potentiodynamic polarization curves of 1018 CS in seawater at 55^{o}C, 10 ppm inhibitor concentration and pH 8.2.

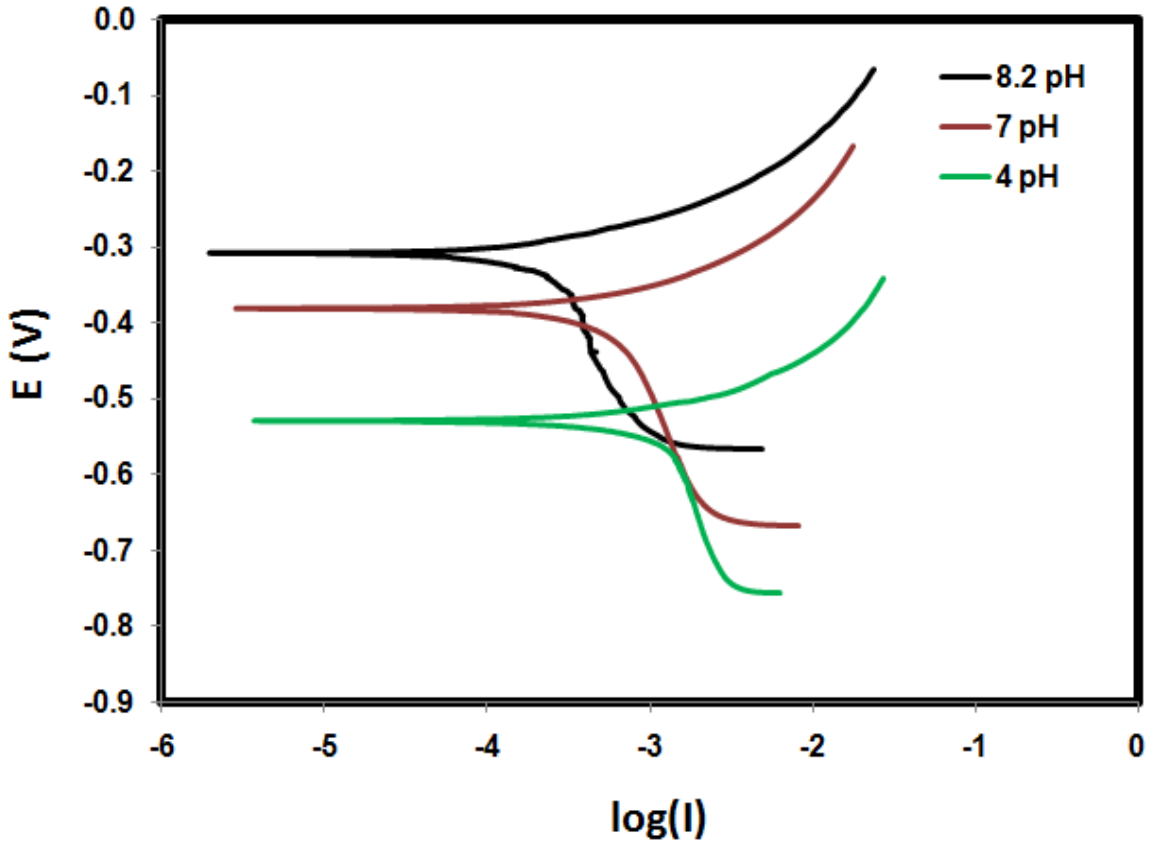

Figure 4-17 d: Effect of solution pH based on Potentiodynamic polarization curves of 1018 CS in seawater based on at 10 ppm inhibitor concentration, 55 ^{o}C and 1000 rpm.

4.2.7 Activation Energy Calculation

The apparent activation energy, E_a, for the corrosion of CS in the presence of Corrosion inhibitor was calculated from Arrhenius equation

$$k = A_f e^{-E_a / RT} \qquad (10)$$

Where k is related to the corrosion rate $\theta_m = \frac{mg}{m^2 s}$ $_2$, A_f is the frequency factor and R is the ideal gas constant,(J/mol.K) . A plot of ln (k) versus 1/T yields a straight line with a slope of -1506.5 K and hence the activation energy is 12.525 $\frac{KJ}{mole}$ as shown in Figure 4-18.

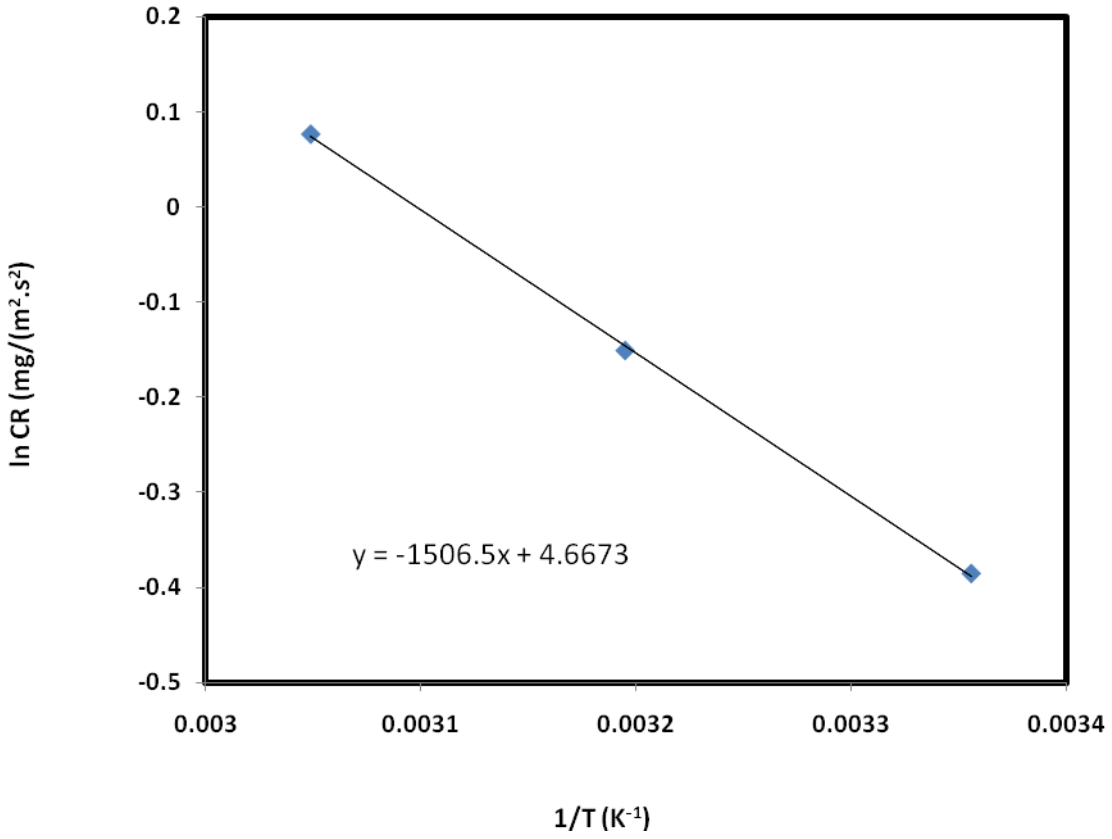

Figure 4-18. Log corrosion rate vs. 1/T for CS in the presence of N-211

4.3 Mixture of N-211 and AR-505 corrosion inhibitors

It was found in this study that the mixture of N-211 and AR505 was enhanced the inhibition efficiency on carbon steel 1018 in seawater solution. Tosun et al. that studied the inhibitor effect of single, binary and ternary mixture of chromate, molybdate, nitrite, tetraborate, ortophosphate, benzoate, acetate, ascorbic acid on the corrosion of carbon steel in neutral aqueous solution containing 100ppm Cl^- at room temperature. The effectiveness of mixtures of inhibitors in all ratios is superior to that of the solution containing molybdate alone [43]. In this part of the study, the inhibitor mixtures are studied while the total inhibitor concentration was kept constant at 10 ppm. It was found that 5 ppm of N-211 and 5 ppm of AR-505 acted as the optimum result.

Kinetic experiments were conducted to study the effect of solution temperature (25, 40, and 55^oC), agitation speed (0, 500, and 1000 rpm), and solution pH (4, 7, and 8.2) on the rate of corrosion of the 1018 CS specimens at 5 ppm of N-211 and 5 ppm of AR-505 and compare results with results in the absence of inhibitor. Thus the inhibition efficiency of the mixture was investigated at different electrochemical techniques using weight loss, polarization resistance and potentiodynamic polarization methods.

4.3.1 Surface Analysis

The SEM of the corroded CS1018 surfaces after exposure to salt solution for 48 hours in the presence and absence of the mixture are shown in Figure 4-19. Image 4-19a shows the corrosion layer on the specimen in the presence of mixture where part of the surface was polished by sand paper.

It is important to stress out that when the mixture compounds were presents in the solution, the

morphology of the steel surface are quite different from the previous work, moreover, the corrosion of specimens is distributed over the whole surface area with uniform appearance. Image 4-19b shows the presence of intense passive film as compared to that in Image 4-19c. The EDS spectra showed the surface was mostly of composed oxides of iron and calcium (Ca) with trace amounts of S, C, and Si as shown in Figure 4-20 and Table 4-9. It can be seen that the presence calcium on the inhibited surface with high distinctive peak result in the adsorption of Ca ions by the surface and the protective film was formed on the surface. It is very obvious that the percentage of iron on this surface is low compared to that not treated with the mixture. The higher oxygen content at the surface that was exposed to the mixture is attributed to the formation film which prevented the surface from corroding.

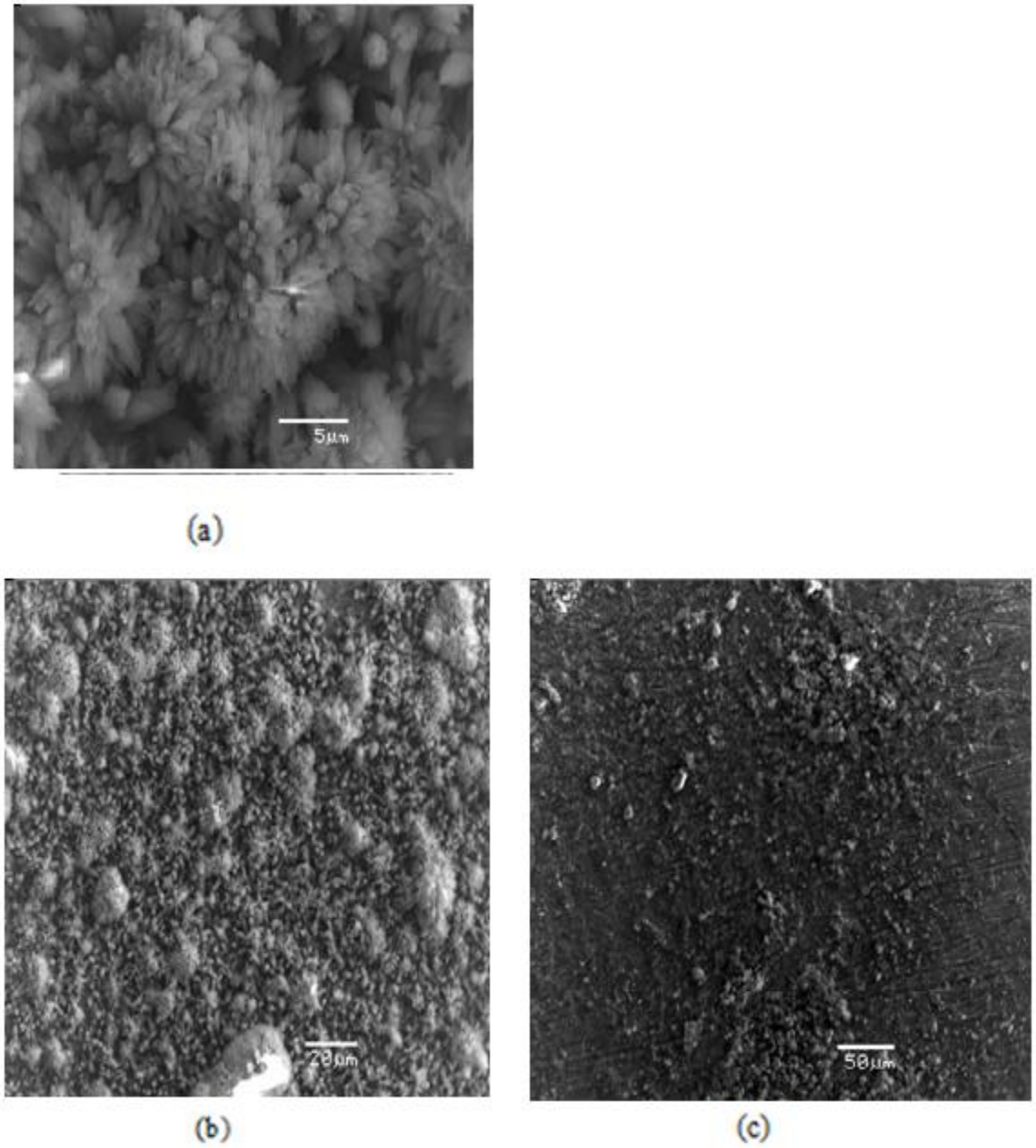

Figure 4-19. SEM micrograph taken on the surface of a specimen exposed to Sea salt; (a,b) mixed with 5 ppm of N-211 & 5 ppm of AR-505 , and (c) without corrosion inhibitor

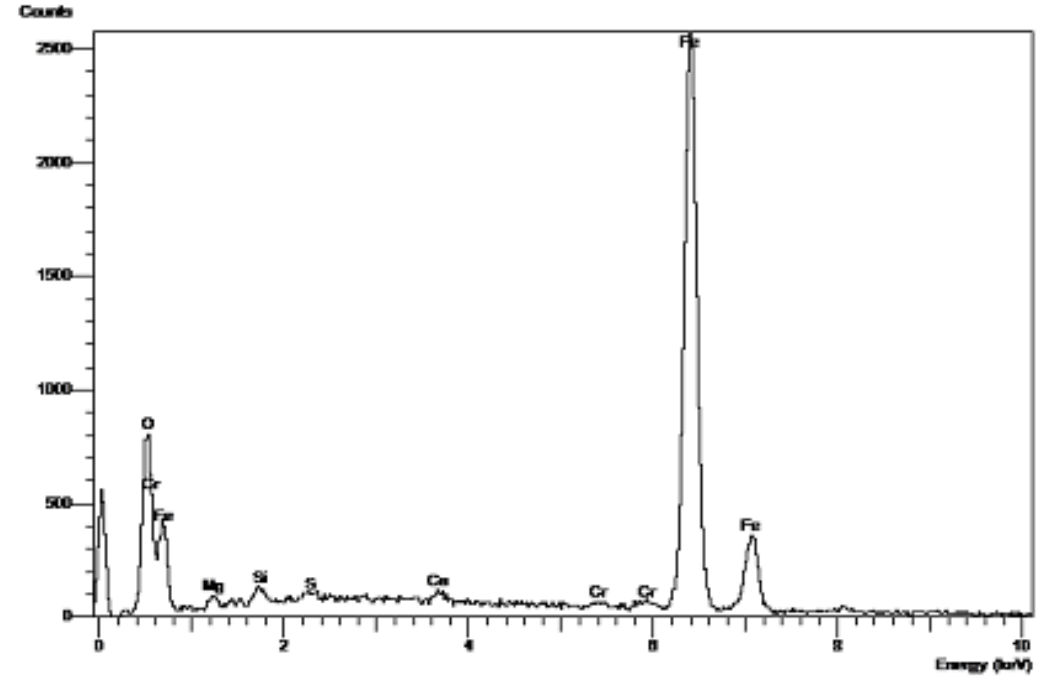

(a)

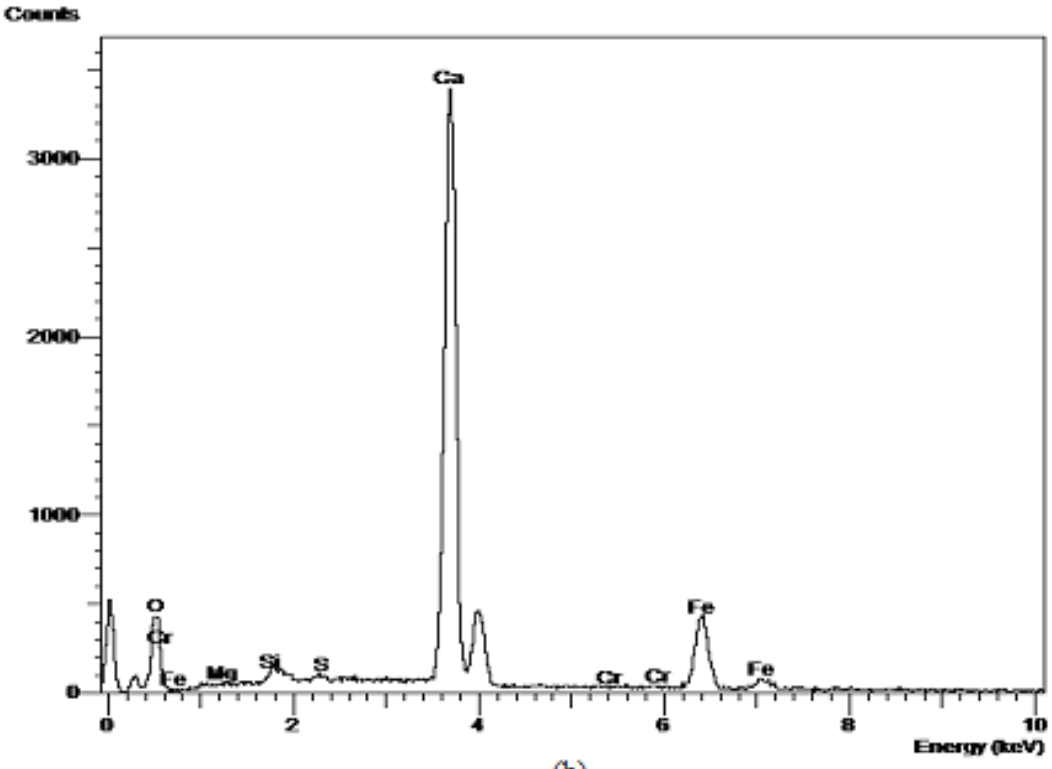

(b)

Figure 4-20: Energy dispersive X-ray analysis of corroded CS1018 specimen; (a) in the absence, and (b) presence of corrosion inhibitor

TABLE 4-9. EDS ELEMENTAL ANALYSIS OF CORRODED CS1018 SPECIMEN; (A) IN THE ABSENCE, AND (B) PRESENCE OF CORROSION INHIBITOR.

Element	**Elemental Percentage in the Absence of Mixture (%)**	**Elemental Percentage in the Absence of Mixture (%)**
O	17.31	42.20
Mg	9.48	---
Si	0.77	0.41
S	0.20	0.25
Ca	0.50	41.13
Cr	0.42	----
C	---	1.94
Fe	71.30	14.07
Total	100.00	100.00

4.3.2 Weight Loss Studies

The weight loss, in term of corrosion rate (CR) of the carbon steel specimen in salt water solution was investigated as shown in Table 4-10. It can be assumed that 5 ppm of N-211 and 5 ppm of AR-505 achieved the best performance at 55 °C, 1000 rpm and 8.2 pH. The corrosion rate increased from 0.42 *mm/y* to 0.71 *mm/y* when solution temperature altered from 25 °C to 55 °C. While CR was decreased with increasing solution pH with a value from 2.03 *mm/y* at pH 4 to 0.71 *mm/y* at pH 8.2. On the other hand, the decrease in mixing speed from 1000 rpm to no stirring was found to reduce the corrosion rate to 0.71 to0 .1 *mm/y* as shown in Table 4-11 and Figure 4-21.

It is noticeable that the mixture of both inhibitor was enhanced the inhibition efficiency. It was assumed that the 5 ppm of N-211 and 5 ppm of AR-505 to be the optimum ratio in this study as shown in Table 4-10.

TABLE 4-10. CORROSION RATE AND INHIBITION EFFICIENCY OF THE INHIBITOR MIXTURE FOR 1018 CS AT DIFFERENT KINETIC CONDITIONS @ 1000 rpm, 55 °C, AND 8.2pH

Inhibitor Concentration (ppm)		Total	CR (mm/y)	Inhibition Efficiency (%)
N-211	AR-505			
30	70	10 ppm	1.37	44.5
50	50	10 ppm	0.71	71.3
70	30	10 ppm	0.69	72.1

TABLE 4-11. CORROSION RATE AND INHIBITION EFFICIENCY OF THE OPTIMUM MIXTURE FOR 1018 CS AT DIFFERENT KINETIC CONDITIONS

Effect of Parameter	Inhibitor Concentration (ppm)	Speed rpm	Temperature (^{o}C)	pH	CR (mm/y)	Inhibition Efficiency (%)
Temperature	10	1000	25	8.2	0.42	83
	10	1000	40	8.2	0.58	76.5
	10	1000	55	8.2	0.71	71.3
pH	10	1000	55	4	2.03	17.8
	10	1000	55	7	1.21	51.0
	10	1000	55	8.2	0.71	71.3
Speed	10	0	55	8.2	0.1	96.0
	10	500	55	8.2	0.58	76.5
	10	1000	25	8.2	0.71	71.3

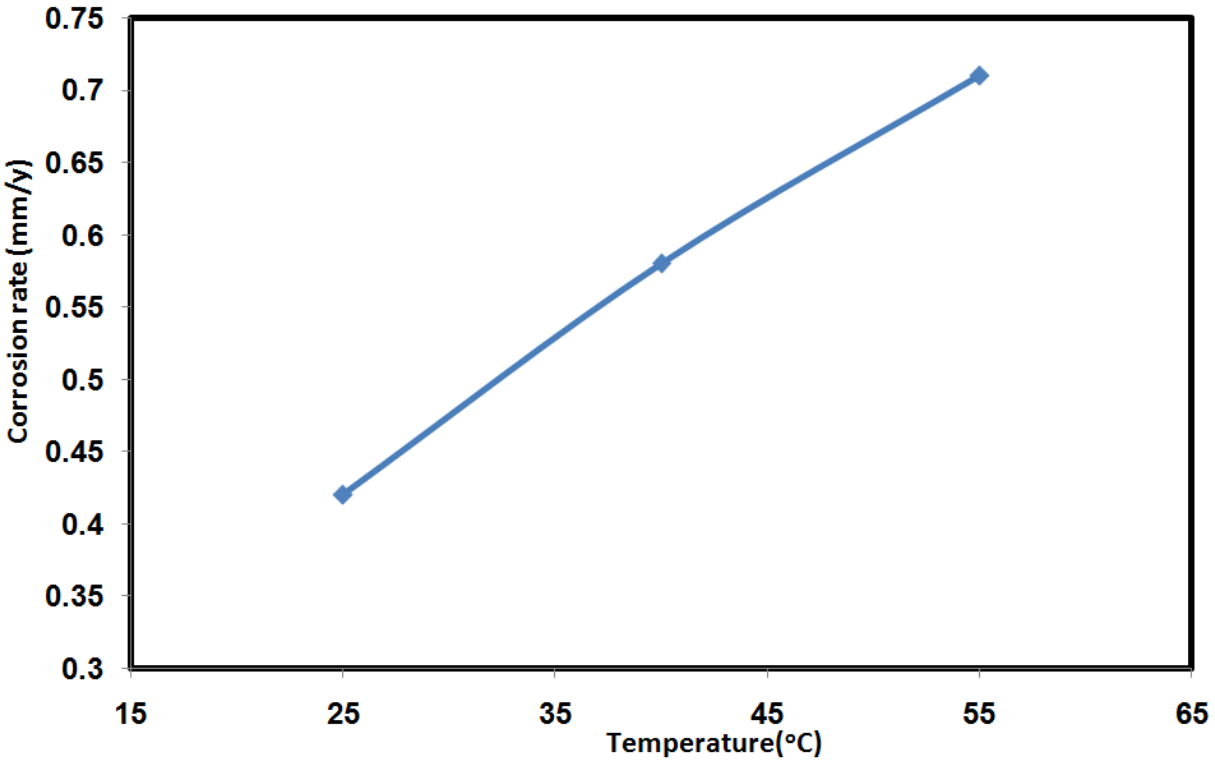

Figure 4-21 a: Effect of solution temperature on the corrosion rate of 1018 CS in sea water obtained by weight loss method at 1000 rpm, 10 ppm inhibitor concentration and pH 8.2.

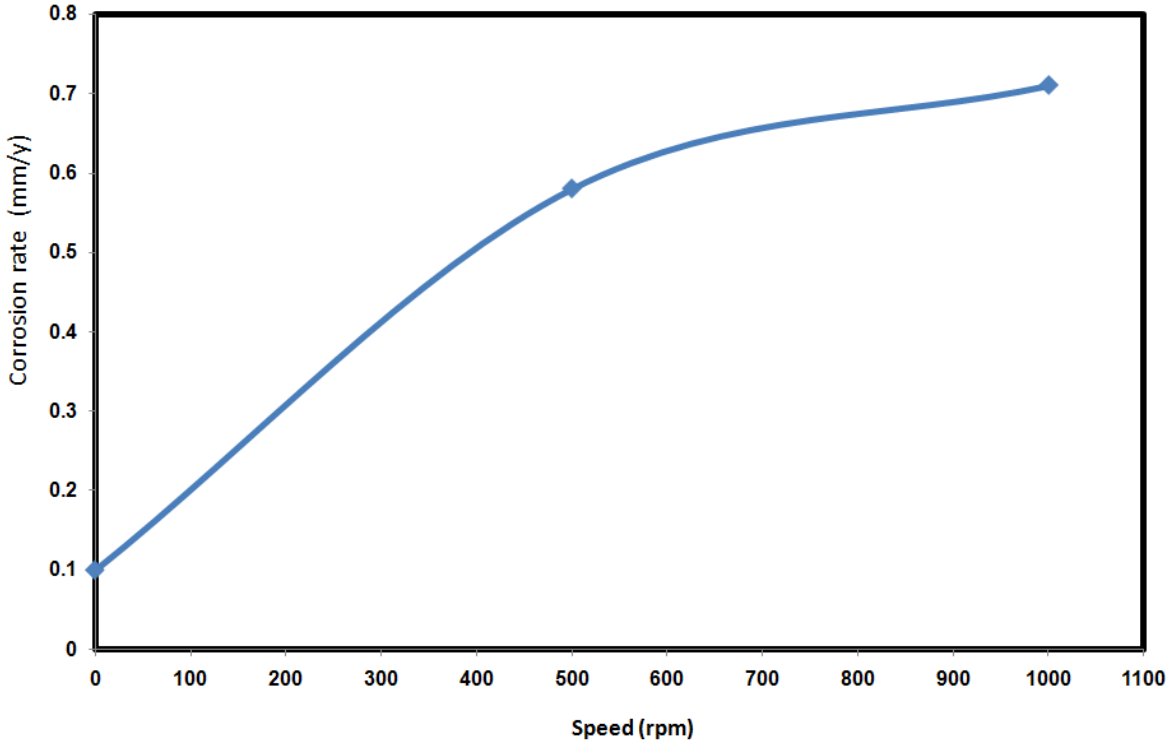

Figure 4-21 b: Effect of mixing speed on the corrosion rate of 1018 CS in sea water obtained by weight loss method at 55^{o}C, 10 ppm inhibitor concentration and pH 8.2.

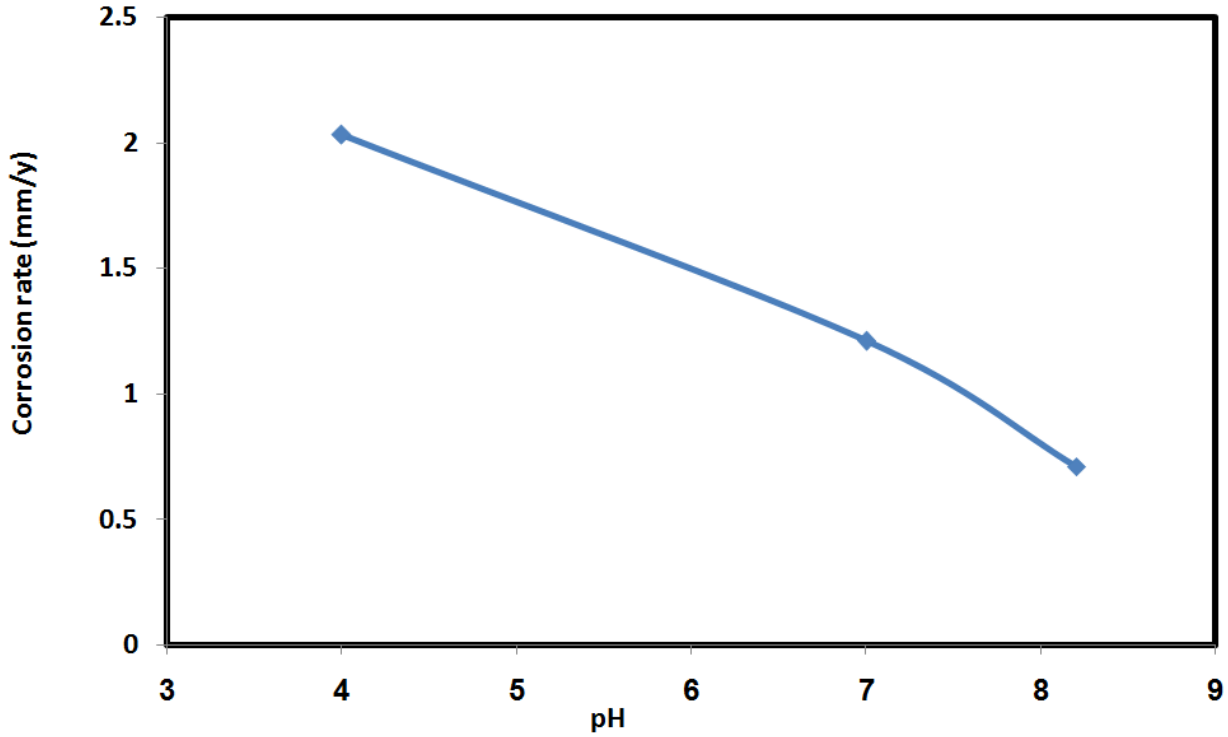

Figure 4-21 c: Effect of solution pH on the corrosion rate of 1018 CS in sea water obtained by weight loss method at 10 ppm inhibitor concentration, 55^{o}C and 1000 rpm.

4.3.3 Linear Polarization Resistance (LPR) Method

The corrosion rates versus time at different experimental conditions are shown in Figures 4-15. Figure 4-22a shows the effect of mixtures of corrosion inhibitor concentrations on the corrosion rate. It is apparent that the increase in percentage of N-211 amine based inhibitor was enhanced the inhibition efficiency and decreased the corrosion rate which is related to the increase in the formation of a protective oxide film. However, it is also concluded that a 5 ppm of N-211 & 5 ppm of AR-505 could be assumed as an optimum concentration to inhibit the surface. The solution temperature has a noticeable effect on the corrosion rate where a value of 0.42 mm/y was achieved at 55 ^{o}C within 4h compared to 0.32 mm/y obtained at 25 ^{o}C within the same period of time as shown Figure 4-22b. As expected, the higher solution temperature yields a higher corrosion rate. This is due to the increase in desorption of the inhibitor with increasing temperature and hence increase the rate of electrochemical reactions and diffusion processes which stimulates corrosive attack. Effect of mixing speed is presented in Figure 4-22c. The corrosion rate has increased within 4 h from 0.19 mm/y for stagnant solution to 0.42 mm/y at mixing speed of 1000 rpm. Increasing mixing speed will reduce the thickness of the diffusion layer at the electrode surface and thus maintaining the concentration of the salt adjacent to surface is relatively equal to that in bulk of the solution [52]. The corrosion rate at 1000 rpm was severely affected by decreasing the solution pH (Figure 4-22d). It is expected that decreasing the solution pH will increase hydrogen ions in solution and the later becomes more aggressive to attack the surface.

The studies of the corrosion potential (E_{corr}) versus time noticeably show up the capability to maintain the passivity of the 1018 CS at different experimental conditions as shown in Figures 4-23. Figure 4-23a shows that the E_{corr} became more positive as the N-211 amine based inhibitor ratio increased. However, it can be seen from figure 4-23b that the decrease in temperatures assists the passivation the surface of iron and the adherence of the passive film is high. The passivity of the carbon steel was decreased as the rotating speed increased as illustrated in figure 4-23c. It is seen that, under the static condition, the E_{corr} shift to highest positive values. Apparently, an increase of rotating speed lead to accelerate the diffusion of oxygen, thus the oxide film will be removed. It is extrapolated from figure 4-23d that the corrosion potential decreases with increase in acidity and this is demonstrated that oxide film have a tendency to dissolve in the solution swiftly when it reached to pH4.

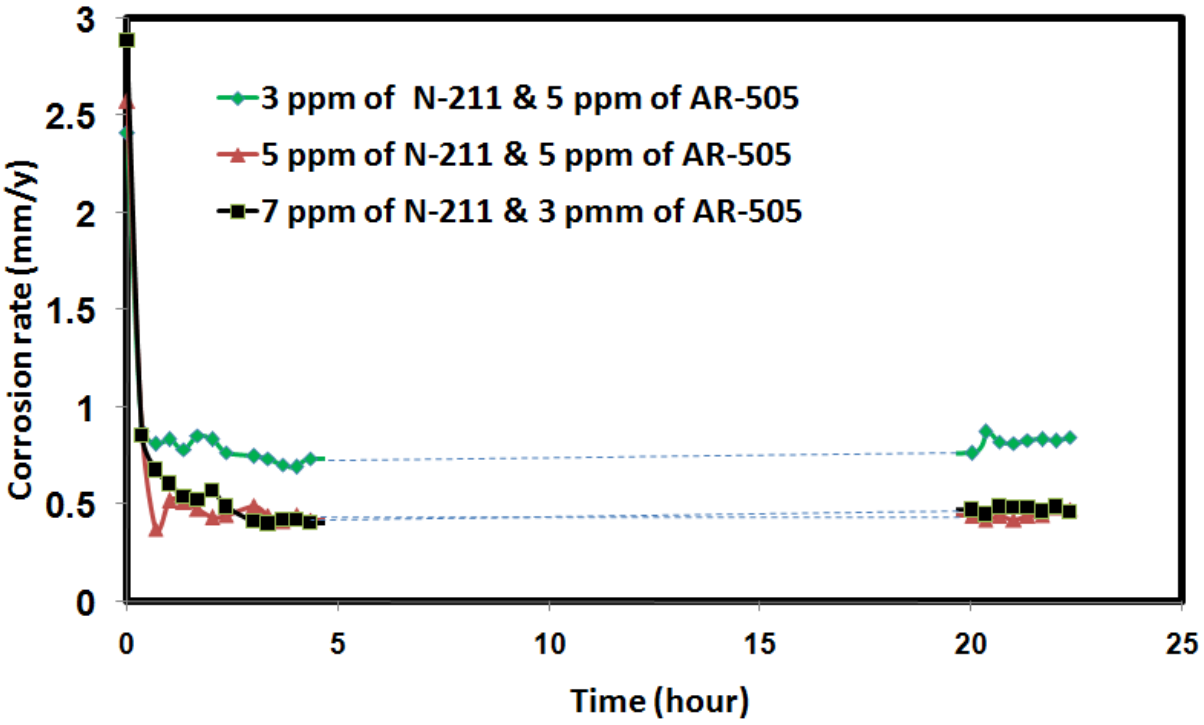

Figure 4-22 a: Effect of inhibitor mixtures on the corrosion rate 1018 CS in sea water obtained by (LPR) Method at 55^{o}C, 1000 rpm, and pH 8.2.

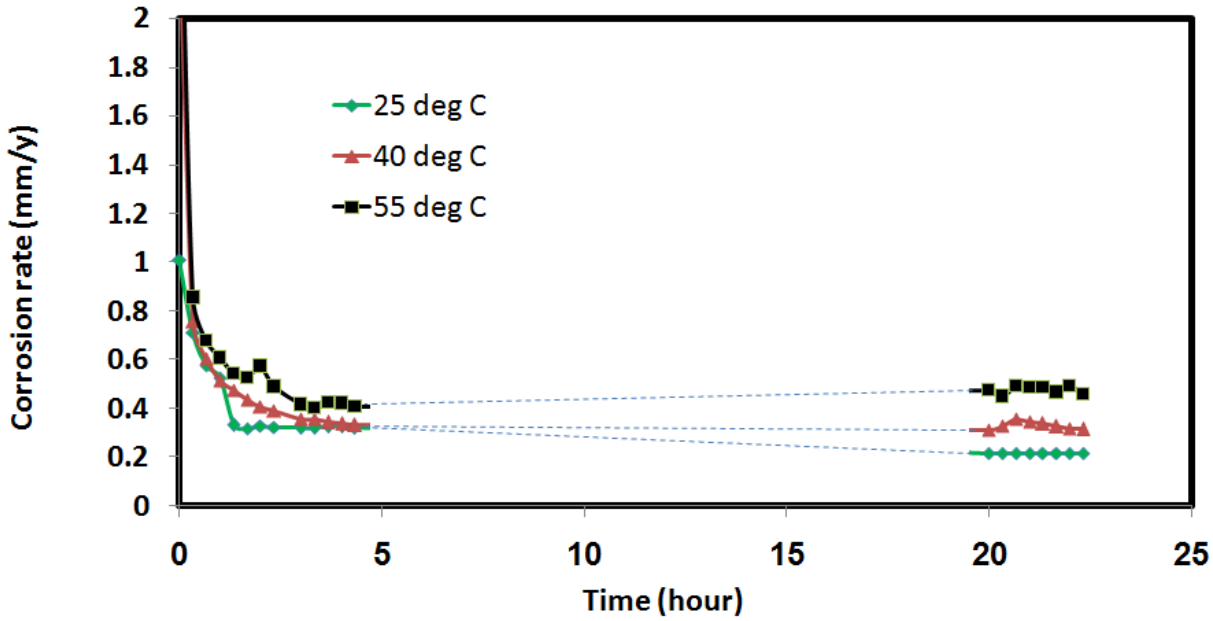

Figure 4-22 b: Effect of solution temperature on the Corrosion rate of 1018 CS in sea water obtained by (LPR) Method at 1000 rpm, 10 ppm inhibitor concentration and pH 8.2.

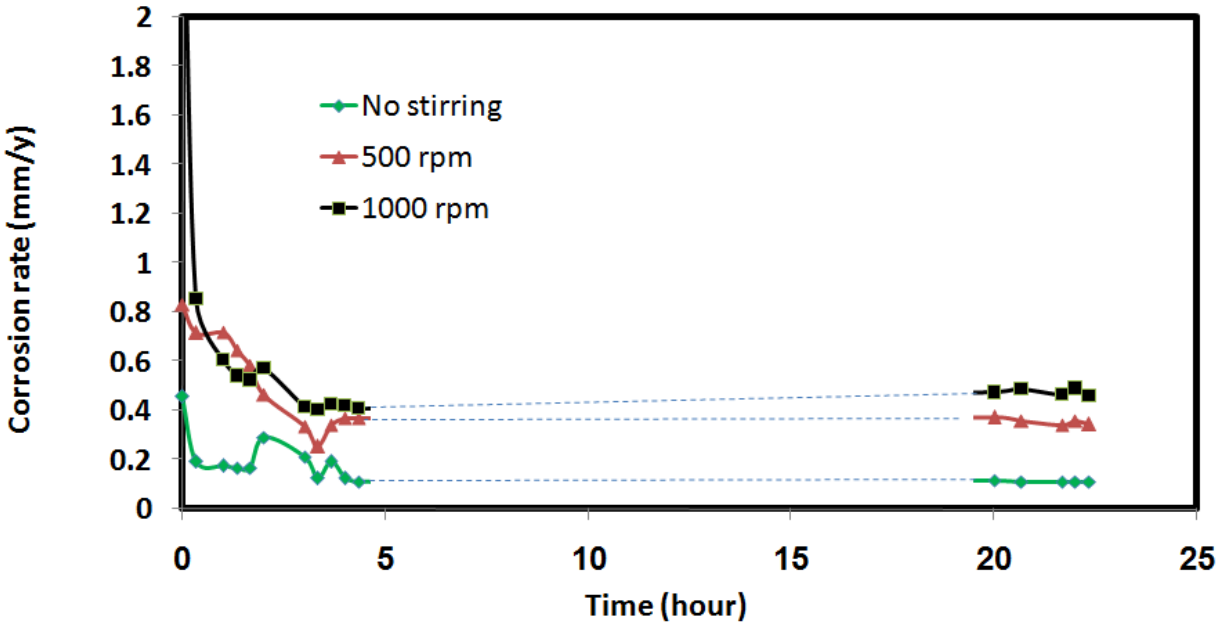

Figure 4-22 c: Effect of mixing speed on the corrosion rate 1018 CS in sea water obtained by (LPR) Method at 55^{o}C, 10 ppm inhibitor concentration and pH 8.2.

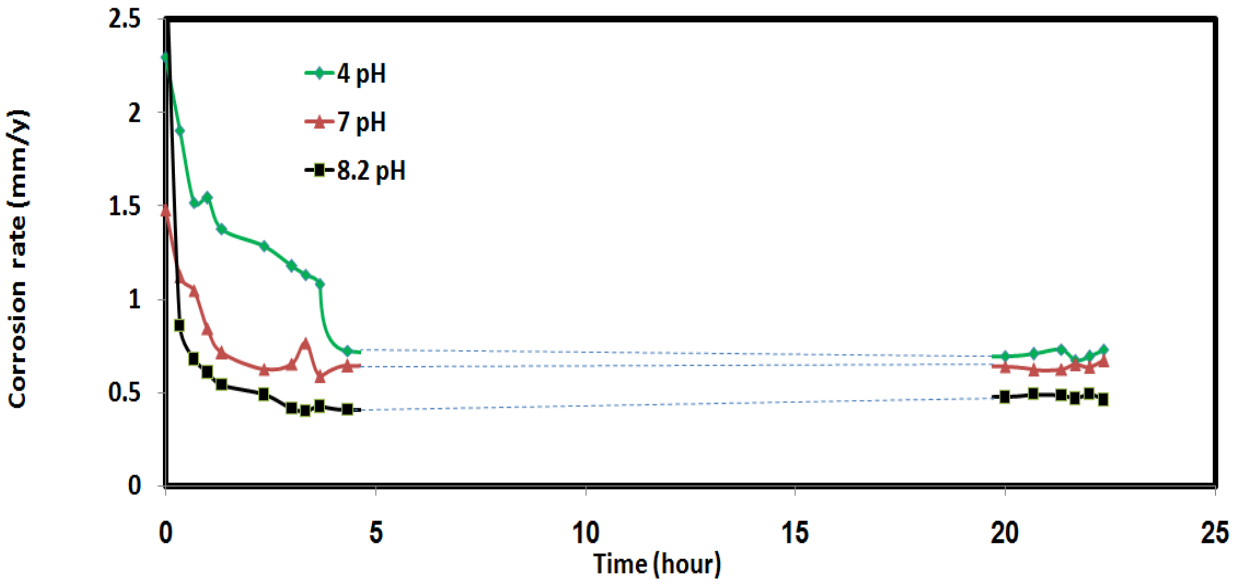

Figure 4-22 d: Effect of solution pH on the corrosion rate 1018 CS in sea water obtained by (LPR) Method at 10 ppm inhibitor concentration, 55^{o}C and 1000 rpm.

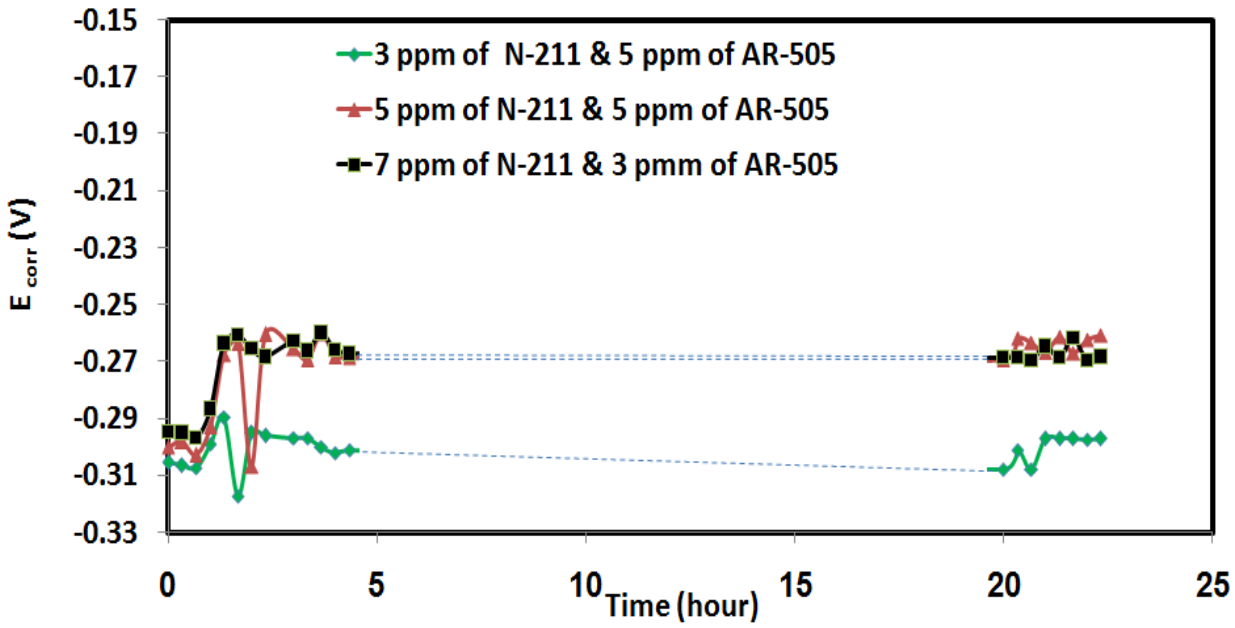

Figure 4-23 a: Effect of inhibitor mixtures on the corrosion potential (E_{corr}) 1018 CS in sea water obtained by (LPR) Method at 55^{o}C, 1000 rpm, and pH 8.2.

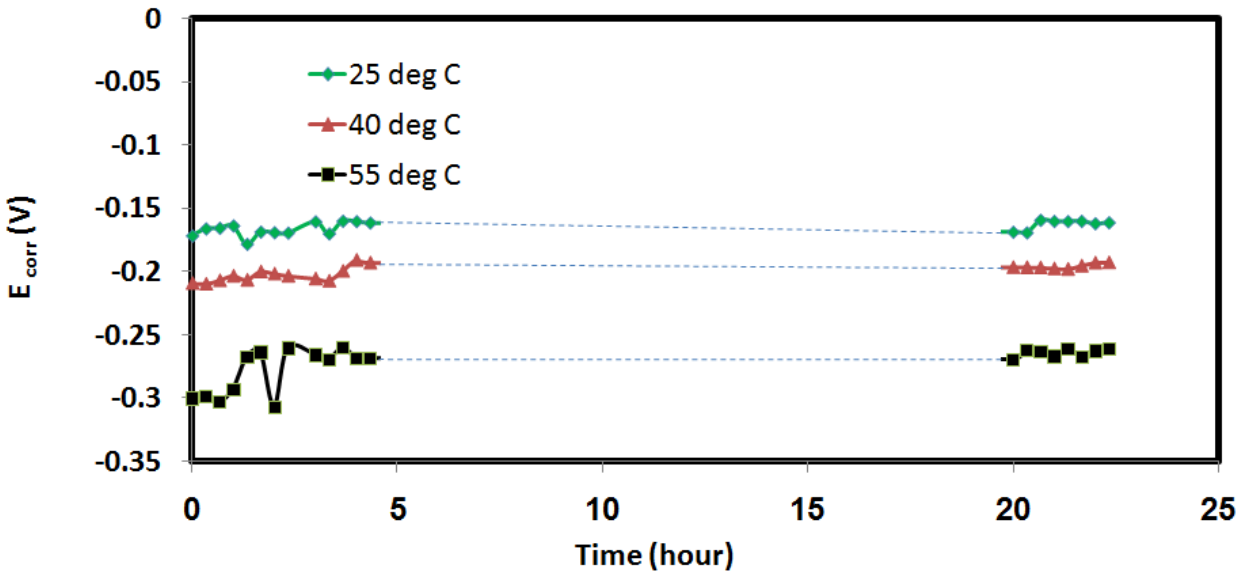

Figure 4-23 b: Effect of solution temperature on the corrosion potential (E_{corr}) of 1018 CS in sea water obtained by (LPR) Method at 1000 rpm, 10 ppm inhibitor concentration and pH 8.2.

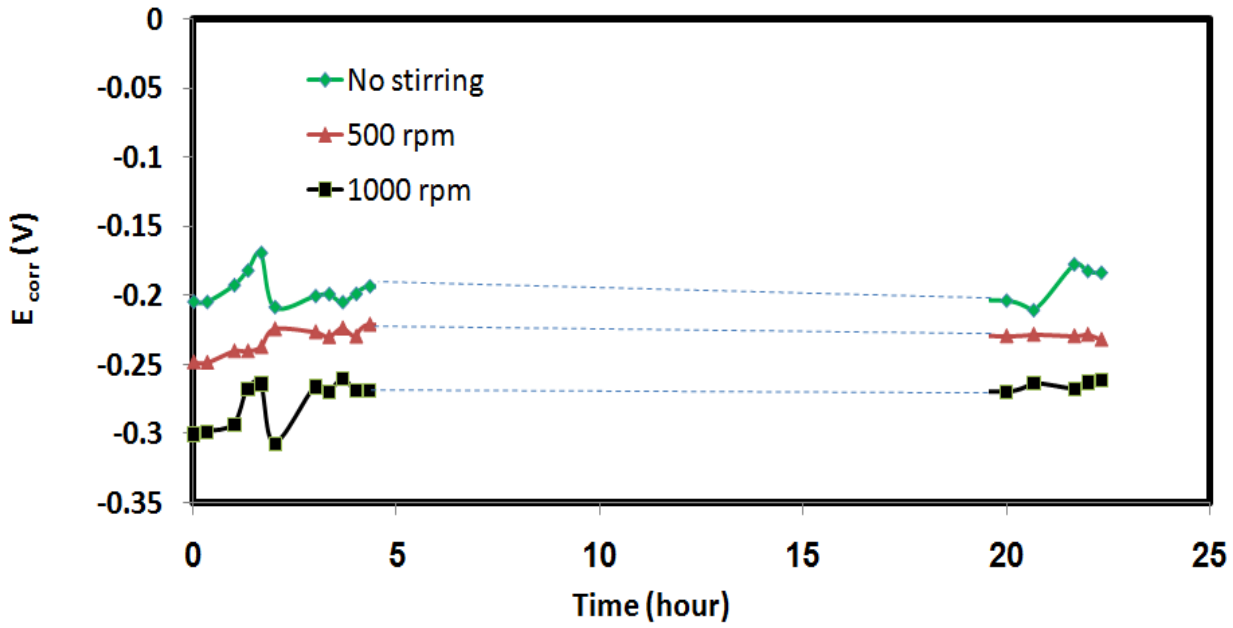

Figure 4-23 c: Effect of mixing speed on the corrosion potential (E_{corr}) 1018 CS in sea water obtained by (LPR) Method at 55^{o}C, 10 ppm inhibitor concentration and pH 8.2.

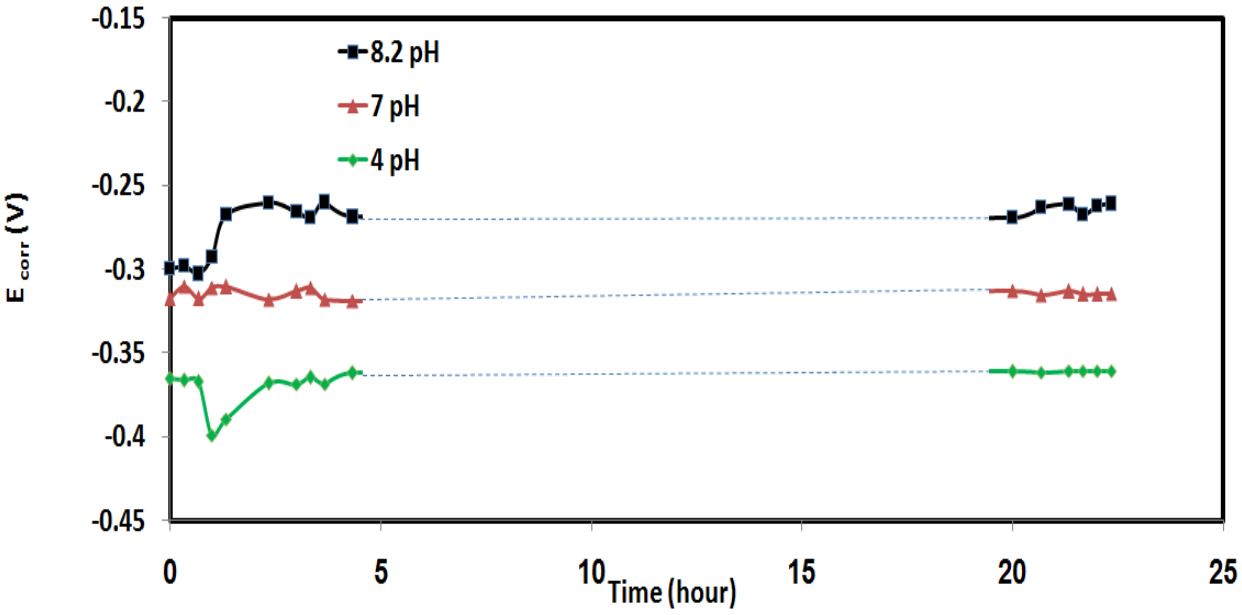

Figure 4-23 d: Effect of solution pH on the corrosion potential (E_{corr}) 1018 CS in sea water obtained by (LPR) Method at 10 ppm inhibitor concentration, 55^{o}C and 1000 rpm.

4.3.4 Potentiodynamic Polarization

The *Potentiodynamic* polarization curves are shown in Figure 4-24 where the corrosion potential, (E_{corr}), has shifted to more positive value with increasing the ratio of the N-211 inhibitor, which indicates that the anodic process of CS is protected from the corrosion as shown in Figure 4-24a. By the similar way to the previous work to and hence to estimate the value of both anodic and cathodic current densities by obtaining the anodic, (α_a) and cathodic, ($\alpha_C = 1-\alpha_a$), transfer coefficients.

Table 4-12 showed the values of anodic and cathodic transfer coefficients are in the average of 0.77 and 0.23, respectively. Butler-Volmer anodic and cathodic slopes were in the order of 36.8 and 141 mV/decade. This anodic current is attributed to the dissolution of the metal surface where a charge transfer reaction at the surface of the CS take place leading to mass transport of the metal ions into bulk solution. Increasing the concentration of CI has decreased the anodic corrosion current and increased the corrosion potential which results in increase in the linear polarization resistance at the surface.

It was shown that the mixture of 5 ppm of N-211 and 5 ppm of AR 505 protect the steel surface better than other mixture due to high value of polarization resistance 6.15×10^4 Ω. Corrosion of CS has noticeably affected by both solution temperature and pH (Figures 4-24b and 4-24c). The current density has increased with increasing temperature which suggests a higher corrosion rate at 55 °C. With increasing the temperature from 25 to 55 °C the corrosion potential decreased from -161 mV to -269 mV while the corrosion current is increased from 31.7 to 200 μA/cm^2.

The anodic transfer coefficient has also increased from 0.69 to 0.86. Increasing the temperature will increase the rate of electrochemical reaction and thus the corrosion rate. Similarly, the decrease in solution pH from 8.2 to 4 resulted in a decrease of potential from -269 to -423 mV and increase in the total current and anodic transfer coefficient from 200 to 1000 $\mu A/cm^2$ and 0.79 to 0.88, respectively. This is due to increasing the hydrogen ions in solution which adsorb to the CS surface and reduced to hydrogen gas. Figure 4-24d shows the polarization curve for the effect of stirring speed on corrosion parameters. As the stirring speed increases from 0 to 1000 rpm the potential decreased from -181 to -269 mV and the total currant is increased from 25.1 to 200 $\mu A / cm^2$.

Table 4-12. Polarization kinetic parameters for corrosion of CS in Sea water solution.

Parameter	value	E_{corr} (mV)	i_{corr} (A/cm^2)	Transfer coefficients		BVE slopes		Rp Ω
				α_a	α_c	β_a (mV/decade)	β_c (mV/decade)	
CI ratio	Blank	-519	4.46E-04	0.87	0.13	32.5	217.4	2.76E+04
	30% N-211 & 70 % AR-505	-295	2.51E-04	0.82	0.18	34.4	159.5	4.90E+04
	50% N-211 & 50 % AR-505	-269	2.00E-04	0.79	0.21	36.0	132	6.15E+04
	70% N-211 & 30 % AR-505	-264	2.22E-04	0.80	0.20	35.4	138.6	5.52E+04
Temperature (^oC)	25	-161	3.17E-05	0.69	0.31	36.2	83.8	3.47E+05
	40	-188	1.26E-04	0.73	0.27	43.0	100.6	1.04E+05
	55	-269	2.00E-04	0.79	0.21	36.0	132	6.15E+04
pH	4	-423	1.00E-03	0.88	0.12	32.2	232	1.23E+04
	7	-318	5.01E-04	0.86	0.14	32.9	200	2.45E+04
	8.2	-269	2.00E-04	0.79	0.21	36.0	132	6.15E+04
Speed (rpm)	0	-181	2.51E-05	0.64	0.36	43.9	79.7	4.90E+05
	500	-229	1.11E-04	0.74	0.26	38.1	110.4	1.11E+05
	1000	-269	2.00E-04	0.79	0.21	36.0	132	6.15E+04

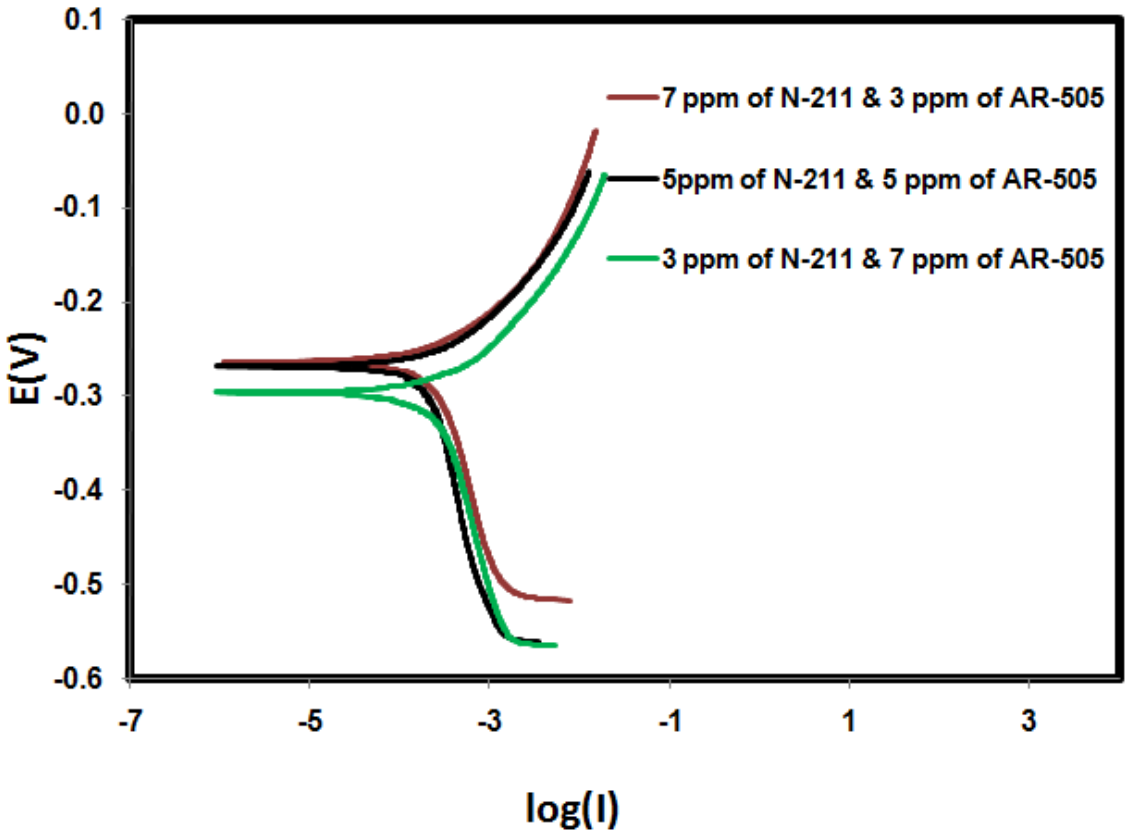

Figure 4-24 a: Effect of inhibitor mixtures based on Potentiodynamic polarization curves of 1018 CS in seawater at 55^{o}C, 1000 rpm, and pH 8.2.

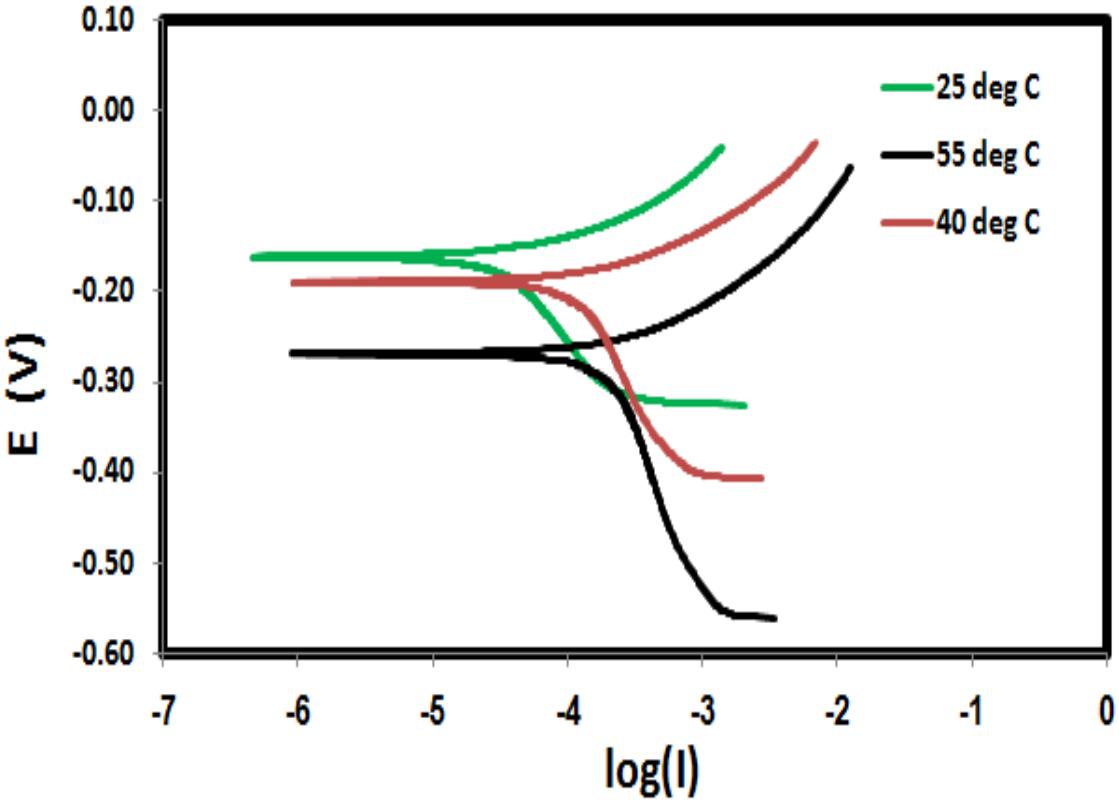

Figure 4-24 b: Effect of solution temperature based on polarization curves of 1018 CS in seawater at 1000 rpm, 10 ppm inhibitor concentration and pH 8.2.

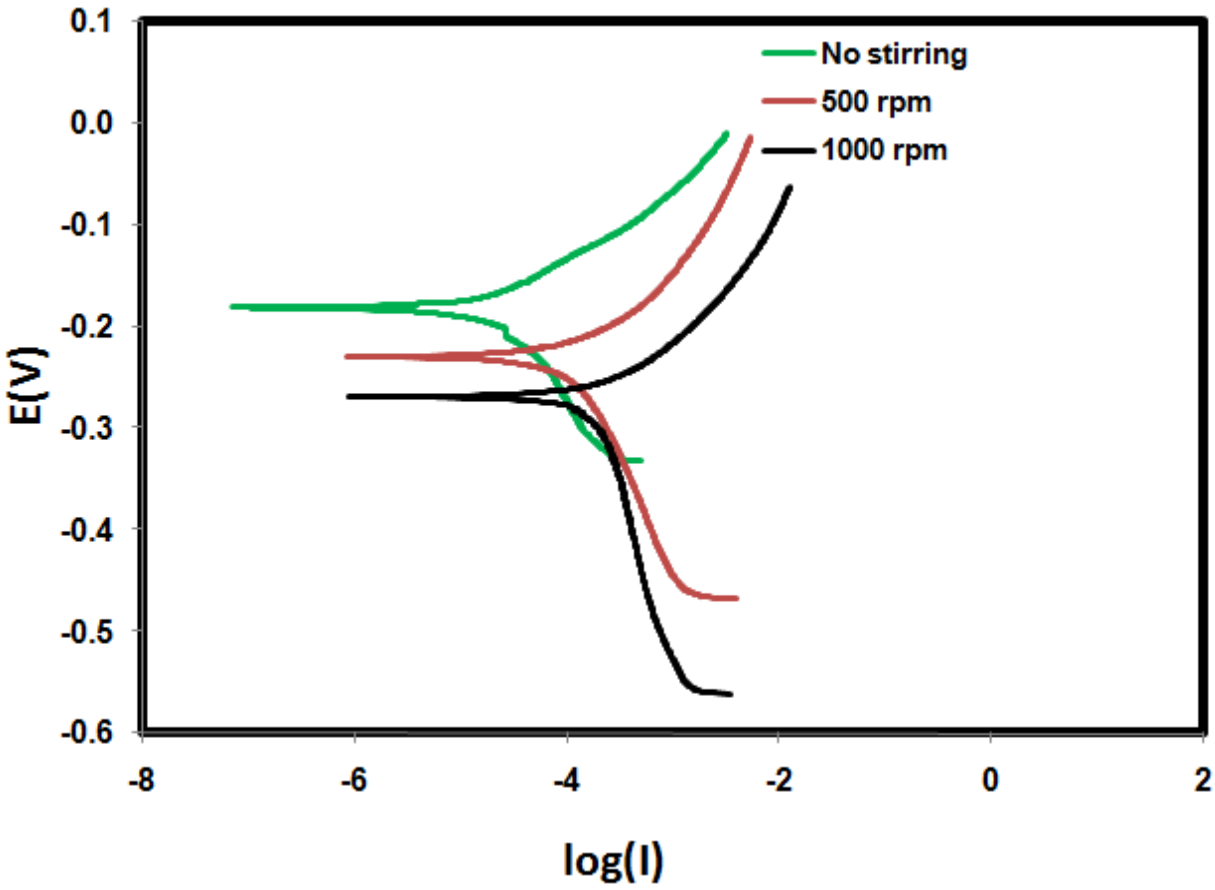

Figure 4-24 c: Effect of mixing speed based on Potentiodynamic polarization curves of 1018 CS in seawater at 55^{o}C, 10 ppm inhibitor concentration and pH 8.2.

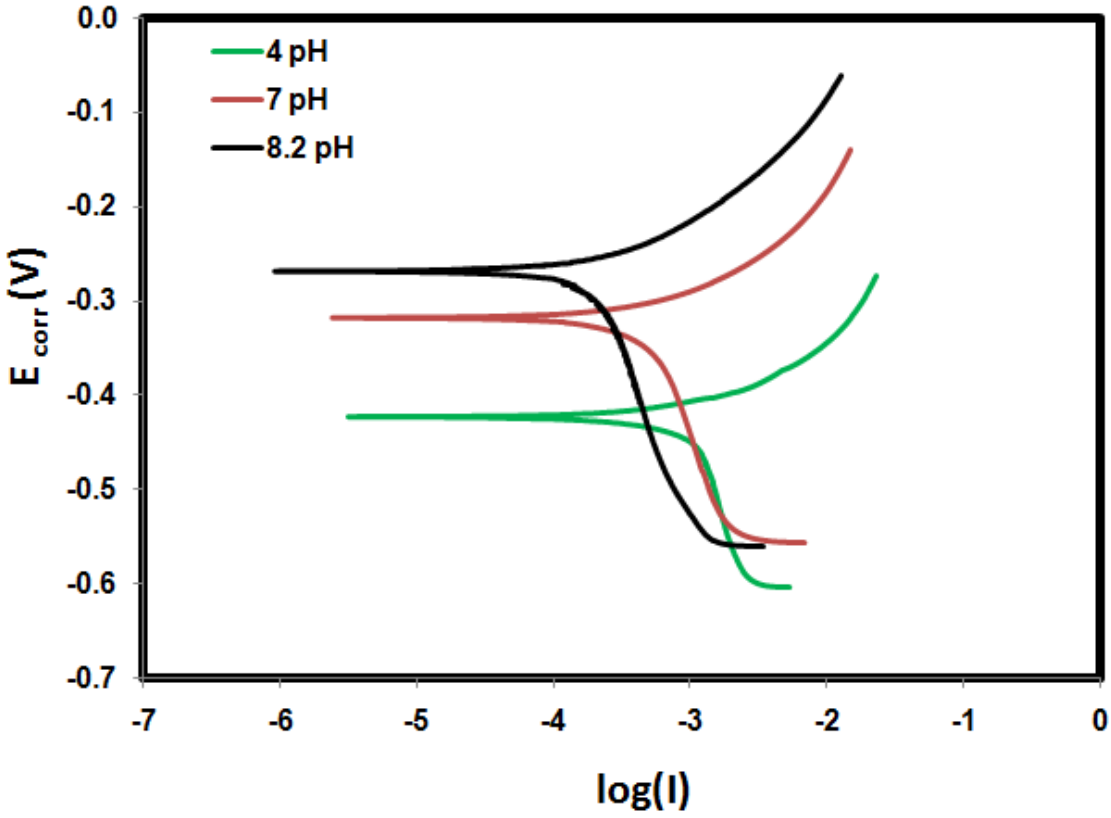

Figure 4-24 d: Effect of solution pH based on Potentiodynamic polarization curves of 1018 CS in seawater based on at 10 ppm inhibitor concentration, 55 ^{o}C and 1000 rpm.

4.3.5 Activation Energy Calculation

The apparent activation energy, E_a, for the corrosion of CS in the presence of Corrosion inhibitor was calculated from Arrhenius equation

$$k = A_f e^{-E_a / RT} \quad (10)$$

Where k is related to the corrosion rate $\theta_m = \frac{mg}{m^2 s}$ $_2$, A_f is the frequency factor and R is the ideal gas constant,(J/mol.K) . A plot of ln (k) versus 1/T yields a straight line with a slope of -1715 K and hence the activation energy is 14.26 $\frac{KJ}{mole}$ as shown in Figure 4-25.

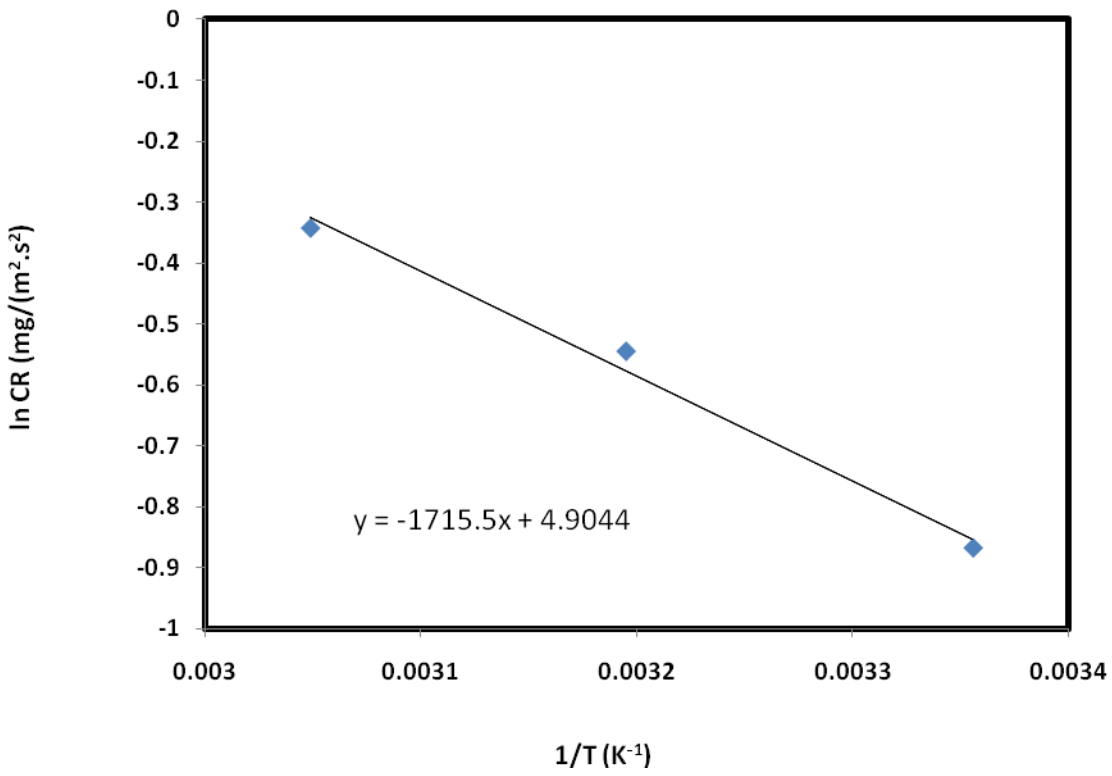

Figure 4-25. Log corrosion rate vs. 1/T for CS in the presence of the mixture

4.4 Comparison Between Inhibitors

In order to exemplify the comparison between the AR505 and N211 amine based inhibitors, with their mixture. This section will be focused on the effect of the inhibitor concentrations on the behavior of the carbon steel corrosion based on the weight loss, linear polarization, potentiodynamic polarization and the activation energy. In addition, the inhibition efficiency of each inhibitor will be compared in general.

4.4.1 Effect of Corrosion Inhibitor Concentration on Behavior of Corrosion

In general, the synergistic effect is described as the presence of one chemical enhances the effects of the other chemical. In this part of research, it is assumed that this effect is the reason for increasing of the inhibition efficiency since the passive film was enhanced once the N-211 was added to the solution. Each inhibitor was studied and compared to others to look for the optimum concentration that provides the best protection to steel surface. Figure 4-26 shows the comparison between the inhibitors based on the weight loss. It is obvious that the mixture of inhibitor 5 ppm of N-211 and 5 ppm of AR-505 is the best one and provide the required protection to the steel against the carbon steel corrosion and further increase in N-211 percentage had little effect on behavior of corrosion rate. Several studies were conducted based on the following observations:

1. From the weight loss study in Figure 4-26 and Table 4-13, it was shown that the inhibitor mixture of 5 ppm of N-211 and 5 ppm of AR-505 has the lowest value of corrosion rate which is the most effective amount of the corrosion-inhibiting to be used as Figure 4-26-a, b and c. The inhibitor interaction nature on the surface of working electrode can be explained in terms of its adsorption characteristics. That mixture was optimum because of the capability to increase the strength of the adsorption film and therefore, protect the metal surface form the corrosion [1].

2. The linear polarization and Potentiodynamic Polarization study confirmed that the mixture of 5 ppm of N-211 with 5 ppm of AR-505 had the highest surface coverage, due the inhibitor adsorption on the metal surface that acts as a barrier between the metal surface and the solution by blocking the active sites. The studies of the corrosion potential (E_{corr}) versus time noticeably show the capability to maintain the passivity of the CS. It was seen that the E_{corr} in the mixture exhibits more positive as the inhibitor concentration increased due to the formation of film to retard the metal dissolution of the metal surface. It was shown that the mixture protect the steel surface better than other mixture due to high value of polarization resistance 6.15x104 Ω and low value of anodic transfer coefficient which suggesting that anodic dissolution of carbon steel substrate is suppressed. In addition, it is very clear that significant shift towards less logarithm corrosion current density because of the interaction of anodic and cathodic Tafel lines decreases as Figure 4- 27, 4-28 and Table 4-14.

3. In general, the smaller the activation energy of a reaction (the lower the height of the energy barrier and located under the physical adsorption border while at higher values, it becomes under the chemical adsorption process. The activation energy showed that the increase in E_a, representing that the energy barrier for the interaction of corrosion became high which is proportional to the nature of inhibitor [34, 40]. From Figure 4-29, the results show that, all activation energy (Ea) for the corrosion of carbon steel in the presence of the inhibitors are close to the chemisporion mechanism. However, it was highest when the inhibitor mixture is present in the solution compared to the activation energies of other inhibitor. This can be attributed to the fact that higher values of Ea induce the energy barrier for the corrosion reaction. It was found that the optimum mixture was achieved with a higher activation energy compared to the each inhibitor individually.

4. The mechanism of corrosion inhibition can be explained by adsorption of the corrosion inhibitor to the surface of the metal. The efficiency of this inhibitor depends on its ability to occupy the respective vacant sites forming a chemisorbed inhibitor film. This efficiency depends on the composition of the metal and corrodent, inhibitor structure and concentration as well as temperature. The degree of surface coverage by the inhibitor, θ_m can be related to the weight loss in the absence and presence of corrosion inhibitor, respectively as illustrated by this Equation. In this study, when we used Langmuir model that predict the physical adsorption, the maximum adsorption capacity was it higher in N-211 than AR-505 suggesting more adsorption reached to the surface system. However, It can be seen that Shawabkeh-Tutunji correlation which is applied for chemisorption

adsorbent-adsorbate system was the best fits to the experimental data due to regression coefficient.

5. In the presence of mixture, we got a wonderful result and the morphology of the steel surface is quite different from the previous inhibitors. This observation indicated that corrosion rate almost suppressed in the presence of the mixture. This might be due to the highly achievement for the adsorption of inhibitor molecules on the metal surface suggesting that mixture bring better passive effect to carbon steel which easily adhered to carbon steel and form a fine structure for anti-corrosion. In addition, the surface was mostly of composed oxides of iron and calcium while the percentage of iron on this surface is very low compared to that treated with each inhibitor and this presumably is due to the enhancing of the passive layer by the surface and thus improves the corrosion resistance.

TABLE 4-13. COMPARISON BETWEEN INHIBITORS CORROSION RATE AND INHIBITION EFFICIENCY FOR 1018 CS AT DIFFERENT KINETIC CONDITIONS

Inhibitor		AR-505 amine based inhibitor		N-211 amine based inhibitor		Mixture of 5 ppm N-211 & 5 ppm of AR-505	
Parameter	value	CR (mm/y)	Inhibition Efficiency (%)	CR (mm/y)	Inhibition Efficiency (%)	CR (mm/y)	Inhibition Efficiency (%)
Temperature (^{o}C)	25	0.93	62.4	0.68	72.5	0.42	83
	40	1.01	59.1	0.86	65.2	0.58	76.5
	55	1.29	47.8	1.08	50.6	0.71	71.3
pH	4	3.67	-	2.88	-	2.03	17.8
	7	1.98	19.8	1.43	42.1	1.21	51.0
	8.2	1.29	47.8	1.08	50.6	0.71	71.3
Speed (rpm)	0	0.34	86.2	0.16	93.5	0.1	96.0
	500	1.18	52.2	0.73	70.5	0.58	76.5
	1000	1.29	47.8	1.08	50.6	0.71	71.3

TABLE 4-14. COMPARISON BETWEEN INHIBITORS RATIO BY *POTENTIODYNAMIC* POLARIZATION FOR 1018 CS

	value	E_{corr} (mV)	i_{corr} (A/cm^2)	Transfer coefficients		BVE slopes		Rp Ω
				α_a	α_c	β_a (mV/decade)	β_c (mV/decade)	
Inhibitor ratio	Blank	-519	4.46E-04	0.87	0.13	32.5	217.4	2.76E+04
	10 ppm of AR -505	-501	2.51E-04	0.82	0.18	34.6	156	4.91E+04
	10 ppm of N-211	-310	2.24E-04	0.80	0.20	35.4	138.8	5.47E+04
	30% N-211 & 70 % AR-505	-295	2.51E-04	0.82	0.18	34.4	159.5	4.90E+04
	50% N-211 & 50 % AR-505	-269	2.00E-04	0.79	0.21	36.0	132	6.15E+04
	70% N-211 & 30 % AR-505	-264	2.22E-04	0.80	0.20	35.4	138.6	5.52E+04

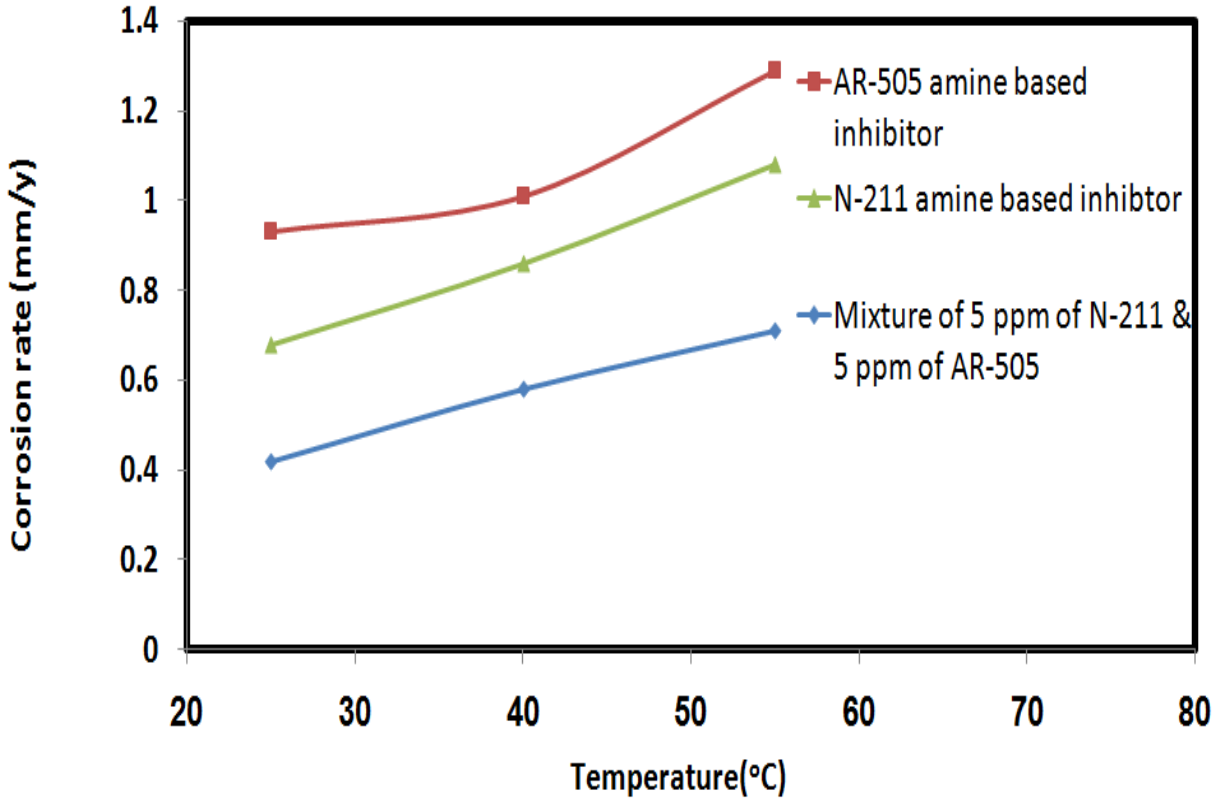

Figure 4-26 a: Comparison between inhibitors 1018 carbon steel corrosion at different temperature.

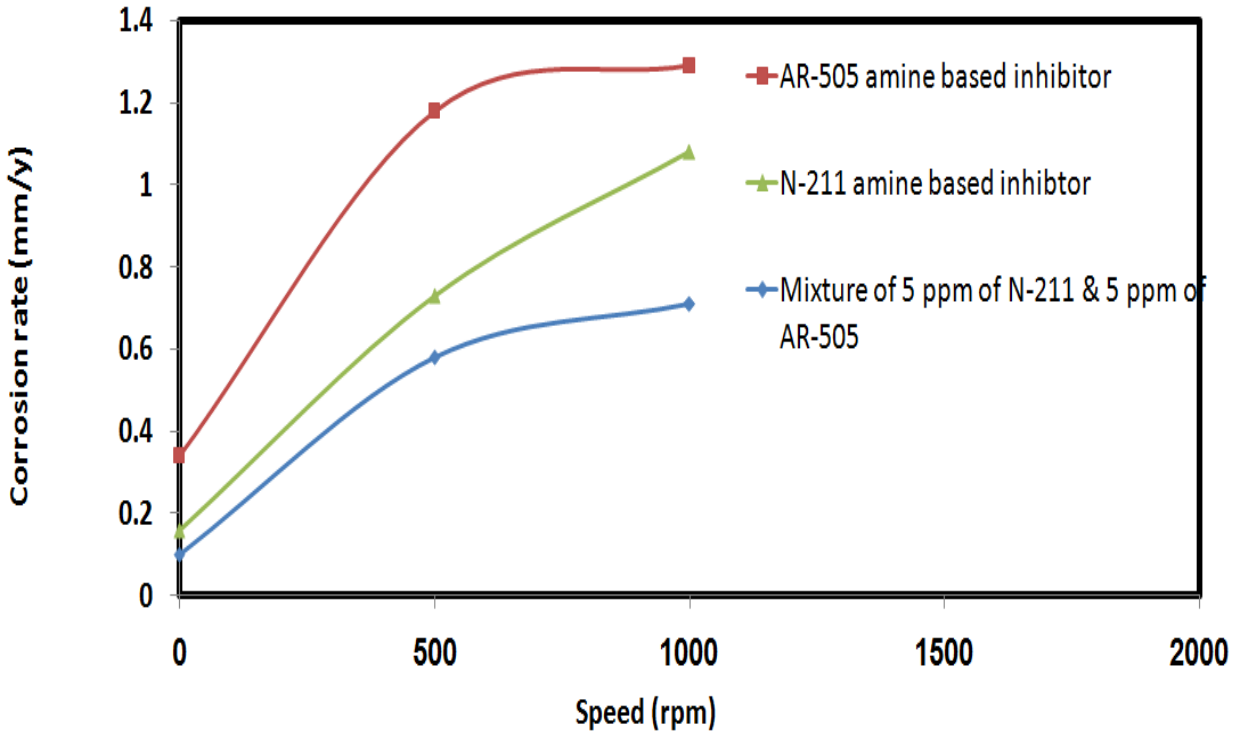

Figure 4-26 b: Comparison between inhibitors 1018 carbon steel corrosion at different mixing speed.

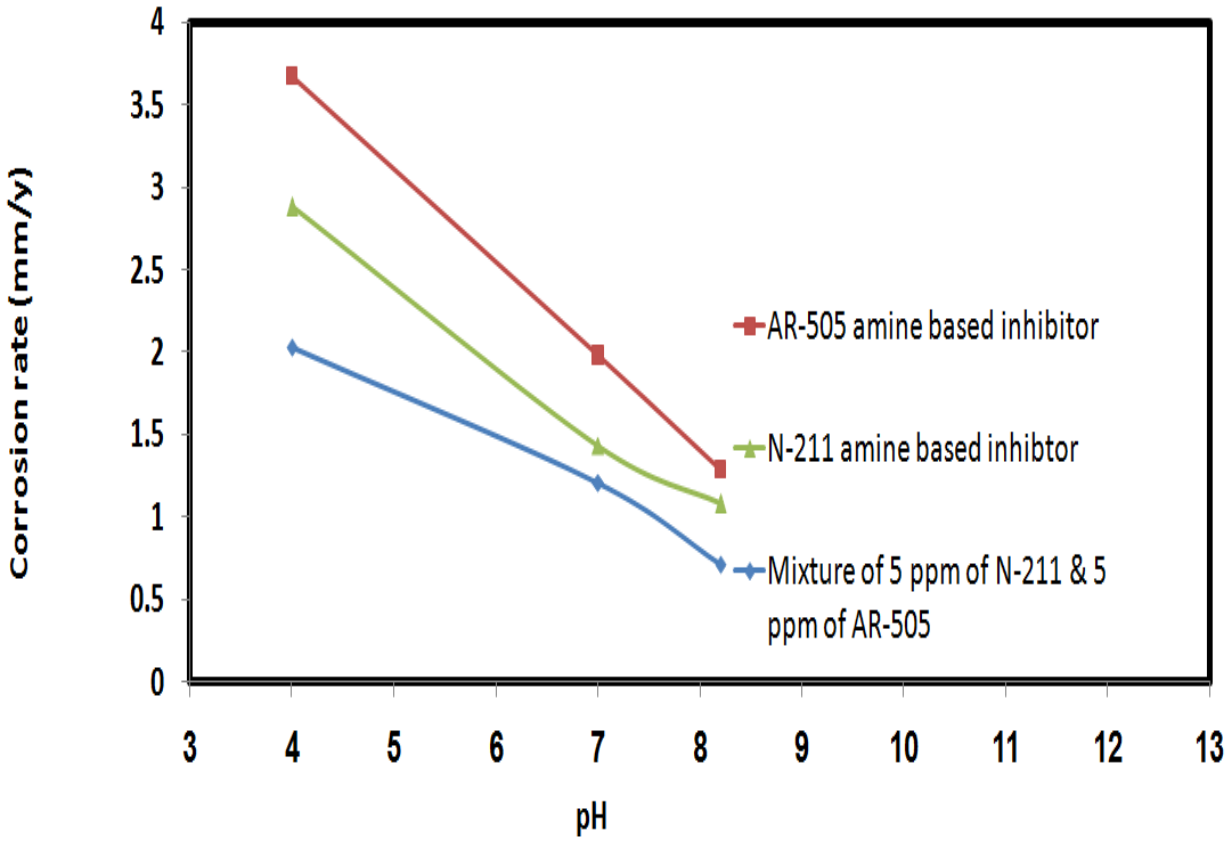

Figure 4-26 c: Comparison between inhibitors 1018 carbon steel corrosion at different value of pH.

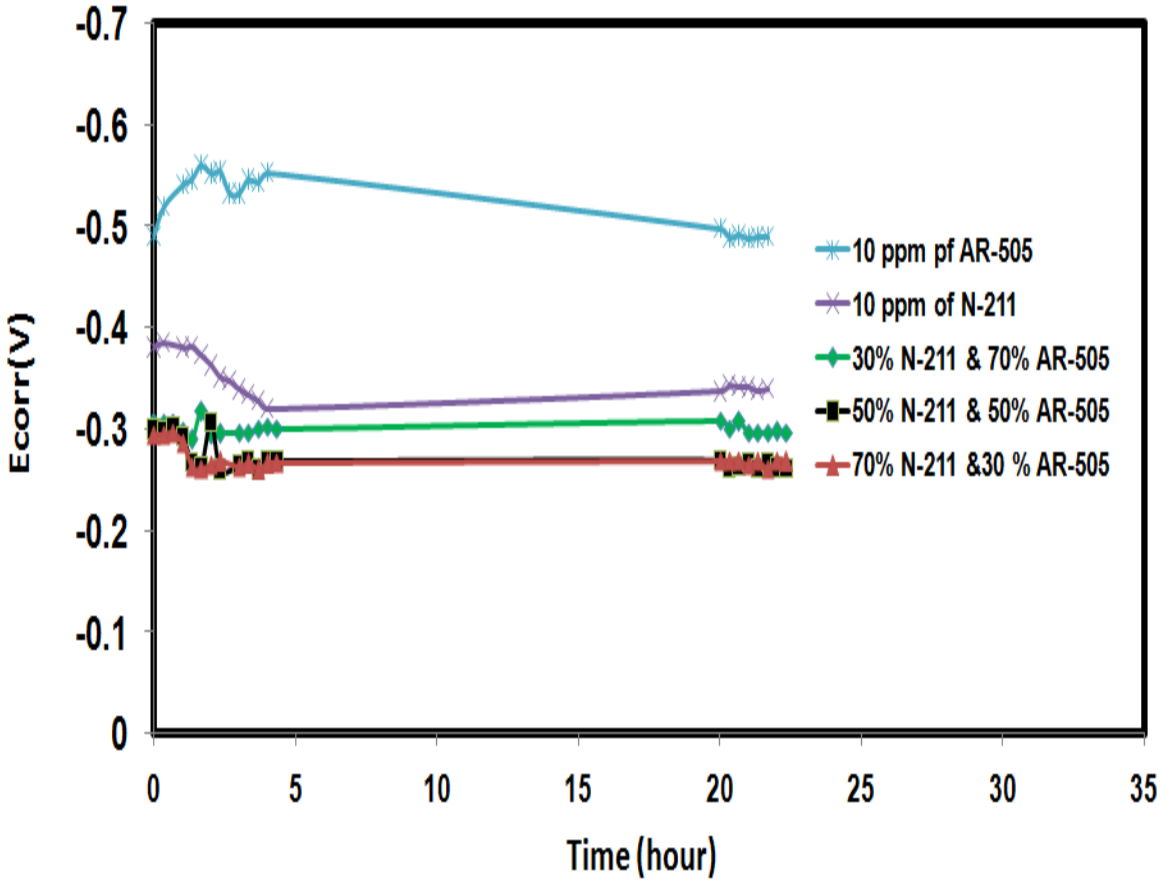

Figure 4-27: Comparison between inhibitors on 1018 carbon steel corrosion based on Linear Polarization technique

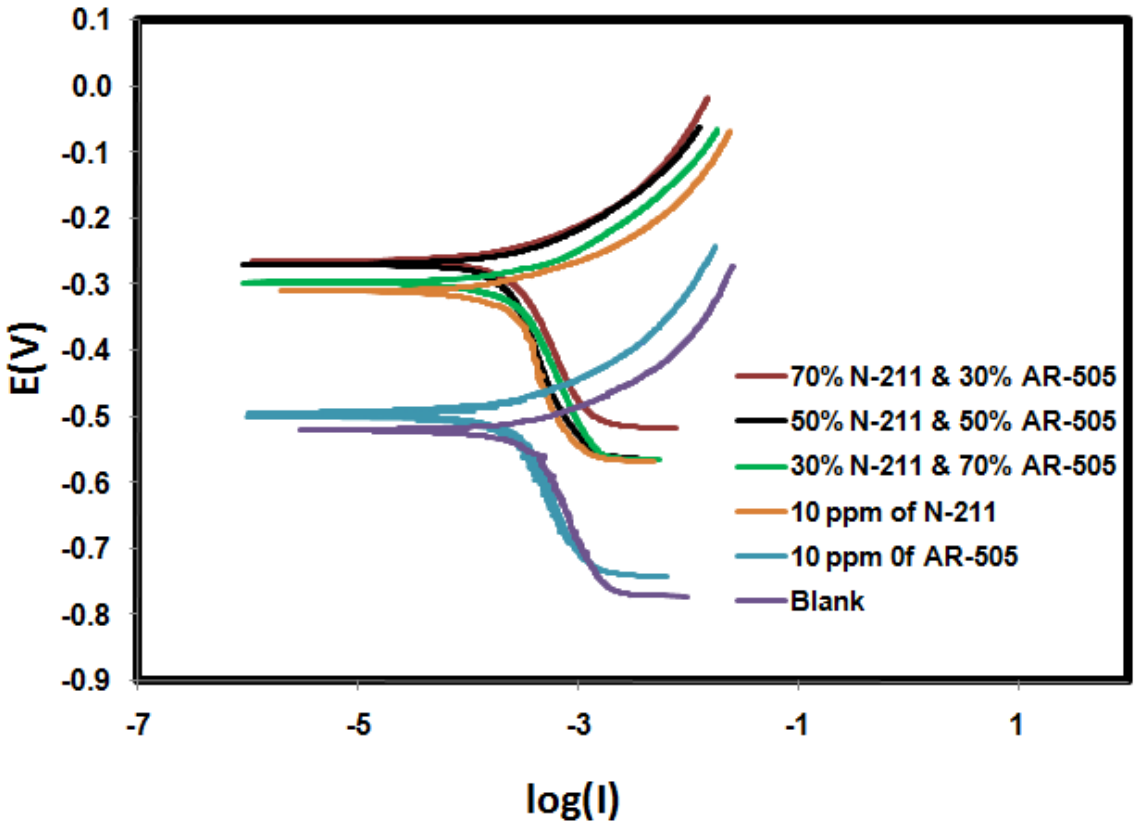

Figure 4-28: Comparison between inhibitors on 1018 carbon steel corrosion based on Potentiodynamic Polarization technique

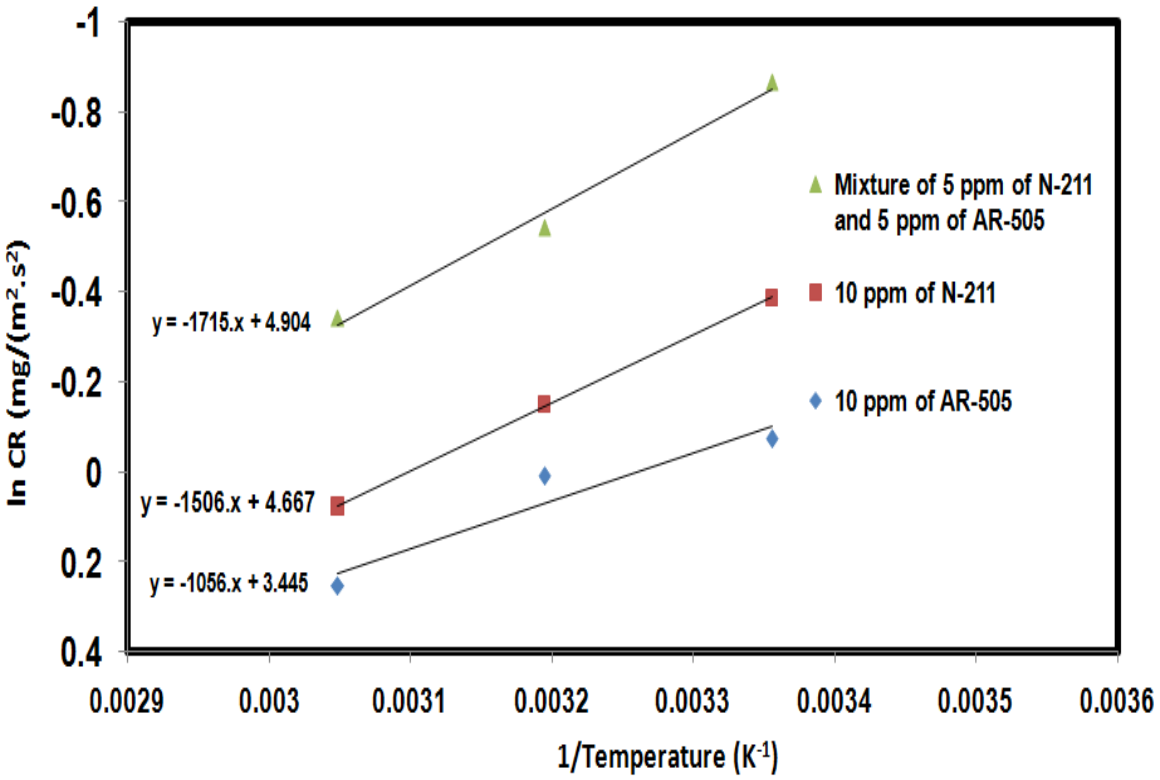

Figure 4-29: Comparison between inhibitors on 1018 carbon steel corrosion based on Activation Energy Calculation

CHAPTER 5

5 CONCLUSIONS AND RECOMMENDATIONS

5.1 Conclusions

The following conclusions are made based on the experimental results of this research:

1. The inhibitor mixture has the lowest value of corrosion rate under any kinetic conditions which is the most effective amount of the corrosion-inhibiting to be used.

2. The mechanism of corrosion inhibition was attributed to the adsorption of the corrosion inhibitor to the surface of the metal. The maximum adsorption capacity of N-211 was higher than AR-505 suggesting more adsorption reached to the surface system.

3. From the weight loss study, it was shown that the mixture of inhibitor 50 % of N-211 and 50% of AR-505 is the best one to protect the metal surface against the temperature, the mixing speed, and the value of pH.

4. The linear polarization and Potentiodynamic Polarization study confirmed that the increasing in the N-211 inhibitor quantity mixture was achieved better protection since it shifted the values of corrosion potential towards more positive (noble) and by formation

of film to retard the metal dissolution of the metal surface. On the other hand, it was shown that the AR-505 had the lowest protection compared with the other inhibitors that were conducted in the experimental work.

5. The study of the activation energy showed that the increase in E_a, representing that the energy barrier for the interaction of corrosion became high which is proportional to the nature of inhibitor. However, It was highest when the inhibitor mixture is present in the solution compared to the activation energies of other inhibitor. This can be attributed to the fact that higher values of E_a induce the energy barrier for the corrosion reaction.

6. The morphology of the steel surface is quite different from the previous work. This observation indicated that corrosion rate almost suppressed in the presence of the mixture. This might be due to the highly achievement for the adsorption of inhibitor molecules on the metal surface suggesting that mixture bring better passive effect to carbon steel which easily adhered to carbon steel and form a fine structure for anti-corrosion.

5.2 Recommendations

The following recommendations could be useful for future work:

1. The mixture of 5 ppm of N-211 and 5 ppm of AR-505 could be used in pipelines which reduce the internal corrosion and extend the lifetime.

2. More inhibitor concentrations should be studied in order to make a more inclusive conclusion on the inhibiting effect of the tested inhibitor.

3. The Conducting of Electrochemical Impedance Spectroscopy (EIS) should be done in order to confirm the data obtained by this research work.

4. Further investigation is required for the mixture of both inhibitors to recognize the mechanism for protection the carbon steel in the seawater.

REFERENCES

1. Mobin Salasi, Taghi Shahrabi, and Emad Roayaei., "Effect of inhibitor concentration and hydrodynamic conditions on the inhibitive behaviour of combinations of sodium silicate and HEDP for corrosion control in carbon steel water transmission pipes" Anti-Corrosion Methods and Materials, 2007, vol. 54, no. 2, pp. 82–92.
2. CS, Corrosion of Carbon Steel. In Key to Metal, http://steel.keytometals.com/default.aspx?ID=CheckArticle&NM=60.
3. Katerina Bılkova, Egil Gulbrandsen, ,"Kinetic and mechanistic study of CO_2 corrosion inhibition by cetyl trimethyl ammonium bromide", Electrochimica Acta 53 (2008) 5423–5433.
4. Tems, R.; Al Zahrani, A. M., Cost of corrosion in oil production and refining. *Saudi Aramco* Journal of Technology 2006, (SUMMER), 2.
5. A. Deyab, S.S. Abd El-Rehim, "Inhibitory effect of tungstate, molybdate and nitrite ions on the carbon steel pitting corrosion in alkaline formation water containing Cl^- ion", Electrochimica Acta 53 (2007) 1754–1760
6. B. Ramesh Babu, K. Thangavel, "The effect of isomers of some organic compounds as inhibitors for the corrosion of carbon steel in sulfuric acid", Anti-Corrosion Methods and Materials 52/4 (2005) 219–225
7. E.E. Oguzie, A.I. Onuchukwu, P.C. Okafor, and E.E. Ebenso," Corrosion inhibition and adsorption behaviour of Ocimum basilicum extract on aluminum". Pigment and Resin Technology, 2006, vol. 35, no. 2, p. 63

8. H. Amar, T. Braisaz , D. Villemin, B. Moreau, "Thiomorpholin-4-ylmethyl-phosphonic acid and morpholin-4-methyl-phosphonic acid as corrosion inhibitors for carbon steel in natural seawater", Materials Chemistry and Physics 110 (2008) 1–6.
9. A.A. Al-Sarawy, A.S. Fouda, and W.A. Shehab El-Dein, "Some thiazole derivatives as corrosion inhibitors for carbon steel in acidic medium". De salination, (2008), no. 229, pp. 279–293.
10. L. Herrag, B. Hammouti, S. Elkadiri, B. El Bali, M. Lachkar, and R. Ouarsal, "Inhibition of steel corrosion in HCl media by phosphite compound". Pigment & Resin Technology 2008, vol. 37, no. 3, pp. 167–172.
11. M. S. Morad, "The inhibitory effect of bis-2,6-(3,5 dimethylpyrazolyl)pyridine on the corrosion behavior of mild steel in HCl solution". Materials Chemistry and Physics 2008, no. 109, pp. 492–499.
12. P.H. Suegama a, H.G. de Melo a, A.A.C. Recco b, A.P. Tschiptschin b, I.V. Aoki, "Corrosion behavior of carbon steel protected with single and bi-layer of silane films filled with silica nanoparticles" Surface & Coatings Technology 202 (2008) 2850–2858.
13. J.Z. Ai, X.P. Guo, Z.Y. Chen "The adsorption behavior and corrosion inhibition mechanism of anionic inhibitor on galvanic electrode in 1% NaCl solution", Applied Surface Science 253 (2006) 683–688
14. M. Sahin , G. Gece, F. Karcı ,S. Bilgic ,"Experimental and theoretical study of the effect of some heterocyclic compounds on the corrosion of low carbon steel in 3.5% NaCl medium", J Appl Electrochem (2008) 38:809–815.
15. Guo Gao, Cheng Hao Liang, Hua Wang,"Synthesis of tertiary amines and their inhibitive performance on carbon steel" corrosion" Corrosion Science 49 (2007) 1833–1846.

16. Akzo, Corrosion Inhibitors for Oilfield Production. In AzoNoble Companey, http://www.se.akzonobel.com/bulletins/Corrosion%20Inhibitors%20for%20Oilfield%20Production.pdf.
17. Jones,D.A.," Principles and Prevention of Corrosion", 2nd Edition, Prentice-Hall (1996).
18. M. Abdallah , E.A. Helal , A.S. Fouda., " Aminopyrimidine derivatives as inhibitors for corrosion of 1018 carbon steel in nitric acid solution", Corrosion Science 48 (2006) 1639–1654.
19. A. Yurt, G. Bereket, A. Kivrak, A. Balaban and B. Erk, "Effect of Schiff bases containing pyridyl group as corrosion inhibitors for low carbon steel in 0.1 M HCl", Journal of Applied Electrochemistry (2005) 35:1025–1032.
20. Y. Abboud, A. Abourriche, T. Saffaj, M. Berrada, M. Charrouf , A. Bennamara, N. Al Himidi, H. Hannache"2,3-Quinoxalinedione as a novel corrosion inhibitor for mild steel in 1M HCl". Materials Chemistry and Physics 105 (2007) 1–5.
21. A.Y. El-Etre, "Inhibition of acid corrosion of carbon steel using aqueous extract of olive leaves", Journal of Colloid and Interface Science 314 (2007) 578–583.
22. E. Machnikova, Kenton H. Whitmire, N. Hackerman, "Corrosion inhibition of carbon steel in hydrochloric acid by furan derivatives", Electrochimica Acta 53 (2008) 6024–6032.
23. Ying Yan, Weihua Li, Lankun Cai, Baorong Hou "Electrochemical and quantum chemical study of purines as corrosion inhibitors for mild steel in 1M HCl solution", Electrochimica Acta 53 (2008) 5953–5960.
24. Ganesha Achary, Y. Arthoba Naik, S. Vijay Kumar, T.V. Venkatesha, B.S. Sherigara, "An electroactive co-polymer as corrosion inhibitor for steel in sulphuric acid medium", Applied Surface Science 254 (2008) 5569–5573.

25. O. Olivares-Xometl, N.V. Likhanova, M.A. Dom´ınguez-Aguilar, E. Arce, H. Dorantes, P. Arellanes-Lozada, "Synthesis and corrosion inhibition of α-amino acids alkylamides for mild steel in acidic environment", Materials Chemistry and Physics 110 (2008) 344–351.
26. A R Sathiya Priya, V S Muralidharan, A Subramania, "Devolvement of Novel Acidizing Inhibitors for Carbon Steel Corrosion in 15% Boiling Hydrochloric acid", ProQuest Science Journals pg. 541.
27. Ayssar Nahle´, Ideisan Abu-Abdoun , Ibrahim Abdel-Rahman, "Inhibition of carbon steel corrosion by 4-vinylbenzyl triphenyl phosphonium chloride in HCl solution" Anti-Corrosion Methods and Materials 55/4 (2008) 217–224.
28. M.S. Morad *, A.A.O. Sarhan"Application of some ferrocene derivatives in the field of corrosion inhibition" Corrosion Science 50 (2008) 744–753.
29. M.Z.A. Rafiquee, Nidhi Saxena, Sadaf Khan, M.A. Quraishi, "Influence of surfactants on the corrosion inhibition behavior of 2-aminophenyl-5-mercapto-1-oxa-3,4-diazole (AMOD) on mild steel", Materials Chemistry and Physics 107 (2008) 528–533.
30. 20. M. S. Morad, "Some environmentally friendly formulations as inhibitors for mild steel corrosion in sulfuric acid solution", J Appl Electrochem (2007) 37:661–668
31. Salah Merah, Lahcene Larabi, Omar Benali, Yahia Harek, "Synergistic effect of methyl red dye and potassium iodide on inhibition of corrosion of carbon steel in 0.5M H2SO4", Pigment & Resin Technology 37/5 (2008) 291–298.
32. Sha Cheng, Shougang Chen, Tao Liu, Xueting Chang, Yansheng Yin, "Carboxymenthylchitosan as an ecofriendly inhibitor for mild steel in 1 M HCl" Materials Letters 61 (2007) 3276–3280.

33. A.S. Fouda, A.A. Al-Sarawy, E.E. El-Katori, "Pyrazolone derivatives as corrosion inhibitors for C steel in hydrochloric acid solution", Desalination 201 (2006) 1–13.

34. L.R. Chauhan, G. Gunasekaran, "Corrosion inhibition of mild steel by plant extract in dilute HCl medium", Corrosion Science 49 (2007) 1143–1161.

35. MOHAMED ISMAIL AWAD"Eco friendly corrosion inhibitors: Inhibitive action of quinine for corrosion of low carbon steel in 1 M HCl", Journal of Applied Electrochemistry (2006) 36:1163–1168.

36. E.E. Oguzie, Y. Li, F.H. Wang, "Effect of 2-amino-3 mercaptopropanoic acid (cysteine) on the corrosion behaviour of low carbon steel in sulphuric acid", Electrochimica Acta 53 (2007) 909–914

37. A. Ouchrif , M. Zegmout, B. Hammouti, A. Dafali , M. Benkaddour ,A. Ramdani, S. Elkadiri," New synthesised diamine derivatives as corrosion inhibitors of steel in 0.5M H2SO4", Progress in Organic Coatings 53 (2005) 292–296

38. Baojiao Gao*, Xin Zhang, Yanling Sheng, "Studies on preparing and corrosion inhibition behaviour of quaternized polyethyleneimine for low carbon steel in sulfuric acid", Materials Chemistry and Physics 108 (2008) 375–381.

39. 56. Policarpo Galicia, Ignacio Gonz´alez,"Modification of 1018 carbon steel corrosion process in alkaline sour medium with a formulation of chemical corrosion inhibitors", Electrochimica Acta 50 (2005) 4451–4460.

40. *Mohammed A. Amin, Sayed S. Abd El-Rehim, E.E. F. El-Sherbini, and Rady S. Bayoumi,* "Chemical and Electrochemical (AC and DC) Studies on the Corrosion Inhibition of Low Carbon Steel in 1.0 M HCl Solution by Succinic Acid - Temperature Effect, Activation Energies and Thermodynamics of Adsorption" *Int. J. Electrochem. Sci.,* 3 **(2008)** 199 – 215.

41. B. Ramesh Babu, A.K. Parande, and P.L. Ramasamy,"Effect of N-cetyl-N,N,N-trimethylammonium bromide and orthophenylenediamine on the corrosion inhibition of carbon steel in 1 mol/L HCl", Can. J. Chem. **84**: 1658–1666 (2006).
42. S.U. Rahman, M.T. Saeed, Sk.A. Ali,"Cyclic nitrones as novel organic corrosion inhibitors for carbon steel in acidic media", Anti-Corrosion Methods and Materials 52/3 (2005) 154–159.
43. Ayşe Tosun*, Mübeccel Ergun, "Protection of Corrosion of Carbon Steel by Inhibitors in Chloride Containing Solutions", *G.U. Journal of Science 19(3): 149-154 (2006).*
44. A. A. Chirkunov, Yu. I. Kuznetsov, M. A. Gusakova, "Protection of Low-Carbon Steel in Aqueous Solutions by Lignosulfonate Inhibitors" published in Zashchita Metallov, 2007, Vol. 43, No. 4, pp. 396–401.
45. A. Amadeh, S.R. Allahkaram, S.R. Hosseini, H. Moradi and A. Abdolhosseini "The use of rare earth cations as corrosion inhibitors for carbon steel in aerated NaCl solution" Anti-Corrosion Methods and Materials 55/3 (2008) 135–143.
46. Nakarin Srisuwan, Nathalie Ochoa, Nadine Pebere, Bernard Tribollet, "Variation of carbon steel corrosion rate with flow conditions in the presence of an inhibitive formulation", Corrosion Science 50 (2008) 1245–1250.
47. A.M. Alsabagh, M.A. Migahed, Hayam S. Awad, "Reactivity of polyester aliphatic amine surfactants as corrosion inhibitors for carbon steel in formation water (deep well water)", Corrosion Science 48 (2006) 813–828.
48. S Rajendran, S P Sridevi, N Anthony, A John Amalraj, M Sundaravadivelu, "Corrosion behavior of carbon steel in polyvinyl alcohol", ProQuest Science Journals pg. 102

49. R. Naderi, M.M. Attar, "Electrochemical assessing corrosion inhibiting effects of zinc aluminum polyphosphate (ZAPP) as a modified zinc phosphate pigment", Electrochimica Acta 53 (2008) 5692–5696

50. Bin Yao, Gengchao Wang , Jiankun Ye, Xingwei Li, "Corrosion inhibition of carbon steel by polyaniline nanofibers", Materials Letters 62 (2008) 1775–1778.

51. M. Salasi, T. Shahrabi, E. Roayaei, M. Aliofkhazraei, "The electrochemical behaviour of environment-friendly inhibitors of silicate and phosphonate in corrosion control of carbon steel in soft water media" Materials Chemistry and Physics 104 (2007) 183–190

52. N. Srisuwan, N. Ochoa, N. Pébèret, B. Tribollet, "Variation of carbon steel corrosion rate with flow conditions in the presence of an inhibitive formulation", Corrosion Science (2008) doi: 10.1016/j.corsci.2008.01.029

53. Langmuir, I., Journal of the American Chemical Society, (1916), vol. 38, no. 11, p. 2221.

54. Shawabkeh, R. and Tutunji, M., *Experimental Earth Journal*, 2003, vol. 1, no. 5, p.

55. Ma, Y., Li, Y. and Wang, F., Corrosion Science, 2009, vol. 51, no. 5, p. 997.

56. Smith, D.C. and McEnaney, B., Corrosion Science, 1979, vol. 19, no. 6, p. 379.

57. K.N. Mohana, A.M. Badiea, "Effect of sodium nitrite–borax blend on the corrosion rate of low carbon steel in industrial water medium", Corrosion Science 50 (2008) 2939–2947.

NOMENCLATURE

i_{corr}: the corrosion current density in A/m^2

R_p: the polarization resistance in $\Omega.m^2$

B: the proportionality constant in V/decade

β_a: anodic Tafel constants

β_c: cathodic Tafel constants

w: the equivalent weight of steel

F: Faraday constant

ρ: the density of the steel in kg/m^3

K: 8.76×10^6 (mm/m)(h/y)

T: the time of exposure in hour

A: the exposed area of the electrode in m^2

(CR_{blank}) the corrosion rate in the absence of the inhibitor

(CR_{inh}) the corrosion rate in the presence of the inhibitor

θ_m The degree of surface coverage by the inhibitor

m_{free} the weight loss in the absence of corrosion inhibitor

m_{inh} the weight loss in the presence of corrosion inhibitor

θ_{max} the maximum adsorption capacity could be reached by the inhibitor-surface system

Ce the equilibrium concentration of the inhibitor in solution

b Constant

q_0 Constant

α Constant

β Constant

BVE	Butler-Volmer Equation
α_a	anodic transfer coefficient
α_c	cathodic transfer coefficient
i:	the net current density of the electrode
i_o:	the exchange current which equals to the anodic current at equilibrium
η:	is the over potential which equals to the difference between the equilibrium and the applied potentials
R:	Ideal gas constant
T:	The temperature of the solution
E_a:	The apparent activation energy
K:	the corrosion rate
$A_{f:}$	the frequency factor

VITA

Name	Nawaf Ibrahim Al-Bakr
Religion	Islam
Nationality	Saudi
Place and Date of Birth	Jeddah, Saudi Arabia, March 1980
Address	Saudi Aramco Company Saudi Aramco Box 1995, Dhahran 31311, Saudi Arabia Dhahran, Eastern Province, Saudi Arabia
E-mail Address	bakrni@aramco.com.sa
Contact information	Office: +966 3 874-1488 Fax: +966 3 874-1431 Mobile: +966 504808008
Education	Bachelor of Science in Chemical Engineering from King Fahd University of Petroleum & Minerals in February 2003 Master of Science in Chemical Engineering from King Fahd University of Petroleum & Minerals in January 2010.